

**GEDIZ UNIVERSITY ★ GRADUATE SCHOOL OF NATURAL AND APPLIED
SCIENCES**

**FABRICATION and ELECTRICAL CHARACTERIZATION of
SONOCHEMICALLY GROWN NANOSTRUCTURED ZnO DYE SENSITIZED
SOLAR CELLS**

M.Sc. THESIS

Telat GÜLER

Nanotechnology Programme

JUNE 2015

**GEDIZ UNIVERSITY ★ GRADUATE SCHOOL OF NATURAL AND APPLIED
SCIENCES**

**FABRICATION and ELECTRICAL CHARACTERIZATION of
SONOCHEMICALLY GROWN NANOSTRUCTURED ZnO DYE SENSITIZED
SOLAR CELLS.**

M.Sc. THESIS

Telat GÜLER

(600712007)

Nanotechnology Programme

Thesis Advisor: Asst. Prof. Dr. Yavuz BAYAM

JUNE 2015

GEDİZ ÜNİVERSİTESİ ★ FEN BİLİMLERİ ENSTİTÜSÜ

**SONOKİMYASAL METODLA BÜYÜTÜLMÜŞ ZnO NANO YAPILI BOYA
DUYARLI GÜNEŞ PİLLERİNİN FABRİKASYONU VE ELEKTRİKSEL
KARAKTERİZASYONU**

YÜKSEK LİSANS TEZİ

Telat GÜLER

(600712007)

Nanoteknoloji Programı

Tez Danışmanı: Yrd.Doç.Dr. Yavuz BAYAM

HAZİRAN 2015

Telat GÜLER a M.Sc. student of Gediz University **Graduate School of Natural and Applied Sciences** 600712007, successfully defended the **thesis** entitled “**FABRICATION and ELECTRICAL CHARACTERIZATION of SONOCHEMICALLY GROWN NANOSTRUCTURED ZnO DYE SENSITIZED SOLAR CELLS**”, which he prepared after fulfilling the requirements specified in the associated legislations, before the jury whose signatures are below.

Thesis Advisor : Asst. Prof. Dr. Yavuz BAYAM

Gediz University

Thesis Co Advisor: Assoc. Prof.Dr. Ceylan ZAFER

Ege University

Jury Members : Asst. Prof. Dr. Ramazan ATALAY

Gediz University

Jury Members : Asst. Prof. Dr. Mücahit SÜTÇÜ

İzmir Katip Çelebi University

Jury Members : Asst. Prof. Dr. Mehtap ÖZDEMİR KÖKLÜ.....

Gediz University

Date of Submission : 22 May 2015

Date of Defense : 15 June 2015

Dedicated to My Wife and My Son

FOREWORD

First of all, I thank my advisor Asst. Prof. Dr. Yavuz BAYAM in person for his tireless efforts and support towards the success of this thesis. His advice, encouragement and motivation certainly stimulated me to work harder. Working with him was a great experience for my career.

My heartfelt gratitude goes to Assoc. Prof. Dr. Ceylan ZAFER at Ege University, İzmir, Turkey who helped me with the experimental study and to Research Assistant Dr. Burak GÜLTEKİN who assisted in the interpretation of the XRD data.

To my family - I really appreciate your efforts especially my mother and my wife for their moral support and encouragement. I'd like to express my gratitude to my friends especially my group members for their cooperation and assistance whenever I needed it. Special thanks to Ali İhsan Kanlı and İhsan ÇAHA who assisted with the experimental part of the thesis.

I would like to thank all the committee members.

JUNE 2015

Telat GÜLER
(Technical Teacher)

TABLE OF CONTENTS

	<u>Page</u>
FOREWORD	vi
TABLE OF CONTENTS	vii
ABBREVIATIONS	x
LIST OF TABLES	xi
LIST OF FIGURES	xii
SUMMARY	xv
ÖZET	xviii
1. INTRODUCTION	1
1.1 Energy	1
1.1.1 Renewable Energy Sources.....	1
1.1.1.1 Solar Energy	3
1.2 Purpose of Thesis	5
1.3 Literature Review	5
1.4 Hypothesis.....	6
1.5 Nanotechnology Concept	6
2. THEORY	8
2.1 Photovoltaic Solar Cell	8
2.1.1 Classification of Photovoltaic Cells.....	9
2.1.2 Semiconductor Technology	9
2.1.2.1 Intrinsic Semiconductors.....	10
2.1.2.2 Extrinsic Semiconductors.....	10
2.1.3 PN Junction	11
2.1.4 Advantages of Photovoltaic Systems.....	12
2.1.5 Disadvantages of Photovoltaic Systems	12
2.1.6 Stages of Development of Photovoltaic Cells.....	12
2.1.7 Electrical Parameters of Photovoltaic Solar Cells	14
2.1.7.3 Open Circuit Voltage (V_{OC}).....	14
2.1.7.4 Short Circuit Current (J_{SC}) :	14
2.1.7.5 Fill Factor (FF).....	15
2.1.7.6 Maximum Power Point (P_{MAX})	15
2.1.7.7 Efficiency (Power Conversion Efficiency)	15
2.1.7.8 Solar Spectrum	16
2.2 Dye Sensitized Solar Cell (DSSC).....	17
2.2.1 DSSC Working Scheme	18
2.2.2 Used Dyes in Solar Cells;	19
2.2.3 Advantages of DSSC;	19
2.2.4 Disadvantages of DSSC;.....	19
2.2.5 Traditional “Gratzel Type” DSSCs.....	20
2.2.6 Solid State DSSCs.....	20
2.3 Metal Oxide Nanostructures and Their Applications.....	21

2.3.1 Zinc Oxide (ZnO).....	22
2.3.1.9 ZnO Crystal Structures.....	23
2.3.2 Growth and Charazterization Techniques For ZnO Nanorods	24
2.3.2.1 Physical Vapor Deposition.....	25
2.3.2.2 Molecular Beam Epitaxy (MBE)	25
2.3.2.3 RF Sputtering	26
2.3.2.4 Thermal Evaporation.....	27
2.3.2.5 Spin Coating Technique.....	29
2.3.2.6 Chemical Vapor Deposition (CVD).....	30
2.3.2.7 Hydrothermal	31
2.3.2.8 Aerosol Deposition	32
2.3.2.9 Sonochemistry	33
2.3.2.9.1. Sonochemistry Applications	35
2.3.2.9.2. Frequency Range of Audio Spectrum	36
3. EXPERIMENTAL	39
3.1 Production Stages of ZnO DSSC	39
3.1.1 Preparation of Fluorine-Doped Tin Oxide Thin Films	39
3.1.1.1 Cleaning of FTO-Coated Glass Plates	39
3.1.2 Synthesis of ZnO Nanorod for DSSC Application	40
3.1.2.2 ZnO Seeding Process	41
3.1.2.3 ZnO Nano Rods Growth Process.	44
3.1.3 DSSC Device Fabrications.....	47
3.1.3.4 Working Electrode Structure.....	47
3.1.3.5 Preparation of Counter Electrode.....	47
3.1.3.6 Preparation of Liquid Electrode	48
3.1.3.7 Construction of Dye Sensitized Silicon Solar Cell	48
3.2 Characterization Techniques	50
3.2.1 Morphological Characterization	50
3.2.1.8 Optical Microscopy	50
3.2.1.9 Profilometer.....	52
3.2.1.10 AFM	54
3.2.1.11 Scanning Electron Microscopy (SEM)	55
3.2.2 Elemental Analysis;	56
3.2.2.1 Energy Dispersive X-ray Spectroscopy (EDS)	56
3.2.3 Structural Analysis,	58
3.2.3.1 X-ray Diffraction (XRD)	58
3.2.3.2 Spectroscopic Analysis	59
3.2.4 Electrical Characterization.....	60
4. RESULTS AND DISCUSSION.....	61
4.1 Morphological Characterization.....	62
4.1.1 Optical Microscopy Analysis.....	62
4.1.2 Sectional Analysis	65
4.1.3 AFM Analysis	66
4.1.4 Scanning Electron Microscopy Analysis (SEM)	67
4.2 Elemental Analysis.....	72
4.2.1 Energy Dispersive X-ray Spectroscopy Analysis (EDS).....	72
4.3 Structural Analysis	73
4.3.1 XRD Analysis	73
4.3.2 Spectroscopic Analysis	74
4.4 Electrical Analysis	75

4.4.1 Current-Voltage (J-V) Characterization.....	75
4.4.2 Incident Photon to Current Conversion Efficiency (IPCE) Measurement	78
CONCLUSION.....	79
REFERENCES	82
CURRICULUM VITAE.....	88

ABBREVIATIONS

ZnO	: Zinc Oxide
TiO₂	: Titanium Dioxide
HMT	: Hexamethylenetetramine
OM	: Optical Microscopy
SEM	: Scanning Electron Microscopy
EDS	: Energy Dispersive X-ray Spectroscopy
PVD	: Physical Vapor Deposition
PLD	: Pulsed Laser Deposition
MBE	: Molecular Beam Epitaxy
XRD	: X-Ray Diffraction
CVD	: Chemical Vapor Deposition
UHV	: Ultra-High Vacuum
IPA	:Isopropyl alcohol
FTO	:Fluorine Doped Tin Oxide
ITO	:Indium Tin Oxide
HOMO	:Highest Occupied Molecular Orbital
LUMO	:Lowest Unoccupied Molecular Orbital
PV	:Photovoltaic
DSSC	:Dye sensitized solar cell
TCO	:Transparent Conductive Oxide
HTM	:Hole Transport Material
BMGP	:Dye Sensitized Solar Cell
Z907	:Rutenyum(II) dye

LIST OF TABLES

Table 1-1: Renewable Energy Resources	3
Table 2-1: Efficiency Comparison of Well-Known Solar Cell ^[20]	17
Table 2-2: Basic Properties Wurtzite Type of ZnO ^[97]	24
Table 2-3: List of ZnO Nanostructures Synthesis Techniques and Grown Products.	38
Table 3-1: Used Chemicals in The Synthesis of ZnO Nanorods.	40
Table 4-1: Electrical Characterization Results of DSSC	76

LIST OF FIGURES

	Page
Figure 1-1. Generation of Electricity and Consumption Rates of Common Energy Sources ^[3]	2
Figure 2-1: Fotovoltaic Solar Cell.....	8
Figure 2-2: Pure and Doped Semiconductor Bonding.....	11
Figure 2-3: Used Parameters by The Solar Cell ^[10]	14
Figure 2-4: Solar Radiation Spectrum ^[16]	16
Figure 2-5: DSSC Working Scheme.....	18
Figure 2-6: Rutenyum Dye II (Z907).....	19
Figure 2-7: Component of Solid-State Dye Sensitized Solar Cell ^[29]	21
Figure 2-8: ZnO Crystal Structures a. Wurtzite b. Zincblende c. Zincblende Rocksalt.....	23
Figure 2-9: MBE System ^[99]	26
Figure 2-10: RF Sputtering Working Principle ^[101]	27
Figure 2-11: E-Beam Evaporation ^[102]	28
Figure 2-12: Thermal Evaporation.....	29
Figure 2-13: Four Stages of the Spin Coating Process.....	30
Figure 2-14: Schematic Diagram For the CVD Apparatus ^[110]	31
Figure 2-15: Teflon Pot Which is Used in The Hydrothermal Method ^[111]	32
Figure 2-16 : Chemical Spraying Methods Test Setup ^[112]	33
Figure 2-17 : Frequency Range of Audio.....	36
Figure 3-1: Image of FTO-Coated Glass.....	39
Figure 3-2: Cleaning Process for FTO-Coated Glass.....	40
Figure 3-3: Layers of Working Electrode a. Substrate b. ZnO Seed Layer Deposition c. ZnO Nanowire Growth.....	41
Figure 3-4: SEM Image of Seed-Layer Deposited on FTO Substrate.....	41
Figure 3-5: Optical Microscopy Image of ZnO NW Without Seed-Layer Via Sonication. (100X Magnification Applied).....	42
Figure 3-6: Optical Microscopy Image of ZnO NW With Seed-Layer Via Sonication. (100X Magnification applied).....	42

Figure 3-7: Schematic Representation of Sonochemical Synthesis of ZnO Seed Layer.....	43
Figure 3-8: Sonochemical Growth Setup.	44
Figure 3-9 : Picture of ZnO Nanorods Growth Solutions	45
Figure 3-10. Schematic Representation of Sonochemical Synthesis of ZnO Nanorods	46
Figure 3-11 : Image of Working Electrode	47
Figure 3-12 : Picture of Platinum Coated Counter Electrode.....	48
Figure 3-13 : The Schematic Structure of DSSCs	49
Figure 3-14 : Picture of Produced DSSC Device.....	49
Figure 3-15: Optical Microscopy Setup Which was Used for The Thesis.....	51
Figure 3-16: Picture of Profilometer Device.....	52
Figure 3-17: Imaging of ZnO Nanorod Step Height	53
Figure 3-18: Atomic Force Microscopy Working Principle ^[138]	54
Figure 3-19: SEM Device in Duzce University, Device Model: Quanta 250 FEG	55
Figure 3-20 : Schematic Presentation of SEM Instrument ^[139]	56
Figure 3-21: Interaction Between Source of X-ray Excitation and a Sample ^[141]	57
Figure 3-22: XRD Device Diffraction ^[142]	59
Figure 3-23: IPCE (EQE) measurement system.....	60
Figure 4-1: Optical Mic. Image of ZnO Seed Layer 30 min, 50% Amplitude Taken from Sample(64) (100X Magnification applied).....	62
Figure 4-2: Optical Mic. Image of ZnO Nanorods 60 min, 50% Amplitude Taken from Sample(68) (50X Magnification applied).....	63
Figure 4-3: Optical Mic. Image of Additional ZnO NanoParticles Layer on NanoRods Layer 30 min, 50% Amplitude Taken from Sample(83) (a.10X b.100X Magnification Applied).....	64
Figure 4-4: Profilometer Graph of ZnO Nanorod Length , 50% Amplitude Taken from Sample, Growth Time 60min.....	65
Figure 4-5: Profilometer Graph of ZnO Nanorod Length Taken from Sample, Growth Time 5x60min, 50% amplitude.....	66
Figure 4-6: AFM Image of Seed ZnO Layer	67
Figure 4-7: SEM Images of ZnO Seed Layer 30 min, 50% Amplitude Taken from Sample(59) (a) is Low Magnification(20000x Respectively) and (b) is High Magnification (50000x Respectively)	68
Figure 4-8: SEM Images of ZnO Nanorod Layer 5x60 min, 50% Amplitude Taken from Sample(68) (a)is Low Magnification(40000x Respectively) and (b) is High Magnification (80000x Respectively).....	69

Figure 4-9: SEM Images of Additional ZnO 12.5% Concentration Nanoparticle Layer on ZnO Nanorod Layer 5x60 min, 50% Amplitude Taken from Sample. (a) is Low Magnification (50000x Respectively) and (b) is High Magnification (100000x Respectively)	70
Figure 4-10: EDS Spectrum of ZnO Nanorod.....	72
Figure 4-11: XRD Pattern of Sonochemical Growth ZnO Nanorods Taken from Second Device.....	73
Figure 4-12: UV-Vis Spectroscopic Analysis Result	74
Figure 4-13: The Production Phase of the Each Devices and Comparison of the Efficiency	76
Figure 4-14: The Reference Device, Sonochemically Grown Nanorods in One Hour Without Nanoparticles. (Device1)	77
Figure 4-15: Sonochemically Grown Nanorods With Different Nanoparticle Ratios (Device 2-Device 3-Device 4).....	77
Figure 4-16: Incident Photon to Current Conversion Efficiency (IPCE) Result for Devices 3 and 4	78

FABRICATION AND ELECTRICAL CHARACTERIZATION OF SONOCHEMICALLY GROWN NANOSTRUCTURED ZnO DYE SENSITIZED SOLAR CELLS

SUMMARY

Each system, in order to maintain their life in the universe, requires energy. For the Mankind, there are some requirements to continue living on the planet Earth. To meet these needs, a number of devices and systems have produced. To run this system and mechanisms, initially its power used and then, more energy is needed to meet growing needs. This energy was formerly obtained from animals however, to meet the growing needs which require more energy, people turned to fossil based energy which has over time caused global warming while reducing remaining resources. In 1973, following a small-scale oil crisis research for various alternative energy sources increased rapidly. With these studies, the importance of renewable energy sources emerged and with activities in this direction, there has been rapid progress.

Alternative energy sources, especially fotovoltaic cells are getting more and more crucial in our lives as our energy need continues to increase. In this study, solar energy has been worked on as a renewable energy resource.

Although Solar Energy is clean and constant energy, amount of use is relatively low. Solar cells made from inorganic materials are quite costly. It also has limited application as they are not flexible. Because of the advantages of photovoltaic technology such as ease of change depending on the desired functionality, cheaper, high resolution and ability to apply on different types of surfaces, organic molecules with a large molecular weight have become indispensable candidates.

High molecular weight organic molecules present the following advantages: ease of adaptation according to desired property, less expensive, through resolution and ability to apply on many different surfaces. Because of photovoltaic technology

advantages, they are indispensable and will continue to be a constantly evolving candidate.

Organic photovoltaic cells based on organic material between two metal electrodes are formed by compression. The two most popular electrodes are donors (p-type) and receptors (n-type). Organic Photovoltaic Cell is produced by using them together. It also may be possible to make changes in the chemical structure of the material to increase the efficiency with additional material.

Zinc Oxide (ZnO) is a semiconductor, which has a large exciton band gap (3.37 eV). In addition, its compelling diversity in some optoelectronic properties (such as being perfectly transparent) and good conductive characteristics have enabled the use of (ZnO) in a number of application areas, such as solar cells, photodetectors and imaging devices. The piezoelectric effect in the absorbed energy has aroused considerable interest. With these features, different branches of science (such as engineering, materials science, biological sciences) have been used. It is rapid and cost-effective to obtain ZnO nano-rods and series production for nano-electronic applications. Vertically aligned ZnO nanorods in a relatively short time, were obtained by sonication method. However, expensive ZnO coated substrate is used in this method to form the ZnO seed layer thin film. In this thesis, complete in-semination by sonochemical method and ZnO nano-rod sequences will focus on the growth of the substrate. These rods can be formed on different types of substrates at room temperature and growth of the nano rod at ambient conditions by sonochemically method as compared with conventional deposition methods (Such as evaporation, Spray, Chemical Vapour Deposition) require less time.

ZnO crystals can be synthesized in the form very different structures with different physical and chemical methods such as nanorods, nanowires, nanotube and nanoflowers. In order to obtain ZnO thin films, a number of methods were used, such as laser deposition (PLD), metal organic chemical vapor deposition (MOCVD), electroplated coatings (of electrodeposition), hydrothermal, chemical bath storage (CBD) and ultrasonic methods.

In this thesis, ZnO nanorods were synthesized on Fluorine Doped Tin Oxide substrates by a simple, fast and cost efficient method. Prior to synthesis, fluorine doped tin oxide substrate was cleaned. After FTO substrate cleaning, ZnO seed layer was first deposited on the substrate by sonicating the substrate in a solution of zinc acetate dihydrate in isopropyl alcohol, before the growth of ZnO nanorods. Growth of ZnO nanorods were achieved by sonication of substrate in a solution of zinc nitrate tetrahydrate and hexamethylenetetramine in deionized water.

Several different samples were grown by changing the growth condition. The results indicated that the longer reaction time at the maximum amplitude exhibits the best result when the surface was densely coated with nanorods compared to those grown in a short time. It was also observed that the diameter of the ZnO nanorods decreased by refreshing the growth solution and increased in the continuously grown sample. The size of ZnO nanorods was also found to decrease by increasing the ultrasonic amplitude.

In this thesis, the sonochemical method is used to emphasize that ZnO nano-wires can be grown at a low cost surface as mass-manufacturable process, resulting in a reduction of production cost of electronics, optoelectronics and energy conservation practices.

SONOKİMYASAL METODLA BÜYÜTÜLMÜŞ ZNO NANO YAPILI BOYA DUYARLI GÜNEŞ PİLLERİNİN FABRİKASYONU VE ELEKTRİKSEL KARAKTERİZASYONU

ÖZET

Yaşamı çevreleyen her system, hayatını devam ettirmesi için, farklı yöntemlere başvurmuştur. Yeryüzünde yaşıyan insanlığın da, ihtiyaçlarını gidermesi, hayatını kolaylaştırması ve yaşam kalitesini arttırması için bazı sistemlere yada cihazlara ihtiyacı olmuştur. Bu sistemleri çalıştırmak, cihazları kullanabilmek için öncelikle kendi gücünü kullanmış kendi gücünün yetersiz olduğunu zamanlarda da yük hayvanlardan yararlanmıştır. Tükettiği enerji her daim artmaya devam etmiştir. Enerjiyi önceleri yük hayvanları ile gidermeye çalışsa da ihtiyacın ve çalışma sürelerinin artması, insanlığı fosil yakıtlara yöneltmiştir. Enerjiyi fosil kaynakları kullanarak elde etmiş, fakat bu seferde küresel ısınmalara sebep olmuş, hatta dünyanın dengesi bozmuştur. Bunun ötesinde fosil yakıtların fazla kullanılması limitli miktarda bulunan fosil kaynakların azalmasına da neden olmuştur. 1973 yılında petrolün arzı, talebin altında kalmış ve krizlere neden olmuştur. Bu andan sonra da küçük çapta da olsa enerji ihtiyacını karşılamak için farklı enerji kaynakları araştırılmaya başlanmıştır. Bu çalışmalar ile yenilenebilir enerji kaynaklarının kullanımı lüks değil zaruri bir durum haline gelmiştir. Bu yönde çok sayıda araştırma yapılmış etkili sonuçlar elde edilmiştir.

Enerji ihtiyacının gün geçtikçe artması sebebiyle, alternatif enerji kaynaklarının, özellikle fotovoltaik hücrelerin hayatımızdaki önemi gün geçtikçe artmaktadır. Bu çalışmada, yenilenebilir enerji kaynağı olarak güneş enerjisi ile kullanılmıştır.

Güneş enerjisinin temiz ve sürekli enerji olmasına karşın kullanıcı miktarı oldukça düşüktür. İnorganik malzemelerden yapılan güneş pilleri oldukça maliyetlidir. Ayrıca esnek olmadıkları için uygulama alanları da kısıtlıdır. Büyük molekül ağırlığına sahip organik moleküller istenen özelliğe göre kolaylıkla değişim sağlayabilmeleri,

daha ucuz olmaları, yüksek çözünürlükleri ve ayrıca farklı tip yüzeylere uygulanabilmeleri gibi avantajlarından dolayı fotovoltaik teknolojinin vazgeçilmez bir adayı olmuştur.

Organik fotovoltaik hücreler iki metal elektrot arasına organik bazlı malzemelerin sıkıştırılmasıyla oluşmaktadır. En popüler kullanılan aygıt tipi biri donör (p) diğer akseptör (n) malzemelerin birlikte kullanıldığı malzeme tipleridir. Ayrıca malzemelerin kimyasal yapılarında değişiklik yapmak mümkün olabildiği gibi ilave malzemelerle de, verimi arttırmak mümkündür.

Çinko Oksit (ZnO), geniş exciton band aralığına (3.37 eV) sahip bir yarı iletendir. Bu özelliğinin dışında, ilgi uyandıran bazı optoelektronik özelliklerindeki çeşitlilik, (mükemmel derecede transparan olması gibi), iletken karakteristiğinin iyi olması, güneş pilleri, fotodedektörler ve görüntüleme cihazları gibi, uygulama alanlarında fazlasıyla kullanılmasına olanak tanımıştır. Piezoelektrik etkisi ile, enerjinin soğurulmasında konusunda, önemli derecede ilgi uyandırmıştır. Bu özellikleri ile farklı bilimsel dallar (mühendislik, malzeme bilimi, biyolojik bilimler gibi) tarafından kullanılmaktadır. Nano-elektronik uygulamalar için, hızlı ve düşük maliyetli ZnO nano çubuk elde edilmesi ve seri imalatı önemlidir. Dikey olarak hizalanmış ZnO nanoçubuklar nispeten kısa zamanda, sonikasyon yöntemi ile elde edilmişlerdir. Fakat bu yöntemde pahalı ZnO kaplı levhalar kullanılır. Ya da üzerine ince film şeklinde ZnO tohum katmanı kaplamak gerekir. Bu tezde, sonochemical method ile tohumlama ve ZnO nano çubuk dizilerinin levha üzerine büyütülmesi üzerinde durulacaktır. Bu çubuklar, farklı türde levhalar üzerine, oluşturulabilmektedir. Nano çubukların oda sıcaklığında ve uygun çevre koşullarında büyütülmesi, geleneksel biriktirme yöntemleri ile karşılaştırıldığında (Buharlaştırma, Kimyasal Buhar Çöktürme ve Püskürtme gibi) süre olarak oldukça kısadır.

ZnO kristalleri farklı fiziksel ve kimyasal yöntemlerle çok değişik yapılarda örneğin nanoçubuk (nanorod), nanotel (nanowire), nanotüp (nanotube) ve nanoçiçek (nanoflower) şeklinde sentezlenebilir. ZnO ince filmlerin elde edilmesi için laser biriktirme (PLD), metal organik kimyasal buhar biriktirme (MOCVD), elektrolizle kaplama (electrodeposition), hidrotermal, kimyasal banyo depolama (CBD), ultrasonik gibi yöntemler kullanılabilir.

Bu tez çalışmasında, ZnO nano çubuklar uygun bir şekilde, basit, hızlı ve düşük maliyetli bir yöntem olan sono kimyasal metot kullanılarak cam alt-tabakalar üzerinde biriktirildi. Sentezleme işleminden önce FTO levha temizlendi. FTO nun temizlenme işleminden sonra ZnO tohumlama işlemi yapıldı. Bu işlem, zinc acetate dihydrate ve isopropyle alcohol solüsyonu içine FTO levhanın bırakılması ile yapıldı. FTO levha 30 dakika sonike edildi. Daha sonra zinc nitrate tetrahydrate ve

hexamethylenetetraimine karışımı iyonsuzlaştırılmış su içine çözüldü. ZnO tohum kaplanmış FTO levha üzerine, yine ultrasonik sonikasyon yöntemi kullanılarak, ZnO nano çubukların büyütülmesi işlemi yapıldı.

Değişik büyütme şartlarında farklı örnekler büyütüldü. Sonuçlar, yüksek genlikteki uzun reaksiyon süresinde yapılan biriktirmeler, düşük genlikte ve kısa sürede yapılanlara kıyasla daha iyi sonuçlar sergilemiştir. Yüzeyle yoğun kaplanmıştır. ZnO nanotellerin çapının, büyütme solüsyonunun sık değiştirilmesiyle azaldığı ve solüsyonda sürekli büyütme yapıldığında ise arttığı görülmüştür. Yine ZnO nanotellerin şekli ultrasonic genlikte yapılan arttırma/azaltma ile değiştiği anlaşılmıştır.

Bu tezde, sonochemical yönteminin basit olduğu, seri üretimin hızlı yapılabileceği vurgulanmıştır. ZnO nanotellerin düşük maliyetli yüzeylerde büyütülebilir olması, üretim maliyetinin azalmasına ve sonuçta elektronikte, optoelektronikte ve enerji dönüşüm uygulamalarında kullanılan malzemelerin üretim maliyetini düşürebileceği anlaşılmıştır.

1. INTRODUCTION

In a globalized world, the demand for energy continues to grow rapidly. The need to find alternative sources of energy has emerged with increasing demand for energy, but reduction in the use of fossil fuels does not seem possible.

Fossil fuel resources, the most widely used sources of energy, are being depleted rapidly. Forecasts say they will run out entirely circa 2050^[1].

Moreover; use of conventional fossil fuels that have been formed over centuries produce harmful greenhouse gases such as CO₂, SO₂, NO₂, CO leading to a environmental problems such as global warming.

In this context, renewable energy sources are needed to meet the ever growing energy need globally.

1.1 Energy

Development level of a state is marked by different parameters. For example; in a developing society there is an increase in energy use per capita. The need for energy began with the mankind and continues to increase. In particular, increased uses of technological devices have led to the increase in the amount of energy consumed per capita.

1.1.1 Renewable Energy Sources

Energy is one of the primary necessities for daily life and it is indispensable. According to the latest data, humans all around the world consume 13 terawatts (13 trillion watts) of power^[2]. Moreover, by 2050 more than 30 terabytes will be needed as a result of increasing population, growing industry and technology all over the world^[2]. This need for energy is met mostly by fossil fuels and nuclear energy (78% of the energy demand) releasing carbon dioxide and strengthening the greenhouse effect that triggers global warming. As these sources are not renewable, their cost of production increases with increased consumption rates. Soon, fossil fuels will not be

enough to meet the need. The small non-fossil energy sources, such as biomass, hydro and geothermal sources cannot provide sufficient output and their production cost is high.

Produced electricity, fuels, nuclear energy and other small energy sources consumption graph is shown in Figure 1.1 [3]. The energy problem has forced scientists and industry to discover new, clean and cheap energy sources. The most likely renewable energy source is solar cells which directly convert sunlight to electricity.

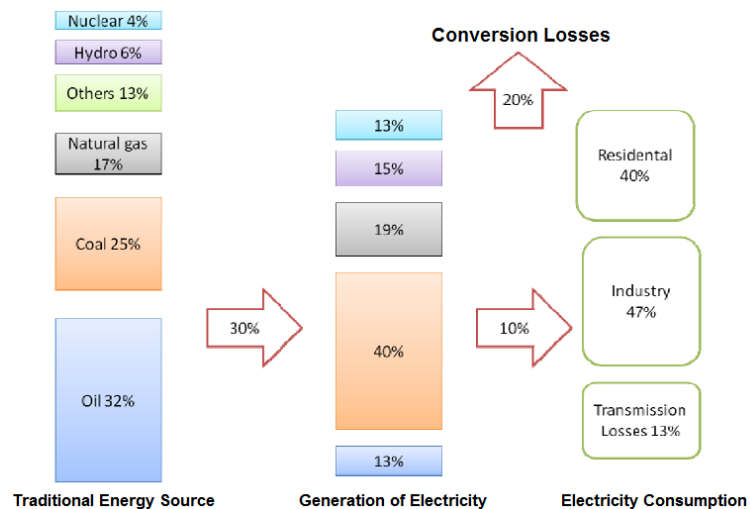


Figure 1-1. Generation of Electricity and Consumption Rates of Common Energy Sources [3].

Non-fossil (coal, oil and carbon derivatives) origin renewable energy sources, which do not require any production process but are available in nature, can be used to produce electric energy with much lower CO₂ emission creating less impact on the environment compared to conventional energy sources. Renewable energy sources such as hydrogen, wind, solar, geothermal, biomass, biogas, wave, and tidal stream energy are readily available in nature permanently replaced through recycling.

Table 1-1: Renewable Energy Resources

	Renewable Energy Resources	Source or Fuel
1	Solar Energy	Sun
2	Wind Energy	Wind
3	Wave Energy	Oceans and Seas
4	Biomass Energy	Biological Waste
5	Geothermal Energy	Groundwater
6	Hydropower	Rivers
7	Hydrogen Energy	Water and Hydroxyls

Energy is obtained from constantly recurring sources such as solar and wind energy and it can naturally renew itself in a short time. Thus, there is no concern for renewable energy sources to be exhausted. Examples for this type of energy include hydropower, wind, biomass and solar energy. Currently, about 20% of the world's electricity is produced using renewable energy sources^[3].

1.1.1.1 Solar Energy

Since the discovery of Silicon-based solar cells in 1954, the conversion of solar energy into electrical energy is used as an alternative energy source^[4].

However; silicon-based solar cells have not presented an alternative energy source due to its long and costly production process and high energy consumption^[5].

Prof. Gratzel blends high conductivity of the inorganic materials with ease of manufacture of organic materials under the name of a new concept “dye-sensitized solar cells”^[6].

Containing liquid electrolyte in its structure photoelectrochemical solar cell efficiency has reached the level of 11%^[7].

The main disadvantage of this new type of solar cell is the need to contain the volatile liquid electrolyte in the structure. Although there have been studies on the electrolyte, the obtained yield is not yet compete to the level with inorganic solar cells.

➤ **The effects of efficiency using dye on solar cells.**

Low mobility and morphology problems in volume heterojunction type cells have been overcome by the inorganic semiconductor coated with organic material and using the electrolyte solution containing redox pairs in dye sensitizing solar cell device^[8].

By realization of the exciton dissociation of inorganic semiconductors with organic material, the electron gap junction is minimized. Load transport occurs between quite high conductivity series, inorganic semiconductor and the electrolyte solution.

Porous structure and electron transport layer of nanoscale features form the center of the system. Moreover; the electron transport layer doped with fluorine, which is growing on oxide layer, allows for the transparent electrode function.

The most productive inorganic oxide which interfaces with the donor featured dye is ZnO wurtzite structure layer. Dye is connected to the film surface in a single layer nanocrystals. Dye is stimulated while photon and an electron pass into conduction band of inorganic material.

The original structure of the dye is preserved by the electron transfer from electrolyte, which consists of generally iodine / iodide solution to the dye. The renewal of iodine occurs by reduction on platinum which is coated counter electrode.

Cycle by the movement of electrons in the external circuit is completed. Voltage output meets the difference between the Fermi level of ZnO and the redox potential of the electrolyte(V_{OC}).

As a result, the system produces electricity without a permanent chemical change. Dye Sensitizing Solar Cell performance is good, despite the restrictions imposed by the liquid electrolyte in the volatile property.(~11%)

1.2 Purpose of Thesis

Although solar energy is clean and renewable, the amount of use is relatively low. Currently, widely used solar cells, which is made of inorganic material is quite costly. Hence, they are not flexible and application areas are limited.

The primary objective of the photovoltaic system is not only to increase efficiency.

Reducing cost of production will lead to widespread use. Use of low cost production techniques will reduce production cost. When solar cells produced under reduced pressure and at low temperatures, the decrease in cost can be achieved. The short production process is a reason for reducing the of cost production. Preferring a system that doesn not produce toxic waste is an important factor for the environment. Therefore, during production the use of alcohol or water-based materials alone have been preferred.

The method I used in my thesis meets the conditions mentioned above. Moreover, Sonochemical system setup is not complicated compared to other growth techniques.

DSSC solar cells were made in different ways. Hydrothermal method has become an increasingly popular method. However, Somochemically grown ZnO nanorod use in DSSCs is a novel application, which led me to choose it as my thesis topic.

1.3 Literature Review

Articles, utilizing the properties of ZnO thin films of ZnO applications were mentioned. Some of these are shown below.

ZnO nanowire grown by sonochemical method was demonstrated. Prior to the nanowire growth, a ZnO seed layer was deposited to increase nanowire density^[9].

Using ZnO thin films electrode in an aqueous solution of zinc nitrate, ITO is covered, with the electrodeposition method and porous ZnO films were obtained. It is reported to give high transmittance of 60% following pore formation^[10].

By chemical vapor deposition method, ZnO films grown on substrate, the obtained films were reported to have high electrical conductivity^[10].

ZnO porous structure of the photo response is very fast and a very high efficiency of electron collection is indicated^[11].

Using the chemical bath deposition method, Approximately 100 nm thin ZnO films were grown on the silicon solar cells at 80 ° C. An increase in the average conversion efficiency was observed^[12].

Nanorods are obtained with different morphologies by the chemical bath growth method. It was observed that temperature and pH affect their morphology. With increasing pH, it is determined that the cluster size increases^[13]

TiO₂ and ZnO are preferred for solar cell applications due to their highly compatible thermodynamics, kinetics and charge carrier properties. TiO₂ and ZnO-based solar cells, in terms of electron transport properties and productivity, have been compared with the current literature^[14].

1.4 Hypothesis

In this thesis, using Sonochemically grown ZnO nano-rods, I will focus on fabrication of dye-sensitized solar cells and electrical characterization. I will compare power conversion efficiency of each device obtained in a different way.

Using different amounts of materials and changing the applied method under different temperatures, pH values and in different concentrations of components I will try to increase the surface of the nano-rods.

Expanding the surface of the nanorods is considered to increase efficiency.

1.5 Nanotechnology Concept

Nanotechnology assumes a role in the nanoscale such as material and electronics production by forming small groups of atoms. Nanotechnology in the nanometer size range (1-100 nanometers) is used to control the material.

Properties of nano materials characteristics are different to the properties of individual atoms, molecules and bulk material properties. Advanced materials used in devices and systems can take advantage of these new features. Nanoscale science, engineering and technology (including nanotechnology), is used in length scale imaging, measuring, modeling, and manipulating the subject.

One-dimensional semiconductor nanostructures (1D) is of great interest for applications such as nanoelectronics and optoelectronics, due to their unusual properties based on nanometer-scale dimension.

Zinc oxide (ZnO) as most important feature serves as the multi-purpose semiconductor. It has a wide direct energy band gap of 3.37 eV, piezoelectric and pyroelectric good transparency, high luminescence at room temperature and its exciton binding energy is very large (about 60 meV).

Based on its unique physical and chemical properties of ZnO nanostructures a great effort has been spent in the field of engineering, material science for their potential applications in electronic, optoelectronic and biomedical devices such as photo detectors.

Examining the most common analytical performance of the ZnO nanostructures, high detection capability and high electron mobility are widely explored for sensor application, such as gas detectors, pH and temperature sensors and biosensors for intracellular measurements. 1D ZnO nanostructures have been the subject of intense scrutiny in the field of emitter electrodes for solar cells, nanolasers, field-effect transistors etc.

Techniques such as Chemical Vapour Deposition, Vapour Liquid Solid, Metal-Organic Chemical Vapour Deposition, Pulse Laser Deposition and hydrothermal technique are used in a variety of applications for well aligned ZnO nanostructures like single crystal, 1-D nanostructures.

Vapor phase techniques are very expensive and require complex mechanisms. Because this technique requires a complex infrastructure, high growth temperature of up to 1400 °C, low pressure, and suitable substrate selection in MBE and MOCVD are required.

Conventional Vapour Phase Techniques are widely used for the expression of different ZnO nanostructures. Solution-based methods are relatively simple and they require a lower temperature compared to vapor phase method (< 200⁰C). The long reaction time required usually few hours a day is a major disadvantage for solution based methods.

2. THEORY

2.1 Photovoltaic Solar Cell

This is the most common method used to convert solar energy directly into electrical energy with photovoltaic cell technology. Photovoltaic cells given in fig 2.1 are made from semiconductor material and the sun light shed on it is generates electricity in electronic devices. Solar energy makes 62,500 MWh/m² energy oscillations in one second. Thus, it is an endless and reliable energy source. Ways to obtain energy from the sun and increasing productivity for existing systems continue to be investigated.

Photovoltaic event occurs in the order described below.

- Photovoltaic effect is created inside a semiconductor material such as silicium.
- Solar cells (Photocells) consist of two semiconductor layers (P and N layers).
- One of these layers enables the removal of electrons by light exposure.
- Free electron is attracted by the other positive layer. And at the same time movement of the holes starts towards the opposite direction.
- In this way, electrons and the holes create an electric current.
- The intensity of light absorbed from the sun is directly proportional to the electric current produced.

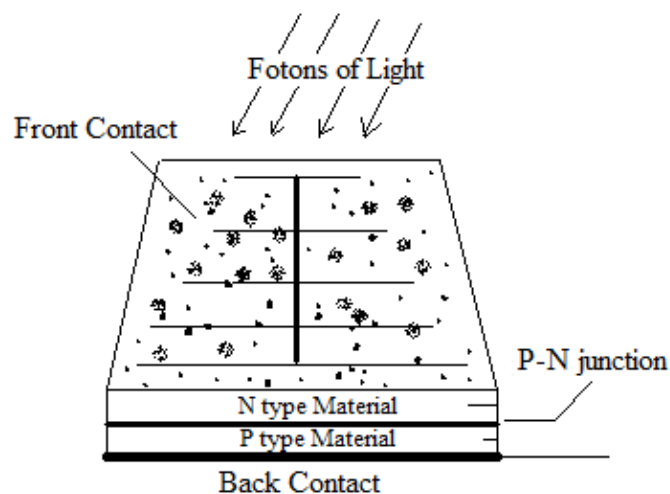


Figure 2-1: Fotovoltaic Solar Cell

2.1.1 Classification of Photovoltaic Cells

Photovoltaic cells are mainly divided into three groups.

- I. 1st Generation
 - Single-crystal Si
 - Multi-crystalline Si

The first generation photovoltaic cells made with monocrystalline or polycrystalline silicon with cut into thin slices and dopings are made. The photovoltaic cell market now constitute almost 90%.

- II. 2nd Generation (low cost-of Thin Film Technology)
 - Amorphous Si
 - Si Thin Film
 - CuInSe₂
 - CdTe

Coating extremely thin layers using photovoltaic cell modules on glass, plastic, metal surfaces present a low-cost support on the photo-sensitive material. This method allows for the production of lower-cost photovoltaic cell although with lower efficiency compared to silicon-based photovoltaic cells. Still, its low cost and fast production have resulted in an increase in its use.

- III. 3rd Generation
 - Organic dye sensitized solar cells
 - Plastic Solar Cells (molecular and polymeric)
 - High-efficiency multi junction tandem solar cells
 - Hot electron converters
 - Quantum dot solar cells
 - Multiple Exciton generation (MEG)
 - Intermediate band solar cells (with intermediate band solar cells)

Third generation solar cell has been developed to increase efficiency in the photovoltaic cell.

2.1.2 Semiconductor Technology

Metal is a very good carrier of electricity and is called conductor. Very poor conductor of electricity is called insulator and metal with lower conductivity (which is between conductor and insulator) is called semiconductor. Copper and aluminium are good examples of a conductor. Diamond, wood, glass are the examples of an

insulator. Silicon and germanium are the examples of a semiconductor, which does not conduct current at low temperatures. When the temperature is increased, it behaves like a good conductor.

According to the Pauli principle, each energy level of the atom, having at most two opposite oriented spins of electrons, can be accommodated. In semiconductor material, atoms are too close. With the influence of strong electric field, adjacent atoms of valence electron band energy level is divided in the form of electron energy bands on the last orbit made up of valence electrons called the valence band. Valence electron excitation level of the atom is called a conduction band. There is a band gap between the conduction and the valence bands.

2.1.2.1 Intrinsic Semiconductors

Sample of semiconductor in its purest form is called an intrinsic semiconductor. The impurity content in intrinsic semiconductor is very small, of the order of one part in 100 million parts of semiconductor. For achieving such a pure form, the semiconductor materials are carefully refined. Intrinsic semiconductors behave as perfect insulator in absolute zero temperature. At room temperature, the numbers of valence electrons absorb thermal energy due to which they break the covalent bond and drift to the conduction band. Such electrons become free to move in the crystal.

2.1.2.2 Extrinsic Semiconductors

In order to change the properties of intrinsic semiconductor a small amount of new material is added to it. The process of adding another material to the intrinsic semiconductor crystal to improve conductivity is called doping. The added impurity is called dopant. Doped semiconductor material is called extrinsic semiconductor. Depending on the type of impurities, extrinsic semiconductors are classified into two groups.

1. n-type
- 2.p-type

Electron doped atoms in semiconductors are called donors. Donor characterized semiconductor in the additives is called **n-type** semiconductor. Electron doped atoms are called acceptors. Conductivity, determined by the acceptor-type semiconductor contributions is defined as **p-type** semiconductor. Majority of charge carriers in N type semiconductors are electrons while holes assume this role in P-type semiconductors.

2.1.3 PN Junction

P-N junctions widely used in photovoltaic cells are established with the doped semiconductor structure. Doped semiconductor conductivity can be increased. Silicon (Si) atoms as a pure semiconductor crystal, jointly establish a bond using the four valence electrons. Crystal structure of phosphorus (P) as the fifth valence electron atoms, when added in small amounts, creates additional electrons by contributing to the system. These electrons are only under the influence of their atomic nuclei, transmission more easily passed and excess electrons in the doped structure takes n-type semiconductor name. The reverse operation creates p-type semiconductor. In the p-type, Boron (B) with three valence electrons is added in pure structure. There is a need for electrons for additional atoms to bond. In this case the system constitutes electron gaps. Moving each electron to fill all gaps, leaving behind a space. N type semiconductor transmission is done by electron, while the p-type occurs by spaces.

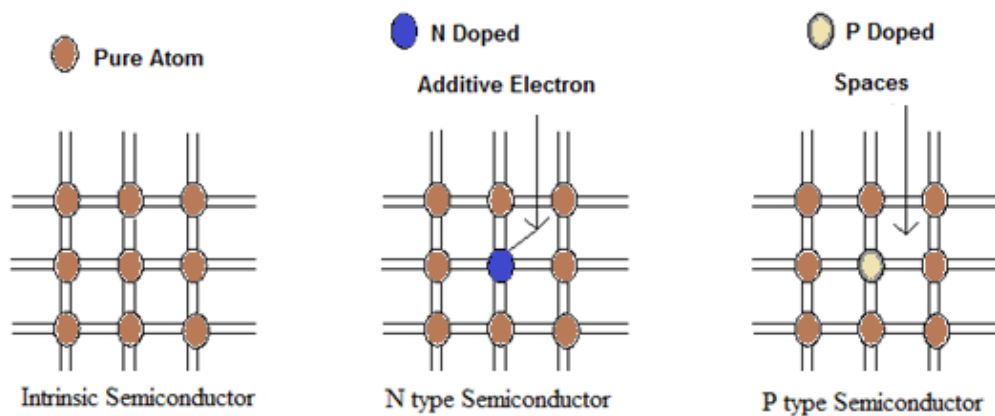


Figure 2-2: Pure and Doped Semiconductor Bonding

2.1.4 Advantages of Photovoltaic Systems

Advantages of photovoltaic systems can be listed as follows;

- They are economic, maintenance cost is almost zero due to the lack of moving parts.
- There is no harm to the environment.
- Fuel not use, do not have any waste.
- Snow, rain, hail are not affected by such climatic events.
- They are installed close to the consumption site, so there is no need for long wiring for installation.
- Can work in modules, so power output can be increased as desired.

2.1.5 Disadvantages of Photovoltaic Systems

- Huge power is required to be produced, requires very large area compared to other systems.
- Do not produce energy in the evening where there is no radiation. Therefore, it needs to storage system independent from the network structure.
- They are brittle batteries need to be framed.
- Photovoltaic cells have a higher cost because they require high production technology.

2.1.6 Stages of Development of Photovoltaic Cells

In 1839, Edmond Becquerel observed light falling on the electrolyte generated a voltage between the electrodes and discovered the photovoltaic event.

In 1876, a similar phenomenon in solids was discovered by GW Adams and RE Day who were working on selenium crystals. By 1914, the efficiency of photovoltaic diodes reached the level of 1%. In 1954, energy efficiency of photovoltaic diodes converting solar energy into electrical energy reached 6% for the first time on silicon crystal. Until early 1970s, such studies were limited to the applications of photovoltaic cells. Photovoltaic cells to be used as an electrical power system began in 1973. National renewable energy laboratory was opened in 1977 in the United States. Worldwide photovoltaic cell production was up to 21.3 MW. By 2010, battery efficiency reached 42%.

Table 1-2: Historical Development of Photovoltaic Cells ^[15]

DATE	PERSON	EVENTS
1839	Henry Becquerel	Discovered photovoltaic effect
1873	Willoughby Smith,	Found photovoltaic effect of selenium.
1876	Adams and Day	Discovered solid selenium photovoltaic effect.
1883	Charles Fritts	Described the first solar cells made from selenium layer.
1904	Hallwachs	Copper is sensitive to light, found.
1905	Albert Einstein	Hallwachs' s findings of the photoelectric effect published.
1916	Millikan	The photoelectric effect was demonstrated experimentally
1918	Polish scientists	Developed technology to produce a single crystalline silicon cell.
1951		A single crystalline structure obtained from Germanium was manufactured.
1954		Cadmium photovoltaic effect was reported.
1954	Chapin and Fuller	Produced the first working silicon solar cells with 4.5% efficiency.
1958	Kearns and Calvin	While working with Magnesium phthalocyanine (mgpc), measured photo voltage of 200mV,
1986	Tang	The first multi-jointed photovoltaic cells were produced.
1991	Hiromoto	First dye additive multi jointed solar cells made.
1993	N.Serdar Sarıçiftçi	Produced the first polymer / C60 organic solar cells.
1994	Yu	Produced the first stack of very articulated solar cells.
1995	Yu/Hall	Produced the first polymer / polymer stack, building of organic solar cells.
2000	Peters/van Hal	Used Oligomer / C60 's active material in photovoltaic cells.

2.1.7 Electrical Parameters of Photovoltaic Solar Cells

The parameters of Photovoltaic cells decide the performance of DSSCs. Six parameters come to the fore.

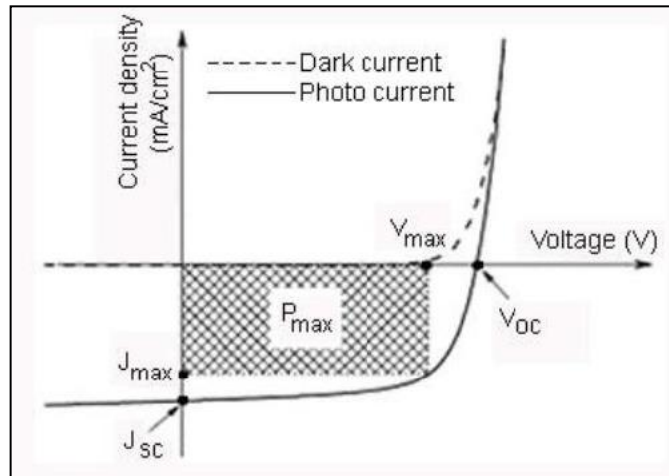


Figure 2-3: Used Parameters by The Solar Cell ^[10].

2.1.7.3 Open Circuit Voltage (V_{oc})

The open circuit voltage (V_{oc}) is defined as the electric potential difference between two electrodes called anode and cathode. There is no current flow when the circuit is opened. This electrical potential difference represents the energy gap between the semiconductor's fermi level and electrolyte redox potential. High voltage is produced by an open circuit voltage of the device. Metal contacts (ITO, Al, etc.) and the material used as the active layer may vary depending on the feature.

2.1.7.4 Short Circuit Current (J_{sc}) :

Current density obtained by short-circuiting the terminal pins of the DSSC cells under light refers to the short-circuit current density. Hence, there will be no electrical inductans on the way of electron flow and maximum current will be obtained from the device. Factors such as light intensity, wavelength, etc. are important parameters in the design of solar cells.

2.1.7.5 Fill Factor (FF)

Another important parameter is the fill factor(FF), defined as the ratio between maximum power (V_m and I_m) and the theoretical power values (V_{oc} and I_{sc}). The closer the Fill Factor is to 1, the more efficient the solar cell. Maximum power is produced.

$$FF = \frac{I_m V_m}{J_{SC} V_{OC}} \quad (2.1)$$

2.1.7.6 Maximum Power Point (P_{MAX})

Is the point at which maximum current and voltage under load of a given amount of light.

$$P_m = V_m \cdot I_m [W] \quad (2.2)$$

2.1.7.7 Efficiency (Power Conversion Efficiency)

It is defined as multiplication of FF and the ratio of theoretical electrical output power to incident sunlight power per unit area.

$$\eta = \frac{P_{max}}{P_{light}} = \frac{J_{sc} * V_{oc} * FF}{P_{light}} \quad (2.3)$$

2.1.7.8 Solar Spectrum

Air mass is the path on which the rays of sunlight pass through the atmosphere. The path of the incoming radiation perpendicular to the ground is called the zenith line.

θ angle of incidence angle and AM eqn $\frac{1}{\cos \theta}$ is defined.

Where Theta (θ) is equals to 48 degree, the value of AM equal 1.5

In the solar simulator, all electronic measurements are based on AM equal 1.5

In Figure 2.4 shows Solar Radiation Spectrum.

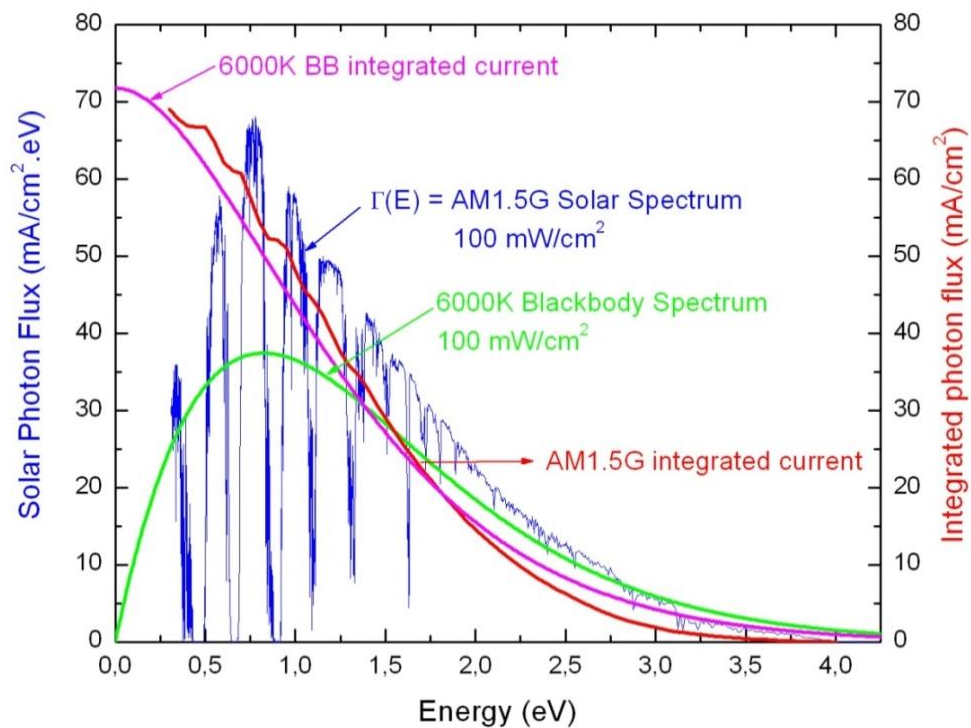


Figure 2-4: Solar Radiation Spectrum^[16].

2.2 Dye Sensitized Solar Cell (DSSC)

Michael Grätzel and O'Regan were developed by the body of DSSC in 1991. Observed in plants, working with photoelectron-chemical mechanism, this feature of the dye-sensitized solar cells is called artificial photosynthesis. Dye sensitized solar cell is a device that absorbs organic molecule layer of sun light to directly convert it into electrical energy. Third-generation solar cells are now arising as an alternative to conventional solar cells. Solar cells are included in the group of photovoltaic cells. Sensitization to the Photo electrode was first reported by Moser^[17]. Previously, by using the dyes of wide band gap semiconductor had been sensitized to visible region. The photo-electrochemical cells produced in the previous study presented very low effectiveness.

Single sensitized crystal semiconductor surface yield is very low compared to the results of a single layer of dye and the amount of absorbed light is minimal. A single crystal electrode surface was sensitized with multiple dye layers to absorb more light. This was one of the alternatives. However, the use of multiple dye layers did not contribute to current production.

The outermost layer of the dye molecules act as filters to prevent the absorption of light by the dye molecules in the substrate. For this purpose, nanocrystalline layer is used instead of a single crystal layer. Grätzel and O'Regan reported 7% efficiency in solar cells, in 1991^[18]. Today, the yield has reached 11%^[19].

Table 2-1: Efficiency Comparasion of Well-Known Solar Cell^[20]

Cell Type	Efficiency (%)	Research Needs
Crystalline Silicon	24	Higher production yield
Multicrystalline solid	18	Manufacturing cost
Amorphous Silicon	13	Lowering cost, product stability
CuInSe ₂	19	Finding replacement for Indium
DSSC-liquid electrolte	10-11	Improve efficiency and stability
DSSC-Solid State	4-5	Improve efficiency and Stability

2.2.1 DSSC Working Scheme

DSSC starts to work by light absorbed dye molecules through on the ZnO nanorods. Light-absorbing dyes become excited and induced dye molecule transmits an electron to the conduction band of ZnO. Electrons reach transparent electrode throughout the nano-crystalline ZnO film network and they are transmitted to the external circuit. Dye cations with the passage of electrons to the conduction band of ZnO are reduced to neutral by the electrolyte containing redox pairs. The oxidized electrolyte is reduced by electrons from the platinum-coated electrodes through the out-circuit. This way, net charge is always zero during operation of the organic dye-based solar cells. Consequently, chemical changes do not occur. At the end of the electron transfer processes, photo-current occurs. To achieve continuous current of organic dye-based solar cells, oxidation-reduction process be must continually repeated.

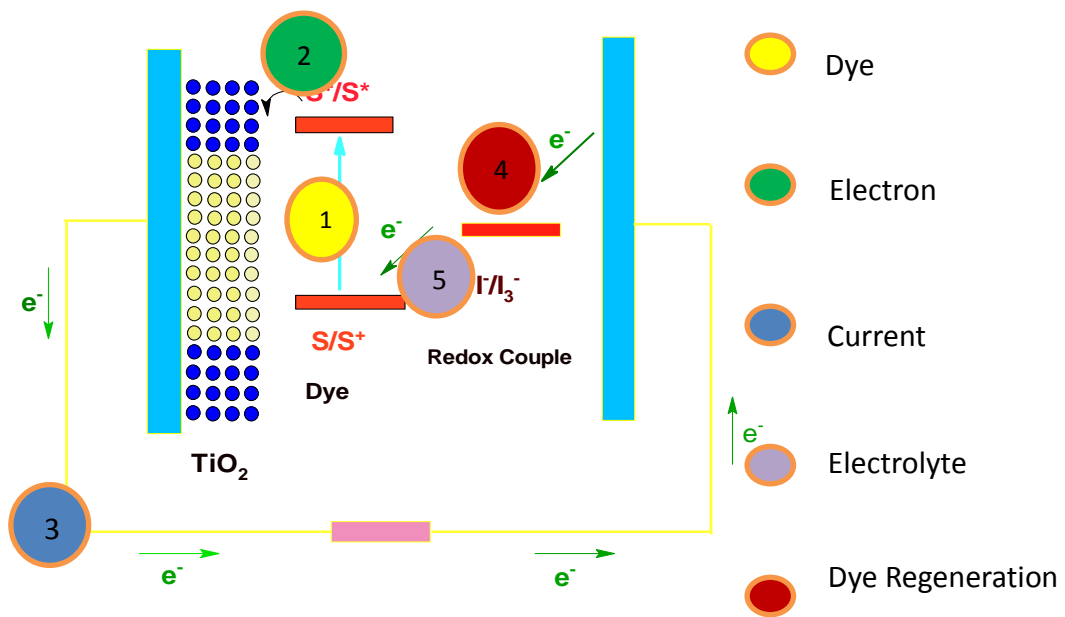


Figure 2-5: DSSC Working Scheme

2.2.2 Used Dyes in Solar Cells;

- A wide variety of dyes are used in organic dye-based solar cells, (DSSC).
- Porphyrin, phthalocyanine, polipiridil, coumarin, indoline, triphenylamine, conjugated polymers, perylenes are among the dye classes used.
- Organic dyes have a higher molar absorption coefficient based on ruthenium chromophore. It is possible to synthesize the dye to achieve desired absorption range.

Dyes are used in organic dye-based solar cells. Some of the basic features should include the ability to convert light energy into high efficiency electric energy:

1. Dye (368nm) absorption is sufficient for single-layer solar cells to provide bandwidth 3.37 eV.
2. Dye should make strong adsorption on semiconductor surfaces.
3. The dye should have good solubility and contain a functional group that may be binding to the semiconductor surface.
4. In light of the solar cell, only to be absorbed in the dye layer is desired. Otherwise, side reactions may adversely affect the battery performance and stability.



Figure 2-6: Ruthenium Dye II (Z907)

2.2.3 Advantages of DSSC;

1. Can work in low light conditions.
2. Can be applied to flexible substrates.
3. Continuous / spot adapted to production conditions.
4. Stable and lighter structure.

2.2.4 Disadvantages of DSSC;

1. Liquid electrolytes create the problem of temperature stability.
2. Volatile organic compounds contained in the liquid electrolyte materials pose a threat to human health and the environment.

2.2.5 Traditional “Gratzel Type” DSSCs

Traditional Gratzel type dye-sensitized solar cells are photo-anode and photo inert electrodes (cathode) with two electrodes. These two electrodes sandwich a liquid electrolyte. This electrolyte provides electrical conductivity and charge recombination.

DSSCs typical ionic electrolyte solutions contain free ions. In most conventional DSSC, redox couples are used as liquid electrolyte in a solution ^[21-27]. Five main ingredients are used to set up the device (Figure 2.5). First is fluorine doped tin oxide (FTO), classified as conductive and transparent oxide (TCO). Second material is a nanocrystalline titanium oxide (TiO₂) thin film as a semiconductor. It is largely preferred for its low price, ease of production, being in the visible light range, absence of any toxic materials and optical excellence ^[28]. Third component is a dye sensitizer. The fourth is an electrolyte, in other words a redox couple. The last two materials work as counter electrode, which is platinum coated on glass substrate. On the side of photo-anode, there exists dye as a sensitizer adsorbed on TiO₂ and FTO covered by TiO₂ – dye complex. The outermost layer is FTO. Semiconductor thickness is about 7-10 nm.

2.2.6 Solid State DSSCs

Liquid electrolyte based DSSCs have leakage and solvent evaporation problems which limit practical and commercial use of these cells ^[29]. Solid state DSSCs were introduced to eliminate the disadvantages of liquid electrolyte.

The main difference between liquid electrolyte and solid state DSSCs is that (I/I₃⁺) redox couple and solid state hole-transport material (HTM), have been relocated. ^[30,31]

In this regard, organic compounds ^[32] and p-type semiconductors ^[33] were used. Solid state DSSC mainly consists of a fluorine doped tin oxide (FTO), blocking TiO₂ layer, semiconductor (mesoporous TiO₂) ^[34], sensitizer dye chemisorbed on semiconductor, hole transport material and a gold counter electrode.

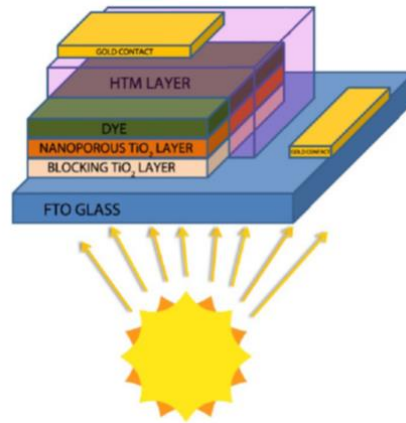


Figure 2-7: Component of Solid-State Dye Sensitized Solar Cell ^[29].

Solid-state DSSC is the alternative to solvent-free dye-sensitized solar cells. It presents practical use and eliminates some of the disadvantages of conventional DSSC. On the other hand, electrical conversion efficiency of sunlight is lower than traditional DSSCs^[35,36]. This lower yield is due to two problems. First, solid-state DSSC thickness is about 4-5 microns, limiting the absorption of the dye and resulting in a retention of less sunlight^[37]. Secondly, HTM based DSSCs electron diffusion length is shorter than a liquid electrolyte based DSSC^[38,42].

2.3 Metal Oxide Nanostructures and Their Applications

Metal oxide nano structures have provided a significant benefit in different application areas. In particular, the production of energy and storage, Lithium ion batteries^[43-47], fuel cells^[48-52], solar cell applications^[53-57], light emitting devices (LEDs)^[58-60], transistor / FET^[61-64] has been very important developments. These benefits are possible in view of different applications.

Such as hydrogen production by water photolysis, air or water to clean the toxic waste applications^[65-69], environmental effects monitoring in applications gas, humidity, temperature. Environmental monitoring by their applications in the fabrication of gas, humidity and temperature sensors^[70-74], UV-screening^[75,76] and photodetectors^[77-79], used as magnetic read, write heads and data storage devices^[80,81], transition metal doped active oxides ZnO, CuO, TiO₂, Al₂O₃^[82-84] are called diluted magnetic semiconductors (DMS) in the fabrication of spin based electronic devices, Phosphor materials for fabrication of LEDs, displays and laser materials^[85-89].

Metal oxides are used in the construction of expensive electronic devices and ICs. Dual semiconducting oxides ZnO, TiO₂, CuO₂/Cu₂O, SnO₂, In₂O₃, and CdO have distinctive features ve they are used as transparent conducting oxide materials ^[90,91] and sensors. Indium-doped tin oxide (In:SnO₂, ITO) is a suitable material for flat panel displays due to high electrical conductivity and optical transparency ^[92-94], futher more because of its lower cost and easier etchability ZnO is regarded as an ideal alternative material for ITO ^[95].

2.3.1 Zinc Oxide (ZnO)

There are lots of nanostructures of ZnO include nanowires, nanobelts, nanorods, nanotubes and nano-tetrapods. Zinc Oxide (ZnO) is an important semiconductor for different applications due to its good transparency, excellent sensitivity, strong room-temperature luminescence, versatility, reliability, high electron mobility and extreme low-cost. Benefits of the property of the semiconductor material, the interest in the scientific community has led to a further increase.

Instead of the material like Si and GaN can be obtained more cheaper zinc oxide material considerable interest has attracted.

Zinc oxide is an n- type material and it has wide band gap semiconductor material using several applications in UV/blue optoelectronics, transparent electronics, spintronics and sensor applications.

Zinc oxide in bulk polycrystalline form has been commonly used in a wide range of applications; such as lubricant additives, paint pigments, piezoelectric transducers, varistors, and as a transparent conducting electrodes.Its makes transparency in the visible region; because of that it has direct band gap energy of 3.37eV and most of the activity in the UV/blue region. When the binding energy compared to GaN (~ 24 meV) and zinc oxide (~ 60 meV), high exciton increases the brightness efficiency. The electrical properties of ZnO nanostructures is more important for their applications especially in nanoelectronics. ZnO nanowires and nanorods are carried out in the electrical transport measurements. ZnO is a semiconductor which has a wide band gap binding energy between 3.37 eV and 60 meV at room temperature. Because of this, it has advantages in high breakdown voltages, ability to sustain large electric fields, low electronic noise, high-temperature, and high-power operation.

Zinc oxide has lots of other specialties; ZnO can grow easily in single-crystal surface it has a low threshold and in compliance with the bio structure. Zinc oxide is widely used for the fabrication of transistors and FETs , dye sensitized hybrid and quantum dot solar cells, light emitting diodes.

2.3.1.9 ZnO Crystal Structures

Zinc oxide at normal pressure and temperature, exhibits wurtzite oxide crystal structure, which is the hexagonal lattice with space. Moreover, Zincblende and Rocksalt structures are available.

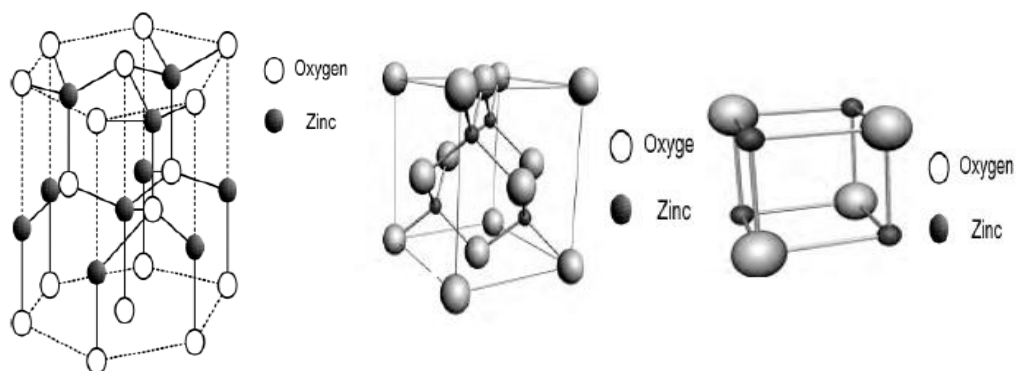


Figure 2-8: ZnO Crystal Structures a.Wurtzite b. Zincblende c. Zincblende Rocksalt

Zinc oxide lattice structure is a combination of the two sub lattices (Zn^{2+} and O^{2-}). In each corner of zinc atoms are surrounded by oxygen atoms tetrahedron. Wurtzite zinc oxide has four common face terminations having Zn^{2+} and O^{2-} polar surfaces and non-polar surfaces containing equal number of zinc and oxygen atoms.

Because of the polar nature of zinc oxide, it shows different properties such as piezoelectricity, which is responsible for its application as nanogenerators. Zinc oxide nanostructures with dimensions may change the physical properties. For example, the quantum restriction of ZnO improves the one-dimensional (1D) band gap energy, which has been confirmed by photoluminescence band gap of ZnO nanoparticles and shows that depending on the size.

X-ray absorption spectroscopy and scanning photoelectron microscope shows that the surface condition increases with reduction of the size of the ZnO nanorods^[96].

Physical properties of zinc oxide are tabulated in Table 2.2.

Table 2-2: Basic Properties Wurtzite Type of ZnO ^[97] .

Properties of ZnO	
Crystal Structure	Hexagonal, Wurtzite
Molecular Weight	Zn:65.38, O:16 and ZnO:81.38
Lattice Constant	a = 3.246 Å, c = 5.207 Å
Density	5.67 g/cm ³ or 4.21 x 10 ¹⁹ ZnO molecules/mm ³
Cohesive Energy	E _{coh} = 1.89 eV
Melting Point	T _m = 2250 K under pressure
Heat of Fusion	4, 470 cal/mole
Thermal Conductivity	25 W/mK at 20 °C
Thermal Expansion Coefficient	4.3x10 ⁻⁶ /K at 20 °C, 7.7x10 ⁻⁶ /K at 600 °C
Band Gap at RT	3.37 eV
Refractive Index	2.008
Electron and Hole Effective Mass	m _e [*] = 0.28, m _h [*] = 0.59
Debye Temperature	370 K
Lattice Energy	964 kcal/mole
Dielectric Constant	ε ₀ = 8.75, ε _∞ = 3.75
Exciton Binding Energy	E _b = 60 meV
Piezoelectric Coefficient	D ₃₃ = 12 pC/N

2.3.2 Growth and Charazterization Techniques For ZnO Nanorods

There are several growth techniques used in order to growth ZnO nanostructure.

These techniques can be divided into three groups. (a) a wet process, (b) a solid-state processing, and (c) vapor-phase processing routes

Wet processing such as, hydrothermal and sonochemistry techniques to grow ZnO nanoparticles in an aqueous solution. Solidstate chemical reaction techniques are applying to solid-state processing routes for the growth of ZnO. The vapor-phase processing routes such as, molecular beam epitaxy (MBE), RF (Radio Frequency) sputtering, aerosol, thermal evaporation and chemical vapor deposition (CVD) techniques are used in order to grow ZnO nanostructures ^[98].

2.3.2.1 Physical Vapor Deposition

Physical vapor deposition (PVD) is a kind of vacuum deposition and physical vapor deposition is a general term used to describe the various methods used to produce thin films by the condensation of a vaporized form of the material onto surface of various substrates.

Coating method involves purely physical processes. For example, high temperature vacuum evaporation or plasma sputter bombardment. There are different PVD techniques which are synthesis of zinc oxide thin films or for obtaining nanostructured materials. These are thermal evaporation or evaporation deposition, electron beam physical vapor deposition, sputtering (magnetron and RF sputtering), cathodic arc deposition etc. These precipitation methods for producing zinc oxide is described briefly as follows.

2.3.2.2 Molecular Beam Epitaxy (MBE)

Molecular Beam Epitaxy (MBE) is an epitaxial thin film growth technique that provides exceptional quality. MBE in high vacuum (10⁻¹¹ torr) to enlarge single crystal epitaxial thin films is an advanced control techniques.

Films, single crystal surface of the elemental or molecular components is formed by evaporating slowly.

The films are formed on single-crystal substrates by slowly evaporating the elemental or molecular constituents of the film from separate Knudsen effusion source cells (deep crucibles in furnaces with cooled shrouds) onto surfaces are set to the appropriate temperature for chemical reaction, epitaxy and re-evaporation of excess reactants.

The furnace is directly heated the surface and relatively small atoms or molecules produced beams. Fast shutters are placed between the source and surfaces and the substrates and by controlling these shutters, superlattices can be grown properly by controlling accurately. Also uniformity, lattice match, composition, dopant concentrations, thickness and interfaces down to the level of atomic layers can be controlled.

MBE, is a suitable method for ZnO thin films grown. But there are some factors that limit the efficiency of the technique significantly. These are complex operation of the process and expensive equipment.

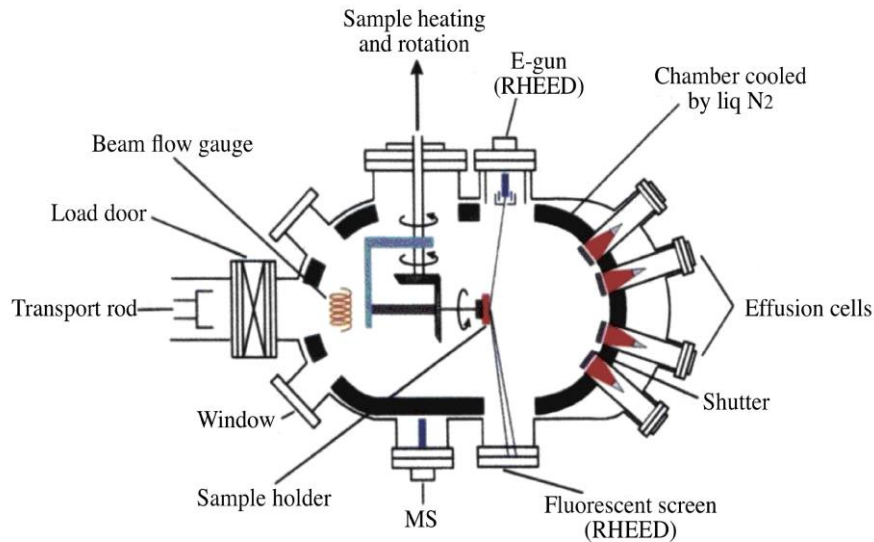


Figure 2-9: MBE System ^[99].

2.3.2.3 RF Sputtering

Sputtering is widely used for ZnO thin films growth techniques and there are three types of sputtering (a) DC sputtering, (b) RF sputtering, and (c) Reactive sputtering.

The sputtered ZnO thin film deposition properties are known to depend on several parameters, such as RF power, pressure, substrate temperature and gas atmosphere. Zinc oxide thin films were deposited at room temperature by radio frequency magnetron sputtering and gas mixture of an argon and oxygen with a metallic zinc target. Gas pressure and oxygen/argon gas ratio, plasma power, substrate temperature is adjusted.

The source material is placed in a vacuum chamber. This is referred to as a target and inert gas at low temperature (such as argon) is introduced. Using the RF power source, gas plasma is ionized. The ions are accelerated toward the target surface, causing the break of the particles from the source material and the particles are deposited on all surfaces including the substrate.

These particles travel in a straight line through the substrate and the substrate would be deposited. The deposition is usually carried out in pressure of 10^{-3} – 10^{-2} Torr with O₂ (as a reactive gas) and Ar (as sputtering enhancing gas) ambient in a vacuum

chamber. RF sputtering systems use high-frequency generator, typically use 13.56MHz for generating electromagnetic power. RF sputtering only occurs in the extremely high kinetic energy of the bombarding particles^[100].

RF sputtering technique is much preferred, because of low cost, simple, operation realize at low temperature.

The properties of sputtered ZnO thin films are known to depend on deposition parameters such as RF power, pressure, substrate temperature and gas atmosphere. As for evaporation, the basic principle of sputtering is the same for all sputtering technologies.

There are several advantages of RF sputtering.

1. It is very suitable with insulating targets. The driving RF frequency changes the sign of the electrical field at every surface in the chamber. So, it protects charge-up effects and reduces arcing.
2. RF sputtering doesn't need magnetic confinement. So, it provides optimum coating uniformity,
3. No poisoning of the target, a few or no arcing and a more stable process.

The grown ZnO thin film has a thickness of 250 nm.

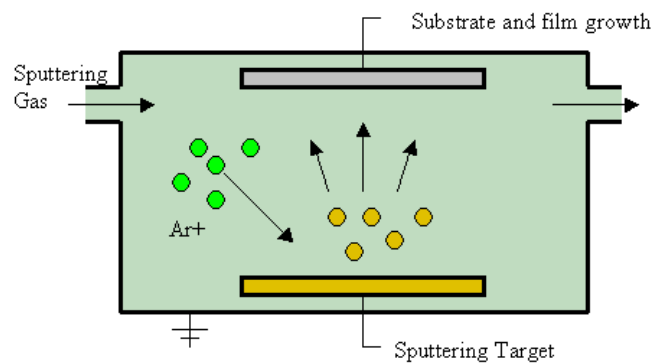


Figure 2-10: RF Sputtering Working Principle^[101].

2.3.2.4 Thermal Evaporation

Another common deposition techniques is the high vacuum thermal evaporation technique. Thermal evaporation technique is ideal method to produce thin films of nano-thickness and high quality. Applied to different substrates such as on glass, plastic films, metals, and almost any other kind of substrates. The purity of the source material is critical for deposition of thermal evaporation.

An e-beam can provide high melting points even above 2000 °C which is a very proper temperature for the purest thin films. This allows us to control the deposition rate is a huge advantage. Such as sequential deposition of material, in the one form storage at low temperature, use of the material as well as controlled.

In evaporation source material layer in the form of blocks is placed in the vacuum chamber. The source material is heated to the boiling point and starts to evaporate. The vacuum in the chamber is required to allow the molecules to evaporate off freely and then the molecules are condensed on all the surfaces.

This principle is the same for all evaporation processes. Only source materials differs. There are two popular evaporation technology these are e-beam evaporation and resistive evaporation each referring to the heating method.

In e-beam evaporation, electron beam is heated the source material locally and leads to evaporation.

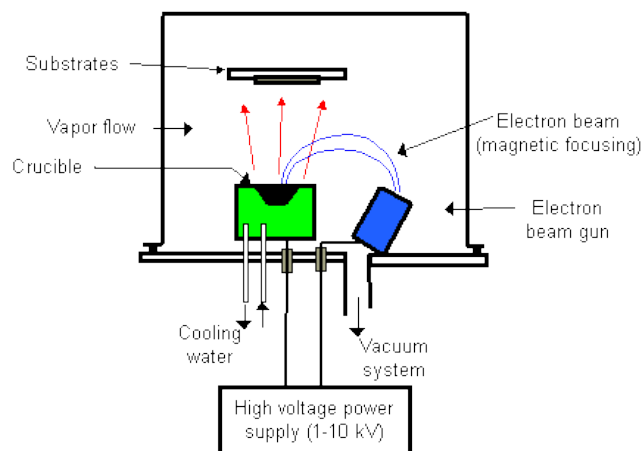


Figure 2-11: E-Beam Evaporation [102]

In resistors tungsten evaporation, boat which include source material is heated electrically by giving high current and allowed to evaporate material. For many materials, the use of evaporation method has restrictive reasons which typically relates to the phase transition properties of that material.

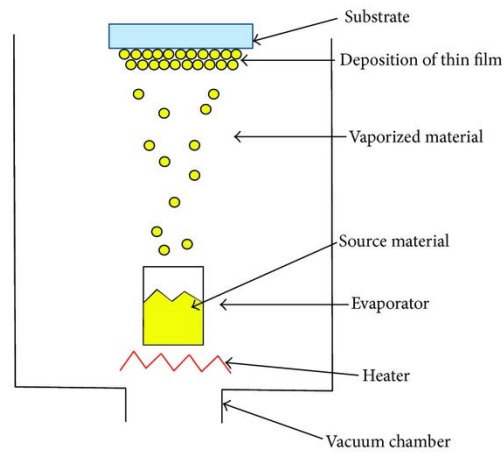


Figure 2-12: Thermal Evaporation

2.3.2.5 Spin Coating Technique

The molten material is dropped on the substrate, the coating is performed by turning. Sol is applied through a nozzle to the center of the substrate. Substrate accelerates to the final spin speed. As rotational forces increase, the sol pulled up and a wave front formed. But because of the fairly uniform layer on the edge of the substrate is formed due to consists of centrifugal force.

Between the 2000 and 8000 RPMs rotation speed can be set. The solution was diluted with a substantially centrifugal force. The solvent was evaporated and the viscosity increases sufficiently then flow stops. The spin off stage events takes approximately 10 seconds after spin up.

Evaporation occurs in a complex process. Excess solvent is absorbed by a portion of the atmosphere. If evaporation occurs prematurely, the liquid surface is formed solid layer which trapped under this layer barriers the evaporation of solvent and the centrifugal forces of the spinning substrate causes coating defects.

The spin coating process can be classified into the four step. Figure 2.13 is shown each stage. The deposition, spin up, and spin off stages occur sequentially while the evaporation stage occurs throughout the process.

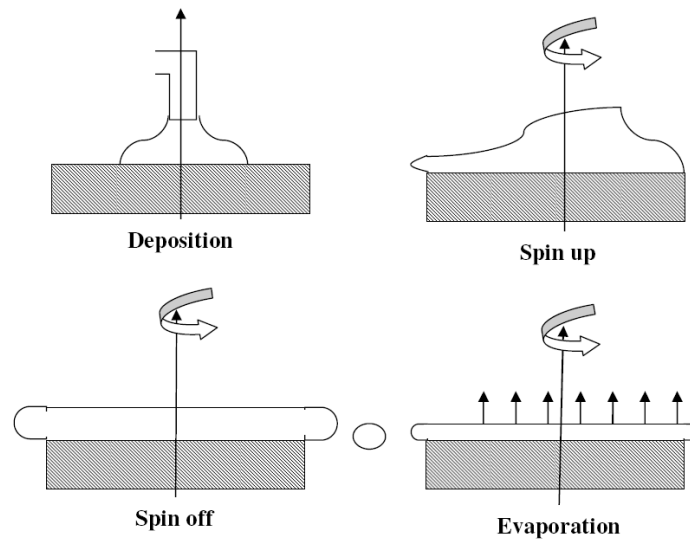


Figure 2-13: Four Stages of the Spin Coating Process

Spin coating has many advantages like controlling the film thicknesses by changing the spin speed, ability to get progressively more uniform.

Spin coating have few disadvantages such as large substrates cannot be spun at a sufficiently high rate and dry in a timely manner resulting in decreased throughput.

A typical spin coating process, the substrate is used only 2-5% of the administered agents on. The remaining 95-98% coating goes hand without being used.

2.3.2.6 Chemical Vapor Deposition (CVD)

Using a chemical process, high-purity and high-performance solid materials can be produced and it called Chemical Vapor Deposition (CVD). This process is often used in the semiconductor industry in order to produce thin films. In a typical CVD process, the wafer (substrate) is exposed to one or more volatile zinc precursors, which react or decompose on the substrate surface to produce the zinc oxide nanostructures. Usually, volatile products, which are removed by gas flow through the reaction chamber, are also produced.

There are number of reports for the synthesis of zinc oxide nanostructures by CVD method ^[103-109].

Chemical vapor deposition (CVD) is used to form a thin film on sapphire substrates. Separately solid source heater, three-zone (load, center and end zone) furnaces, gas injector, a vacuum pump and with a quartz tube is equipped.

The reaction tube 2 inches x 3 inches over a three-part collection area in order to achieve uniform temperature on the substrate was controlled by a furnace. Source material is mixed with ZnO powder and graphite powder. Solid source is placed in the quartz tube loading zone.

Zn is heated up to high temperatures by the addition of solid heating source for generating steam. Then the steam is moved to the central side in the tube by Ar carrier gas. The reaction gas (O_2) is transferred into the gas injector system from different locations in order to achieve the best uniformity over substrate.

Planar cut sapphire substrates are used. Schematic diagram of the CVD apparatus shown in Figure 2.14. There are two important parameters affecting growth. These are growth (plate) temperature (T_g) and flow rate (F_{O_2}). The surface morphology of the deposited thin films can be analyzed by electron microscopy (SEM) and atomic force microscopy (AFM).

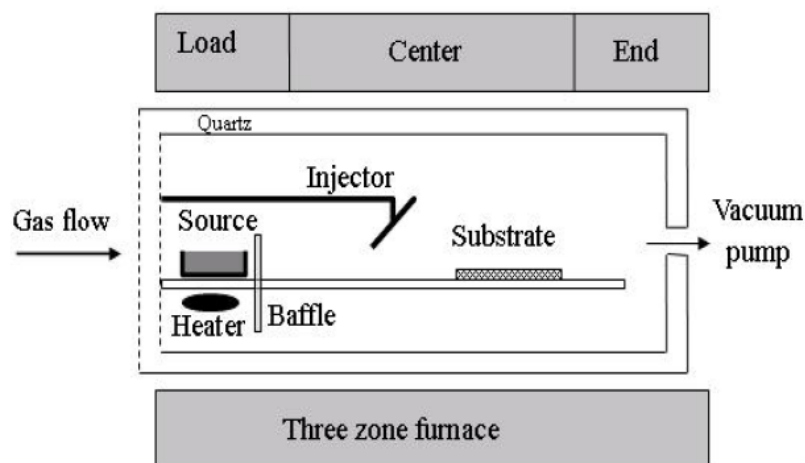


Figure 2-14: Schematic Diagram For the CVD Apparatus ^[110].

2.3.2.7 Hydrothermal

Hydrothermal method preferred method for the acquisition of ZnO nanostructures. Hydrothermal synthesis at high vapor pressure, is a method based on the crystallization of substances from aqueous solution at high temperature. In other words, the hydrothermal synthesis, depending upon the solubility of the mineral in the hot water under high pressure, the crystalline synthesizing methods.

Instruments used in the crystallization by hydrothermal method are stainless steel, autoclave and Teflon pot.



Figure 2-15: Teflon Pot Which is Used in The Hydrothermal Method^[111].

Hydrothermal method is an attractive method for the synthesis of high quality nano materials. Powders prepared by hydrothermal method with high crystallization, have good dispersion and no agglomeration in macroscopic level. By varying the synthesis conditions by hydrothermal method is easy to control the particle size and morphology. The most desirable material for synthesizing the crystalline phase is a suitable method.

Some general advantages of the hydrothermal method are as follows:

- Energy saving is achieved,
- The product is obtained completely pure,
- The experimental setup is not complicated, which makes it possible to synthesize New phases and stable novel complex,
- Homogeneous precipitation is carried out,
- The resulting particles have nano dimensions.

2.3.2.8 Aerosol Deposition

Thin film formation using the spraying method, on a heated pad, the metal salt solution spray process is created. The spray droplets on a base surface, thermal (heat) are exposed to weathering. The size and shape of the film formation is dependent on the arrival rate and the volume of droplet emission. The resulting film is transformed into the oxide on a heated pad, consisting of superposed metal oxide plate.

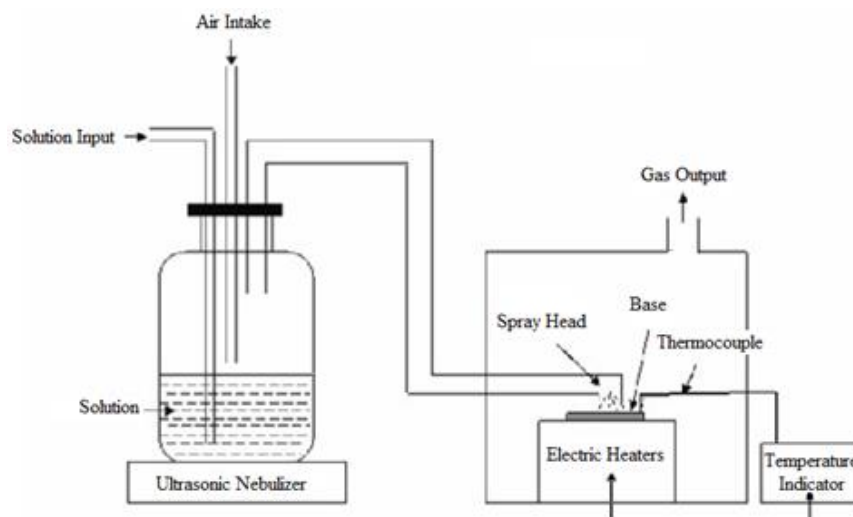


Figure 2-16 :Chemical Spraying Methods Test Setup ^[112].

Some advantages of chemical spraying method can be listed as follows:

- On the lower base films are obtained at the desired temperature.
- The film thickness can be controlled.
- A method of spraying chemicals cost compared with many other methods is low and easy method.

2.3.2.9 Sonochemistry

Sonochemistry is the study that the molecules for applying a strong ultrasonic radiation (20 kHz–10 MHz) exposes a chemical reaction. Acoustic cavitation is physical phenomenon and that is responsible for the sonochemical process.

Chemical effects of ultrasound does not come directly from the interaction of sound waves or molecular species. Sonochemistry, this phenomenon known as an acoustic cavitation occurs. The collapse of bubble growth and formation occurs in liquid environment.

A number of theories have been developed to break chemical bonds with sonic radiation. The main events in Sonochemistry, creating, growth and collapse of bubbles in a liquid form occurs.

Chemical effects of ultrasound can be divided into three parts:

- Homogeneous sonochemistry of liquids,
- Liquid-liquid or liquid-solid systems, heterogeneous sonochemistry,
- Sono catalysis. (The first one and second one overlap)

Generally chemical reactions, do not occur during ultrasonic application in solids or solids-gas mixture system, when exposed to a high intensity sound in the liquid, the alternate expansion and compression of the acoustic wave create bubbles.

The release of the bubble grows, the ultrasonic energy is deposited. Eventually, the bubbles reach an unstable size (maximum size). The concentrated energy stored. With the collapse of the bubble starts to become free. Implosive collapse of bubbles, very high temperature of ~5000 K and ~1000 atm pressure creates short-lived hot spots in the local area. Heating and cooling rate of 10^{10} K/s over occurs^[113]. Sonochemistry, for use in the synthesis of various nano materials have been found. These are high surface area transition metals, carbides, alloys, colloids, and oxides.

"Hot spot mechanism" theory, explains collapse of on the bubble and breaking of chemical bonds. Claimed according to this theory, very high temperatures obtained the collapse of the bubble.

This degradation occurs in less than a nanosecond. Obtained very high cooling rates. (In excess of 10^{11} K / s). High cooling rate of the blocks causes the crystallization product and shaping. As a result, almost all sonochemical reactions led to obtain inorganic products or nano materials.

They are available in various sizes, shape and available in the solid phase. But all in nanometer size. Many methods have been developed to produce nanoparticles. Which makes it superior to the sonochemical method, there are four issues related to nanotechnology.

➤ **The Preparation of Amorphous Products.**

Bulk metals by cold quenching method, amorphous metal can be obtained. However, glass-forming materials must also be added to the mixture. When sonochemistry is applied to an amorphous metal oxide synthase, no need to add glass formers and amorphous products are obtained in nanometer size^[114].

➤ **Insertion of Nanomaterials Into Mesoporous Materials.**

Amorphous nanosized catalysts are inserted into the mesopores by using ultrasonic waves. Detailed studies demonstrate nanoparticles are deposited without blocking them as a smooth layer on the inner pore walls. Sonochemistry presents better properties compared to impregnation or thermal spreading,^[114].

➤ **Deposition of Nanoparticles on Ceramic and Polymeric Surfaces.**

Sonochemistry is used for depositing different nanomaterials (metals, metal oxides, semiconductors) on the surface of ceramic and polymeric materials. Uniform and homogeneous coating layer is formed on the surface. Nanoparticles can be attached to the surface by chemical bonds or interactions with the substrate that cannot be removed by washing^[114].

➤ **The Formation of Proteinaceous Micro- and Nanospheres.**

During sonication, any protein can be converted into a sphere. Some researchers have also illustrated that they can encapsulate a drug, such as tetracycline, in the sphere. Spherical protein is biologically active, although its biological activity is reduced. The spheronization sonochemical process made it shorter than others^[114].

2.3.2.9.1. Sonochemistry Applications

➤ **Sonochemical Synthesis of Nanoparticles**

- Chalcogenides (S_2 , Se_2 , and Te_2) material is so popular because of those semiconductive properties, valuable to fields like on-linear optic detectors, photorefractive devices, photovoltaic solar cells, and optical storage media^[114].
- Metal and alloy nanoparticles have continued to be of interest to synthetic Sonochemistry. Varieties of reducing agents are used. Zinc powder, hydrazine and nanomaterials including ethylene glycol were obtained^[114].
- Nanophases oxides preparation by using sonochemical method began long time ago and is still continuing. Titanium dioxide, strontium titanate, silica, ZnO , ZrO_2 and $MnOx$ was prepared using ultrasonic radiation^[114].

➤ **Shapes of Nanomaterials Created Sonochemically**

Formation of nanocrystalline product is carried out with high efficiency with sonochemical reactions. The products are different morphology for each other. First nanoproductions were either spherical or near spherical structures. Over the years, research groups all around the world have tried to obtain nano-sized products which are unique shapes like nanotubes, nanorods, hollowed spheres, and many others. The dimensionality of nanostructures is shown in semiconductors as best way. This includes 0D (quantum dots), 1D (nanowires), 2D (films), and 3D (bulk)

configurations. On the formation of nanotubes and nano-rods, several reports appeared such as carbon, hydrocarbon, TiO₂, ZnO and MeTe₂.

2.3.2.9.2. Frequency Range of Audio Spectrum

Ultrasound is part of the audio spectrum. It consists of three main regions. Ranges from about 20 kHz to 10 MHz.

- Low frequency, high power ultrasound (20-100 kHz),
- High frequency, medium power ultrasound (100 kHz-1 MHz),
- High frequency, low power ultrasound (1-10 MHz).

The range between 20 kHz and around 1 MHz is used in sonochemistry whereas frequencies far above 1 MHz are used as medical and diagnostic ultrasound^[115].

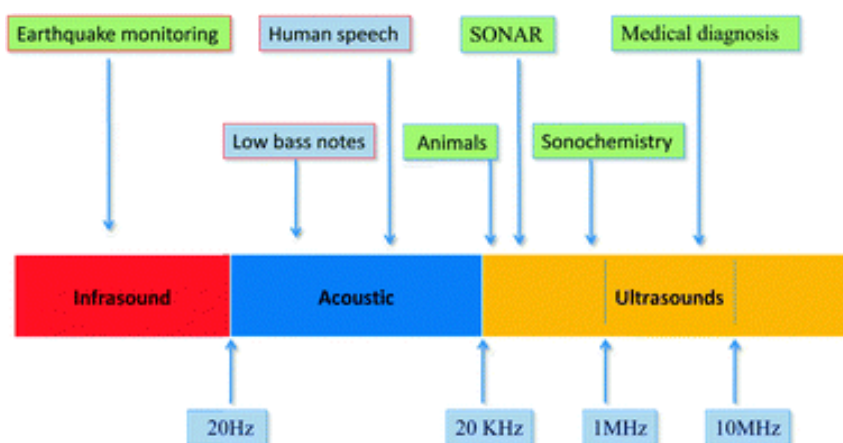


Figure 2-17 : Frequency Range of Audio.

➤ Acoustic Cavitation

Sonochemical effects in liquids involves a phenomenon of acoustic cavitation. Acoustical energy is mechanical energy. Namely, it is not absorbed by molecules. Ultrasound is transmitted through the pressure wave inducing vibrational motion of molecules^[115]. Therefore, the distance between molecules oscillation vary around their average position changes. If the ultrasound intensity is increased so much, intramolecular forces are not able to keep a stable molecular structure. As a result, bonds broken and formed cavity. This cavity is called cavitation bubble.

There are two form for cavitation: Stable and transient.

Stable cavitation means that the bubbles, on their own, duration of refraction/compression cycle, can oscillate around the equilibrium position. During

transient cavitation, the bubbles grow up one (Sometimes two or three) acoustic cycles to double their initial size and finally violently collapse^[115]. The size life time and cavitation bubble status depend on the following parameters: frequency, intensity (acoustic pressure), solvent, bubbled gas, external parameter (temperature, pressure). However, it should be noted that there is often no simple relationship^[115].

ZnO nanostructures can be synthesized in the environmental conditions and one of the most simplest and fastest technique is sonochemical growth method because of that, has been the focus of attention by many researchers. Using the chemical effect of ultrasound, various morphologies of ZnO nanorods are obtained. This method is reasonably priced, mass production can be made easily and environmentally friendly, (non toxic) method. This method has been shown to be suitable for any substrate which is stable in alcohol and aqueous solution.

In this thesis, a sonochemical approach was adopted for the synthesis of ZnO nanorods. For characterization four techniques are used. Firstly, Morphological Characterization of ZnO nanorods such as; Optical Microscopy, Profilometer, AFM, (SEM), Secondly; Elemental Characterization of ZnO nanorods such as; Energy dispersive X-ray spectroscopy(EDS), Thirdly Structural Characterization of ZnO nanorods such as; XRD Image and Spectroscopic Analysis. Finally, electrical characterization of ZnO nanorods is done. Such as; J/V analysis.

Table 2-3: List of ZnO Nanostructures Synthesis Techniques and Grown Products.

Technique	Structure	Substrate/Temperature	Reference
MBE	Nanorods	Silicon 300-500 °C	[56]
Hydrothermal	Nanorods	Glass and Silicon 60-95 °C	[116]
Solothermal	Nanorods	TPU 75 °C	[117]
PLD	Nanorods	Sapphire and Silicon 550-700 °C	[118]
CVD	Nanowires	Chip 700 °C	[119]
Sonochemical	Nanorods	Glass and Si wafer Room conditions	[120]
Thermal evaporation	Nanorods	Porous Si 600-1000 °C	[121]

3. EXPERIMENTAL

3.1 Production Stages of ZnO DSSC

3.1.1 Preparation of Fluorine-Doped Tin Oxide Thin Films

SnO₂: F thin films are used in dye doped solar cells as a base. (FTO) thin films is so important for economic and availability in terms of solar energy conversion. In photovoltaic applications, due to the appropriate atmospheric conditions, exhibit good properties^[122]. SnO₂: F thin films obtained by adding different materials, has higher electrical conductivity, optical transmission and an infrared reflectance properties. Metals and oxides are attractive due to very good adhesion to a multi-crystalline and amorphous surface such as FTO, ITO.

3.1.1.1 Cleaning of FTO-Coated Glass Plates

In this study, slides the glass substrate was used as 25mmx25mmx2.1 mm size. The films will be covered, for good hold on the FTO plate, the cleaning process must be done well. The film will be easy to cover with a clean substrate and improve quality.



Figure 3-1: Image of FTO-Coated Glass

Before synthesized, FTO substrate was cleaned in four steps. Firstly TCO sample, which is coated by FTO was cleaned by detergent solution using sonication device during 10 minutes. Later, sample was cleaned by distilled water using same method. Thirdly, same sample drop in a beaker which is filled with acetone, and sonicated for

10 minutes. And lastly, sample was sonicated with isopropyle alcohol-filled beaker at 10 minutes.

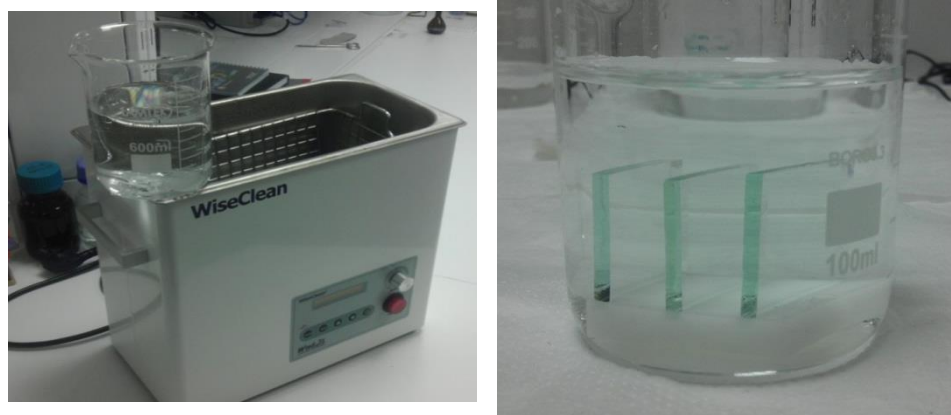


Figure 3-2: Cleaning Process for FTO-Coated Glass

3.1.2 Synthesis of ZnO Nanorod for DSSC Application

In this thesis, I grew up ZnO nanorods on FTO coated glass in the environmental conditions using sonochemical technique. First ZnO seed layer was coated onto substrate then ZnO nanorod grown on ZnO seed layer. This installation method is not complicated. Applicability is described in various publications ^[116-121]. It is not harmful to the environment because of that hazardous waste not leave to outside, Changing the magnification conditions, different examples can be synthesized.

Table 3-1: Used Chemicals in The Synthesis of ZnO Nanorods.

Chemicals	Molar Mass	Supplier
Zinc acetate dihydrate	219.51g/mol	Tekkim
Zinc nitrate tetrahydrate	261.44g/mol	Sigma Aldrich
Hexamethylenetetramine	140.19g/mol	Sigma Aldrich
Isopropyl alcohol	60.1g/mol	Sigma Aldrich

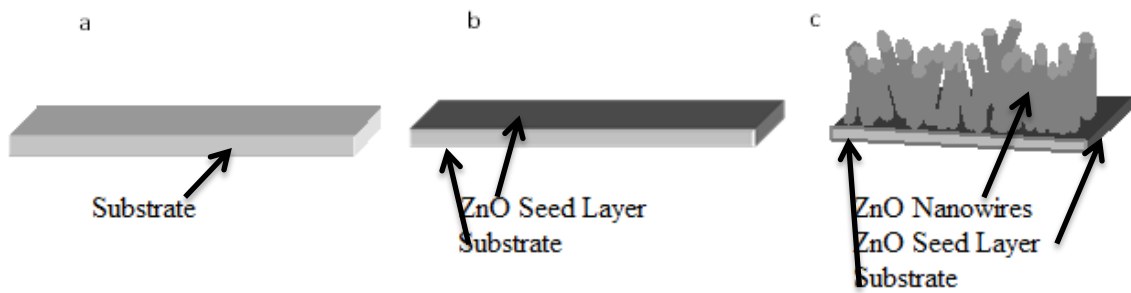


Figure 3-3: Layers of Working Electrode a. Substrate b. ZnO Seed Layer Deposition c. ZnO Nanowire Growth

3.1.2.2 ZnO Seeding Process

For the growth of ZnO nanorods on the substrate is an important first step to do the seeding process extremely. As shown in Figure 3.4, the peaks and valleys that occur in the seed layer deposition process, acts as a nucleation point and ZnO helps the formation of the wire.

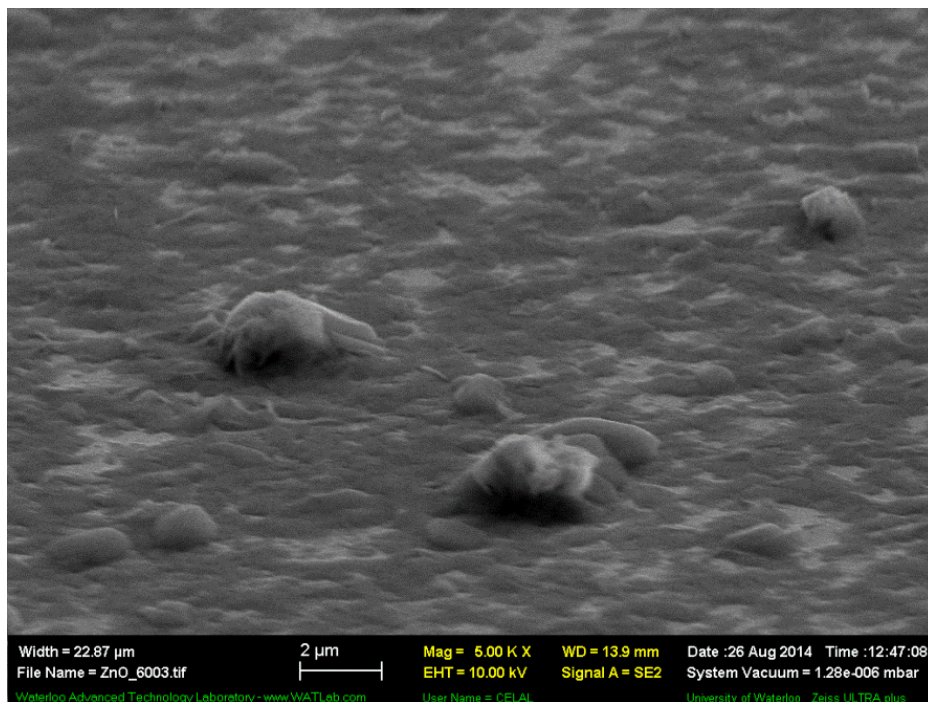


Figure 3-4: SEM Image of Seed-Layer Deposited on FTO Substrate

Figure 3.5 shows the attempted growth of ZnO on a FTO substrate without the deposition of the seed-layer. This control setup shows poor ZnO range and the absence of NW arrays.

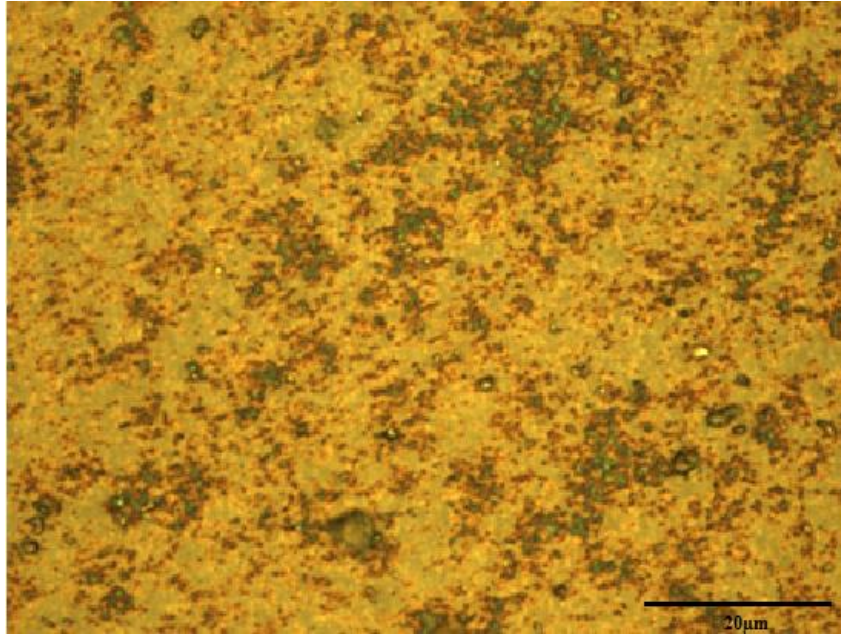


Figure 3-5: Optical Microscopy Image of ZnO NW Without Seed-Layer Via Sonication. (100X Magnification Applied)

We apply that ZnO NWs can be, 50% of the maximum amplitude, with 30 minutes of sonication. Figure 3.6 shows the result.

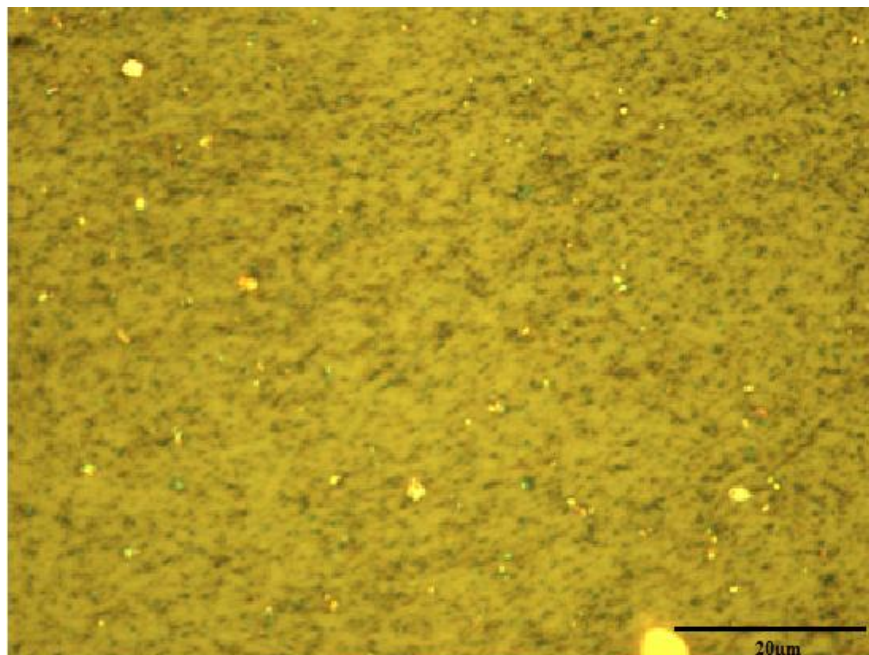


Figure 3-6: Optical Microscopy Image of ZnO NW With Seed-Layer Via Sonication. (100X Magnification applied)

Some reports show that Zn is required catalytic metal film for pretaration of ZnO nanorods^[123-125]. Because of that Zn deposition is required long process and more difficulty. To eliminate these problems, one step is added between process. This step is called seeding process. In this process, Zinc acetate dihydrate and IPA solution are used. Thus, in polar and non-polar surface, a seed layer is formed for the growth of ZnO nanorods^[128].

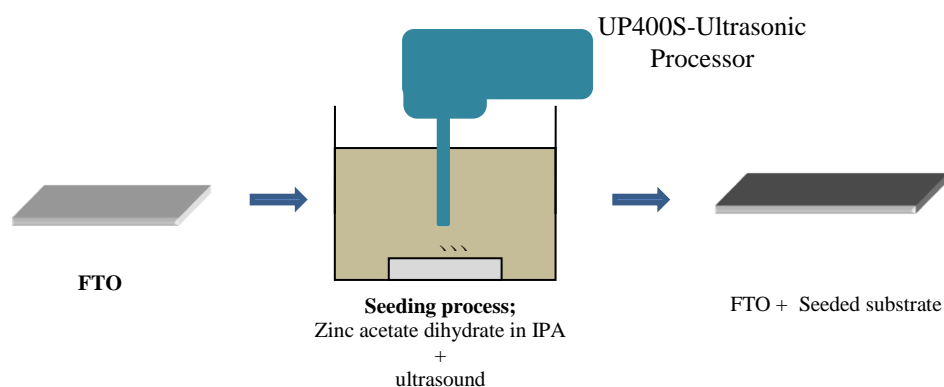


Figure 3-7: Schematic Representation of Sonochemical Synthesis of ZnO Seed Layer

In seeding process, for surface of the FTO glass substrate, 0.005M Zinc acetate dihydrate ($0.5487\text{g}(\text{C}_4\text{H}_{10}\text{O}_6\text{Zn})$) were dissolved in one liter of isopropyl alcohol at room temperature. The solution was stirred with a magnetic stirrer at 1000rpm for 15 min.

The clear solution was obtained and the FTO glass substrate was then immersed into the solution and sonicated for 30 min at 0.8 cycle and 50% of the maximum amplitude of the 24KHz ultrasonic probe working at 400 W.

3.1.2.3 ZnO Nano Rods Growth Process.

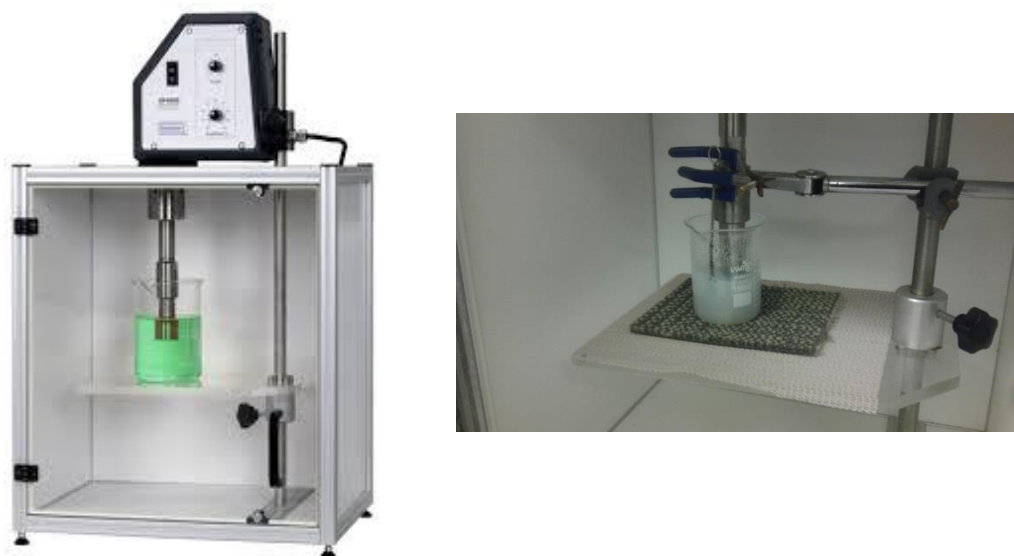


Figure 3-8: Sonochemical Growth Setup.

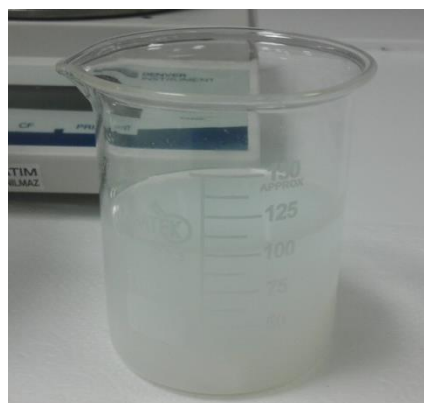
ZnO seed substrate and using in a mixture of zinc nitrate and HMT, the growth of ZnO nano-rods are obtained by ultrasound effect.

Aqueous solution consist of 0.04M Zinc nitrate tetrahydrate($\text{Zn}(\text{NO}_3)_2 \cdot 4\text{H}_2\text{O}$) and 0.04M Hexamethylenetetramine ($\text{C}_6\text{H}_{12}\text{N}_4$). Firstly, 0.004M (2.8038g) of HMT was dissolved in a beaker containing 0.5L deionised water and stirred with a magnetic stirrer at 1000 rpm for 10 min. In another beaker containing 0.5L deionised water and 0.004M (5.2288g) of $\text{Zn}(\text{NO}_3)_2 \cdot 4\text{H}_2\text{O}$ was dissolved and the solution was also stirred at 1000 rpm for 10 min.

Equal volume, it means 50ml HMT solution and 50ml $\text{Zn}(\text{NO}_3)_2 \cdot 4\text{H}_2\text{O}$ solution were mixed in 150ml beaker and stirring 10 minutes. The FTO and seeding covered glass substrate was immersed into the solution and sonicated 0.8 cycle and at 50% of the maximum amplitude of the 24 kHz ultrasonic probe working at 400W for 60 min. Then stimulated with high sound intensity, the solution became cloudy and a white precipitate.



Before Growth



After Growth

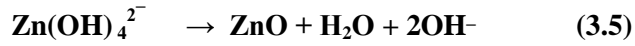
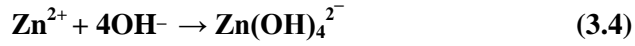
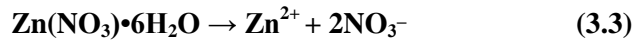
Figure 3-9 : Picture of ZnO Nanorods Growth Solutions

In this procedure, only using ultrasonic energy, without further processing, to provide a molecular structure sufficiently resolved was observed. During sonication process time, increase the temperature of solution between 25°C and 80°C was observed.

ZnO nanorods growth rate tend to slow, as the time goes by. Therefore, each of 60 minutes of ZnO nanorods growth process, fresh solution was prepared. Using the new solution prevented the depletion of the amount of Zn^{+2} ion and ZnO nano-rods aspect ratio has increased.

Dye, to make enough interference into zinc oxide nano rods, the height of the nano rod must grow to be at least 1 micron. At each 60 minute growth process is seen to extend from about 250nm to 300nm of the nanorods. So, I repeat the same procedure 5 times.

After the sonication the sample was heated at 70°C for 10 minutes on the heater in order to evaporate the liquid remains of the sample surface. In the following formula, the chemical reaction for the formation of ZnO nano rod shown.



Both HMT and zinc nitrate participate in the formation of $\text{Zn}(\text{OH})_4^{2-}$ crystal which is produced from the sonochemical reaction of Zn^{2+} and 4OH^- . NH_4^+ cations and OH^- anions are released from the hydrolysis of HMT as shown in equation (1) and (2) above, and Zn^{2+} cations are released from the dissolution of zinc nitrate as in equation (3). Growth of the ZnO nanorods is initiated by the negatively charged ZnO seed layer with O^{2-} ionization, this attracts the Zn^{2+} by coulomb force of attraction and subsequently binds to the ZnO seed surface. By incorporating OH^- available in the solution, $\text{Zn}(\text{OH})_4^{2-}$ crystals are produced. $\text{Zn}(\text{OH})_4^{2-}$ are known to be unstable under sonication, therefore phase transition from $\text{Zn}(\text{OH})_4^{2-}$ to ZnO nanorods is said to occur at this stage^[126].

Alternatively, ZnO nanorods can also be grown from a reaction between Zn^{2+} and $\bullet\text{O}_2^-$ during sonication. Radicals $\bullet\text{OH}$, $\bullet\text{H}$, $\bullet\text{HO}_2$ and $\bullet\text{O}_2^-$ are generated through the sonolysis of water in air atmosphere and the reaction proceeds as follows^[127-136].

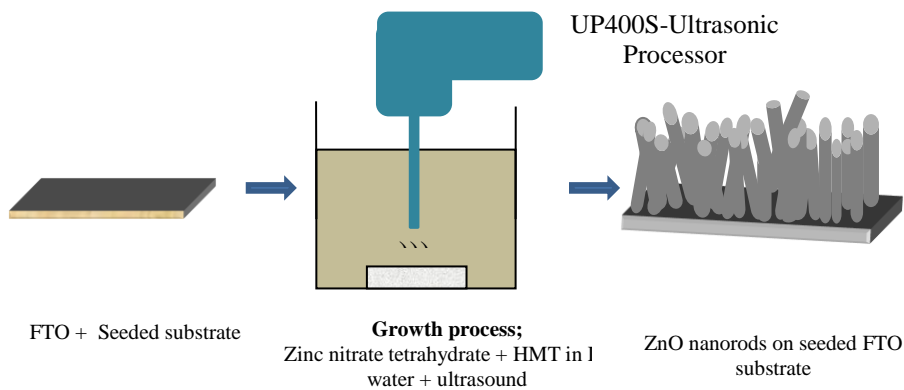


Figure 3-10. Schematic Representation of Sonochemical Synthesis of ZnO Nanorods

3.1.3 DSSC Device Fabrications

3.1.3.4 Working Electrode Structure

ZnO coated layer into the prepared dye solution was allowed. ZnO semiconductor thin film is left into dyes and sample is incubated in the dye for 24 h. ZnO semiconductor film, which is taken from dyes of materials, thrown into dilute ethanol solution. Because of that the outer shell surface, which dyes materials can not hold surface (dead side) is cleaned. It is allowed to dry at room temperature. The obtained layer ($\text{SnO}_2: \text{F} + \text{ZnO} + \text{Dye}$) forms the working electrode. Picture of the working electrode are shown Figure 3.11 which is using dye, the working electrode obtained.

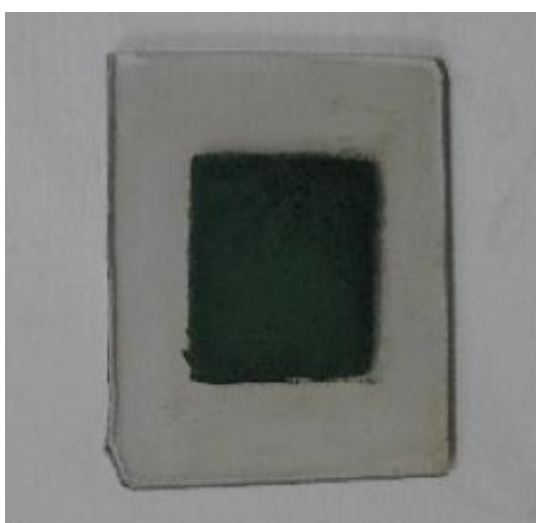


Figure 3-11 : Image of Working Electrode

3.1.3.5 Preparation of Counter Electrode

Dye-sensitized solar cell to operate as a continuous, electrolyte must be supplied electron transfer continuously to the dye sensitized. This electron transfer is performed with iodine-iodide conversion.

Conversion rate which is on the Platinum (Pt) surface is much faster than in the FTO surface. The effects of the Pt catalyst, the conversion reaction is accelerated.

Therefore there is no need to cover the entire surface completely platinum for this process, catalytic purposes only regional cover is sufficient.

Opposing electrode to be used in making 5mm platinumic acid solution in 10 ml of 2-propanol, H_2PtCl_6 (hydro platinumic acid) are prepared by dissolving.

Prepared using platinum acid solution, 2-3 drops on SnO₂: F thin film are dropping, the coating is obtained.

Pt coating electrode, in order to dry at room temperature, expected for a while. After it allowed standing for 1 hour at 350°C to 400°C in the oven. Lastly, it was allowed to cool to room temperature. Image platinum coated counter electrode, Figure 3.12 is shown.



Figure 3-12 : Picture of Platinum Coated Counter Electrode

3.1.3.6 Preparation of Liquid Electrode

Liquid electrolyte 0.05 iodine (I₂) dissolved in 10 ml of pure ethylene glycol, and then into by the addition of 0.5M potassium iodine is formed.

The liquid layer, at which the redox reaction occurs, for the continuity of the electron loop, is preserved in the dark or in a dark glass container after stirring thoroughly.

This solution is the layer at which the necessary reactions DSSC during operation and is located between the working electrode and the counter electrode.

3.1.3.7 Construction of Dye Sensitized Silicon Solar Cell

DSSC can be examined in three main parts. These are;

- i) Working electrode (FTO + ZnO + Dyes)
- ii) Liquid Electrolyte (KI + I₂ + Ethylene Glycol)
- iii) Counter electrode (FTO + Pt)

DSSC's schematic structure shown in Figure 3.13

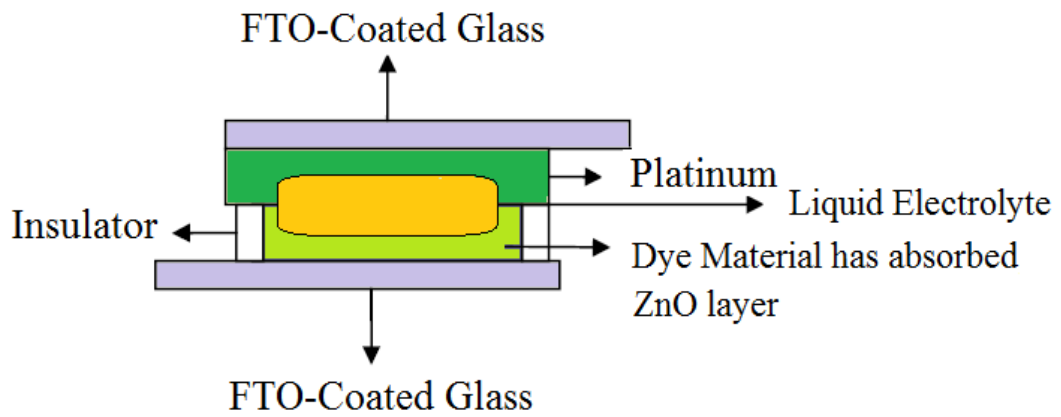


Figure 3-13 : The Schematic Structure of DSSCs

Dye sensitized solar cells item, consist of firstly FTO + ZnO + Dye with the working electrode, secondly FTO + Platinum coated counter electrode layer and located electrolyte fluid therebetween, the structure toast formed by putting on top form.

DSSC battery, dye will overlap with the platinum and the two layers only FTO-coated portion remain outside is attached. A small area as to inject the liquid electrolyte is left without bonding. From this point, the liquid electrolyte between the two layers is injected. DSSC's photo is shown in Fig 3.14.

The liquid electrolyte is consists of dissolved in an organic solvent iodide / triiodide redox couple.

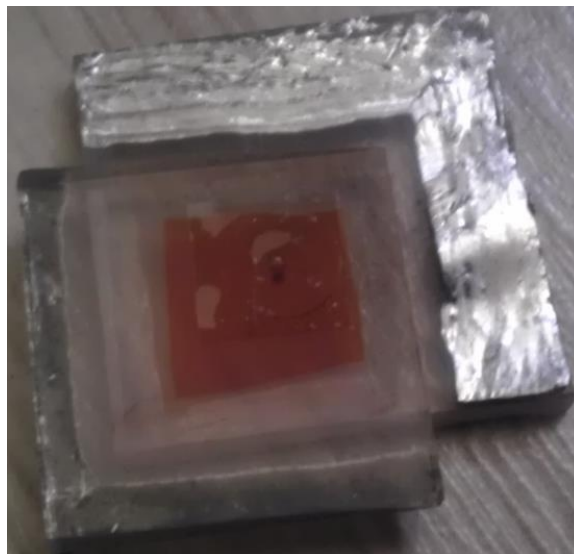


Figure 3-14 : Picture of Produced DSSC Device

3.2 Characterization Techniques

Grown by sonochemical method for the analysis of ZnO nano-rods, elemental analysis, surface characterization was performed. Thereafter, the electrical characteristics were measured.

These include optical microscopy(OM), scanning electron microscopy(SEM), Energy-dispersive X-ray spectroscopy (EDS), Atomic Force Microscopy (AFM), I-V measurement. Details of the characterization techniques are given below.

3.2.1 Morphological Characterization

3.2.1.8 Optical Microscopy

Microscope enables magnified so small objects which can not be seen with the naked eye by lenses and it is a tool to examine the image. Optical microscope consists essentially of two lens system. Given by the first system image (lens), the second with a system (ocular) is further magnified. Thus, a higher magnification power of a magnifying glass, which can be obtained provided.

The closer to the object using the lens. Focuses on the object to be displayed in the microscope. By collecting the light falling on the object, takes an image.

The second lens or lens image magnified by the group, the inverse virtual image of the object in the viewer.

Using the compound objective/eyepiece combination provides a larger magnification. Chromatic aberration is reduced and can be changed by using the objective lens, we can adjust the magnification. A compound microscope also provides improved lighting. Phase contrast adjustment can be made.

The combined microscope is widely used in research field. Receiving the object image with some parts compatibility, are obtained. It has several parts which play together to generate the imate of sample.

Beam of light from the microscope, after passing through the condenser, passes through concave lens. The focal plane of the lens, it will appear enlarged inverted real image of the object (by adjustment).

This image appears as an object in the eyepiece. Finally eyepiece lens forms a further enlarged virtual image of the object. Compound microscope magnification power is multiplication product of magnifying powers of objective and eyepiece.

In this thesis, Nikon H600I optical microscope equipped with digital camera fitted with clemex captiva digital image analysis software was used. to view the surface of the sonochemically synthesized ZnO nanorods.



Figure 3-15: Optical Microscopy Setup Which was Used for The Thesis.

The magnification optical microscope is limited. Light is a wave motion and around a very small objects it can be bent without any influence. This prevents the appearance of very small objects. Therefore, although to be made of microscope magnification providing more than 2000, due to the nature of light, it is impossible to obtain a detailed image. The wavelength of the electron wave is much shorter than the wavelength of light, smaller than 2500 angstrom (or 0.000025 cm) objects for high magnification, electron microscope is used.

3.2.1.9 Profilometer



Figure 3-16: Picture of Profilometer Device

Profilometer is used for recognition of the surface morphology of samples, and a multifunctional device that is used to identify the thickness of these structures.

Especially in recent years to create growing thin film organic electronic applications, polymer coatings and more similar, surface images of different structures can measure high speedly and with precision.

Although this function is similar as in the atomic force microscope, there is some differency. This device can be used for all of the samples what you want to see the surface structure.

A contact profilometer uses a diamond stylus. Tip of the mechanism is moved vertically and laterally in contact with the sample for a specified distance. It precisely measures small variations in stylus displacement. This technique is a real direct measurement of surface. It obtain very high resolution 3D images of scanned area.

It's not required optical constants and an advantage in dirty environments. Works for both research and production environment. Works on non clean surfaces.

Data generated of

1. Surface roughness,
2. Step height,
3. Volume wear,
4. Stress,
5. Bowing,
6. Film thickness,
7. Surface Profiling Defect Studies.

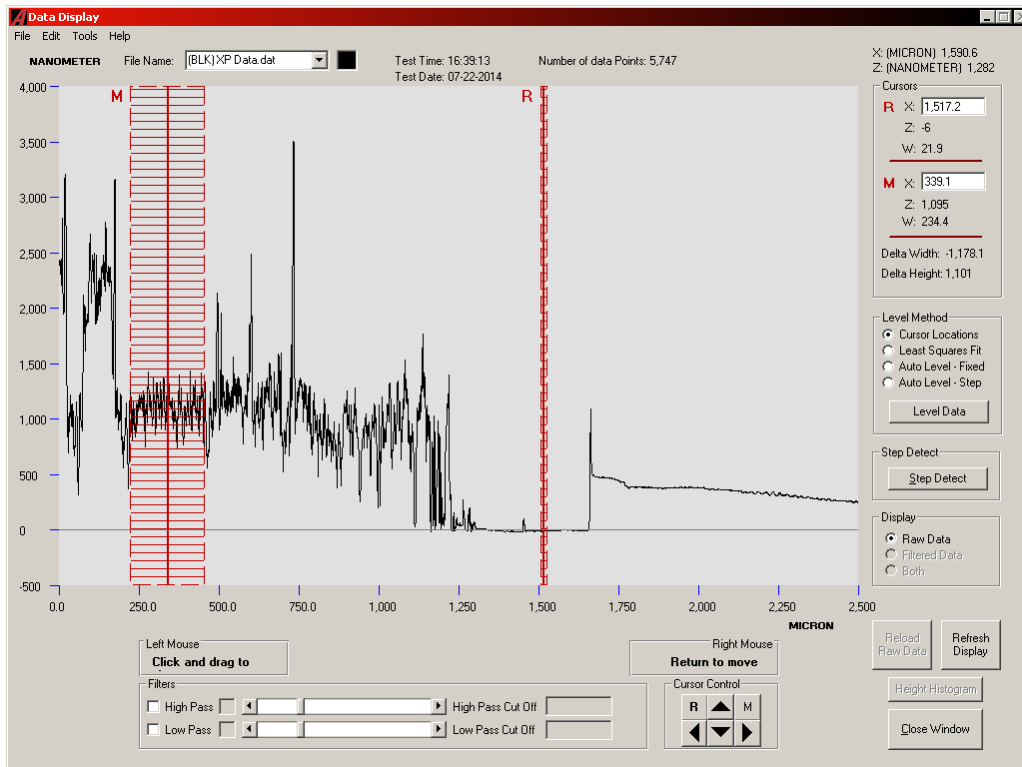


Figure 3-17: Imaging of ZnO Nanorod Step Height

3.2.1.10 AFM

AFM enables us to obtain a 3-dimensional image in local area on the nanoscale by measuring forces between surface and probe (<10 nm) at very short distance (0.2-10 nm probe-sample separation). The probe is located on the end of a cantilever. The AFM tip softly touches the surface on the sample and the small force stored in the memory by up and down movement is exerted between the probe and the surface [137].

The amount of force between the probe and sample depends on the spring constant of the cantilever and the displacement between the probe and the sample surface. Force measured between the surface and sharp probe points scans. If the spring constant of cantilever (typically ~ 0.1-1 N/m) is less than surface, the cantilever bends and the swerves is monitored^[137].

The main difference in instrumentation design is the method of monitoring forces between the probe and sample surface. We can produce an image of an object or surface with atomic force microscope. But with this image, we do not see any atom in a real sense, but we can understand how the arrangement of atoms. The deflection of the probe is typically measure by a “beam bounce” method. A semiconductor diode laser is bounced off the back of the cantilever onto a position sensitive photodiode detector. This detector measures the cantilever deflection while scanning the tip over the sample. The measured deflections of Cantilever is used to create a surface topography maps.^[137].

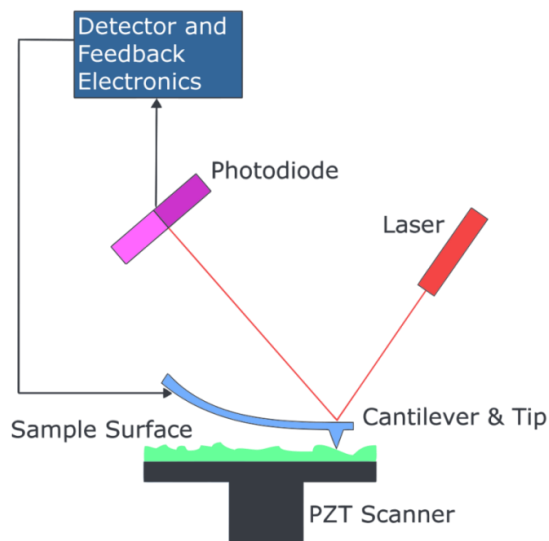


Figure 3-18: Atomic Force Microscopy Working Principle^[138].

3.2.1.11 Scanning Electron Microscopy (SEM)

Scanning Electron Microscope, besides its use in research and development, the production of microelectronic devices, the error analysis in different branch industry, in biological sciences, medicine and criminal practices are widely used.

Including the shape and size of the sample, provide a detailed topographic feature.

In the Scanning Electron Microscope (SEM) to obtain images, the accelerated electrons with high voltage, focus on the sample. It scans the sample surface of the electron beam. During the scan, interference occurring between electrons and atoms samples collected at appropriate sensor. The signal after passing the enhancer is transferred to the screen of a cathode ray tube.

In modern systems, the signals from these sensors are converted into digital signals are given to the computer monitor. Resolution, depth of focus, to combine image and analysis features, the use of areas of the scanning electron microscope is expanding.



Figure 3-19: SEM Device in Duzce University, Device Model: Quanta 250 FEG

There are detectors that as a result of sample interference with electron beam collects various electron and radiation, signal multipliers and at the sample surface a magnetic coil for synchronizing the scanning image.

The system uses a highly focused electron beam. The focused beam is made to scan on the sample in a raster pattern. With condenser and objective contained in the bottom, set the diameter of the electron beam. Consequently small electron probes occurs. The electrons with the atoms of the sample interact mutually.

The interaction between the electrons and the atoms of the sample produce a variety of signals, such as X-rays, backscattered electrons, and secondary electrons signals. These signals give information about the surface topography and composition of the sample.

Scanning electron microscope, a technique which does not destroy the sample. To produce a very high resolution image is used. SEM can achieve a magnification from 10X to approximately 100,000X.

Scanning electron microscope EDS was used for the structural characterization of the sonochemically synthesized ZnO nanorods.

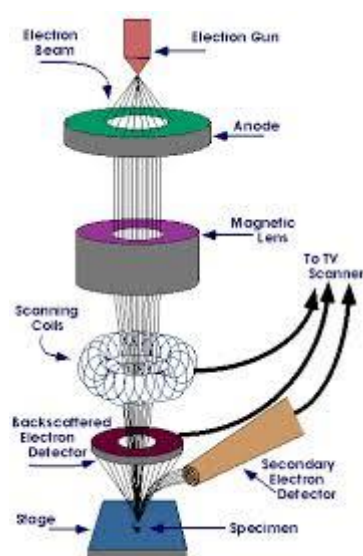


Figure 3-20 : Schematic Presentation of SEM Instrument^[139].

3.2.2 Elemental Analysis;

3.2.2.1 Energy Dispersive X-ray Spectroscopy (EDS)

Discovery of X-rays by Wilhelm Roentgen (German scientist) realized in 1895. Henry Moseley (British scientist) in 1914 showed the relationship between wavelength of characteristic x-rays emitted from an element and its atomic number. The energy is related to the wave length^[140].

$$E = hc/\lambda \quad \text{or} \quad E = 12.4/\lambda \quad (3.7)$$

This led to the finding that energy levels in electron shells varied in discrete fashion with atomic number. For most elements characteristic patterns created in 1920 and they were recorded.

Wavelength dispersive spectrometer prototype was developed in 1948. First commercial Electron Probe Microanalyzer (EPMA) was developed in France in 1956. In late 1960s solid (SiLi) state EDS detectors attached to an SEM^[140] were introduced.

A typical analytical electron microscopy method (energy dispersive X-ray spectroscopy of EDS, sometimes called EDX or EDXS) is shown. Some improvement in the resolution of EDS has been attempted. But there has been no significant modification introduced in the practice of EDS in comparison with electron energy loss spectroscopy (EELS).

This method still is kept standard and reliable in the field of analytical electron microscopy and is widely used.

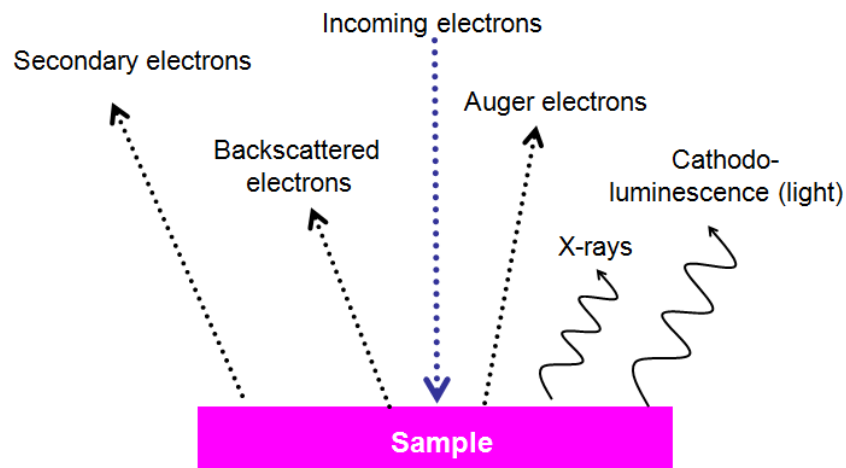


Figure 3-21: Interaction Between Source of X-ray Excitation and a Sample^[141].

Analytical techniques mostly preferred for the elemental analysis of a sample or chemical characterization of sample. Working principle is based on of interaction between the X-ray excitation source and a sample. Determines characteristic of an atom due to the a unique atomic structure.

Place with an atomic binding energy of the electron orbital is held. Ionizing an atom requires a big enough the energy of the incoming electron to knock out the orbital electron: Energy of the electron beam must be greater than the binding energy of the shell. This beam energy is called the Critical Excitation Energy. Each shell and subshell has its own binding energy and each one is peculiar; therefore there are many Critical Excitation Energies. An outer shell electron then “jumps” to fill the

vacancy. A characteristic x-ray (equivalent to the energy change in the “jump”) is generated. The difference in energy between two orbits has a unique value for each element, the energy of the emitted x-ray is also unique to the element.

Obtain atomic number contrast of the surface, a backscattered image are used. There are different gray levels on EDS in the spot mode. We can distinguish the elements in the image. Also we can adjust the design by assigning items that we want on the map.

3.2.3 Structural Analysis,

3.2.3.1 X-ray Diffraction (XRD)

XRD device, with X-ray diffraction method which each owned a crystalline structural atomic sequences, X-ray diffraction based on that principle works.

X-ray diffraction method (XRD), each crystal phase is unique, depending on the atomic sequence, X-rays, is based on diffraction in a characteristic pattern.

This diffraction profiles for each crystalline phase, as a kind of fingerprint, it defines the crystal. X-ray diffraction analysis method does not destroy the sample during analysis and even a small amount of samples (liquid, powder, crystalline and thin film) allows the analysis to be made.

By X-ray diffraction device crystalline materials, thin films and polymers, can be qualitative and quantitative studies.

Scientists are beginning to use effectively probe crystalline structure at the atomic level when X-ray radiation was discovered in 1895. Using X-ray diffraction has been in two main areas. The first of them is that the fingerprint characterization of crystalline materials. The second is to determine their structure. Each crystalline solid has unique characteristic X-ray powder pattern which used as a its identification, called “fingerprint identification” X-ray crystallography can be used to determine its structure to identified of the material in example, what the interatomic distance and angle are and how the atoms pack together in the crystalline structure etc.

X-ray diffraction is one of the most important tools used in the characterization of solid state chemistry and materials science. Using X-ray diffraction we can easily determine the size and shape of the unit cell for any given compound.

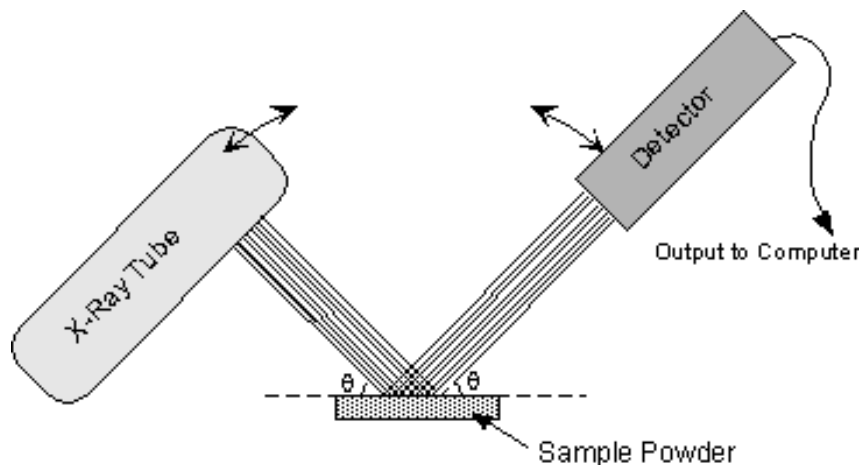


Figure 3-22: XRD Device Diffraction^[142]

3.2.3.2 Spectroscopic Analysis

Most molecules absorb ultraviolet or visible light.

$$A = \epsilon bc \quad (3.8)$$

A, the absorbance of light in the equation represents. c, the concentration of light absorbing agent and b is thickness which is the light will enter into the material. Absorbance values of the light is directly proportional to the those parameters. Absorption measure transitions, from the ground state to the excited level.

$$E = \frac{hC}{\lambda} = \frac{1241}{\lambda} \quad (3.9)$$

H in the equation, plank constant (6.626×10^{-34} J. S.) and C is the speed of light (3.0×10^8 m/s).

The energy of the optical band gap of the nanomaterial (EOBB), 1241 (evm) value divided by wavelength (λ) is calculated. This λ (nm), UV-VIS measurements obtained from the graph corresponds to the absorption edge.

3.2.4 Electrical Characterization

Photovoltaic (PV) cells are non-linear energy sources, weather conditions change as soon as the system operating point has been changed.

Current-voltage values of PV devices; hence the power output and operating efficiency, the seasonal parameters such as radiation intensity and temperature, are affected considerably.

Therefore, PV panels, knowledge of performance that they showed under real atmospheric conditions is important..Installs the most commonly used in the testing apparatus, resistance-type loads, capacitance-type loads, and the loads electronically.

Such devices are able to make measurements automatically or manually.

During the automatic measurement, electronic load in constant current mode, the voltage is measured by the current value of zero, the open circuit voltage of the PV panels (V_{OC}) serves.

Provided it remains below the maximum current value of the PV panels can withstand, the current value at which the voltage is zero, the short circuit current (I_{SC}) serves.

For all of the radiation intensity in the tester, current-voltage (I-V) and voltage-power (V-P) graphs can be generated. Maximum power transfer will allow the load values can be determined.



Figure 3-23: IPCE (EQE) measurement system.

4. RESULTS AND DISCUSSION

In this chapter, the characterization results of ZnO nanorods and electrical characterization of DSSC are given. There are four DSSC samples was performed which are different from each other,

In the first example, after seeding performed on FTO plate, grown ZnO nano-rods takes one hour and sample was allowed to stand in the dye. After Electrolyte applied and preparing the counter electrode it was formed into a solar cell. Finally, electrical measurements were performed.

In the second example, after seeding performed on FTO plate, grown ZnO nano-rods takes six hour and sample was allowed to stand in the dye. After Electrolyte applied and preparing the counter electrode it was formed into a solar cell. Finally, electrical measurements were performed.

In the third and fourth example, seeding done in the same way on the FTO plate, ZnO nano-rods were grown for 5 hour. Then, to extend the active area, located nanorods on the surface, ZnO particles were coated using spin coating (respectively 12.5% and 25%). Finally, Electrolyte applied and preparing the counter electrode it was formed into a solar cell and electrical measurements were applied.

ZnO nanorods of various sizes were successfully synthesized on glass substrates by decomposition of zinc nitrate tetrahydrate and HMT at room temperature using sonochemistry. Growth was carried out within 60 - 360 min, subsequent to a 30 min seeding process as stated in the experimental section. Optical Microscope, Scanning Electron Microscope (SEM), Energy-dispersive X-ray spectroscopy (EDS), X-RAY and electrical Measurement System used to analyze both the structural, elemental composition and lastly, sonochemically grown ZnO nanorods of electrical graphic features were revealed.

4.1 Morphological Characterization

To examine the surface of ZnO nanorods, optical microscopy, AFM and Scanning Electron Microscopy were used. These techniques provide information on the surface of ZnO nanorods accumulation and structures obtained.

4.1.1 Optical Microscopy Analysis

All samples were characterized by an optical microscope. Fig4.1 show us ZnO seed layer deposited on FTO coated substrate, and other one (Fig 4.2) show us ZnO nanorod growth image. The final image(Fig4.3) is taken from the coated ZnO nanoparticles on ZnO nano-rods.

Images were taken from all samples at 100x magnification. It can be seen that higher magnification gives a better resolution. These images also show that the particles are widely dispersed on the substrate. From high resolution of the taken image, The arrangement of seeds seems to be better. However, due to some limitations in the optical microscope image shows superficial.

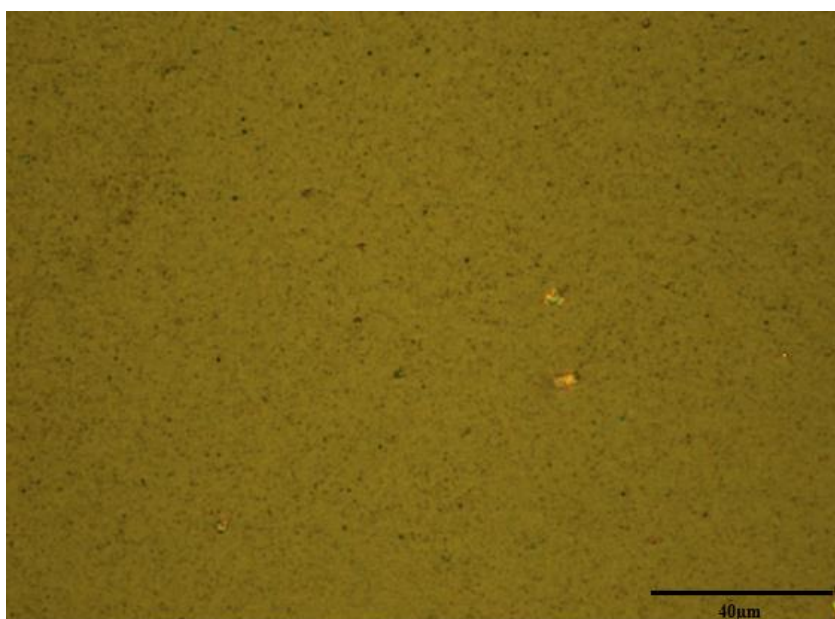


Figure 4-1: Optical Mic. Image of ZnO Seed Layer 30 min, 50% Amplitude Taken from Sample(64) (100X Magnification applied)

Fig 4.1 says that although it is not very clear image received from the optical microscope, creating an idea in our minds. We could infer that seeding is done why the small black dot are placed intermittently. In Figure 4.1, which are ZnO seed layer covers the whole area. But, it's not homogenous. Zn particles accumulated at some

points. ZnO nanorod density is also increased at these points. Without seed layer, ZnO nanorods are lying randomly on the substrate.

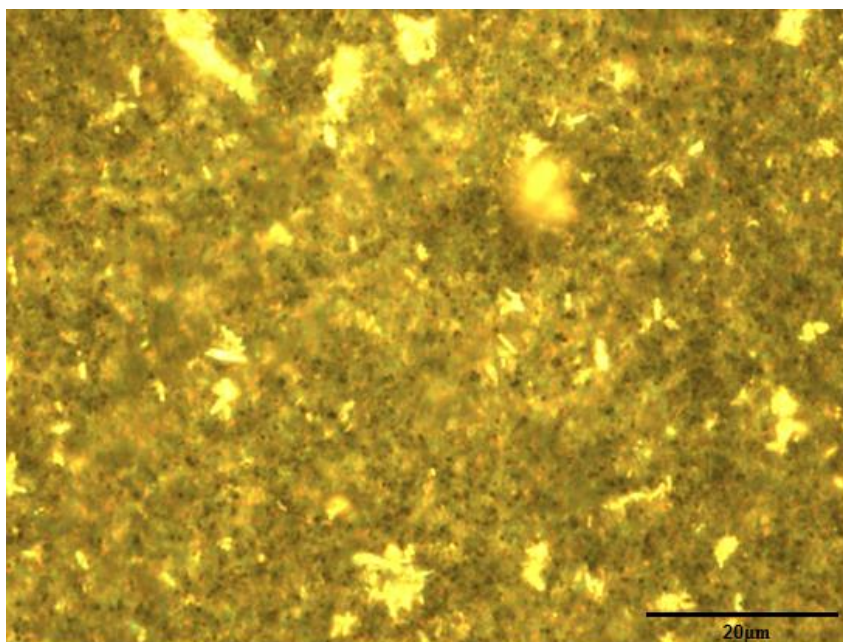


Figure 4-2: Optical Mic. Image of ZnO Nanorods 60 min, 50% Amplitude Taken from Sample(68) (50X Magnification applied)

Fig 4.2 Image was taken after nanorod process. Despite the lack of optical microscopy to measure the length of the nanorods is that the light is bright in some places, it is understood that the gaps between the nanorods.

Growth of the ZnO nanorods is not homogeneous in Figure 4.2. Where the deposition of ZnO seed, ZnO nano rods which is better formation was observed. ZnO nanorods are connected to each other. This connection network in nanorods allows better electrical mobility.

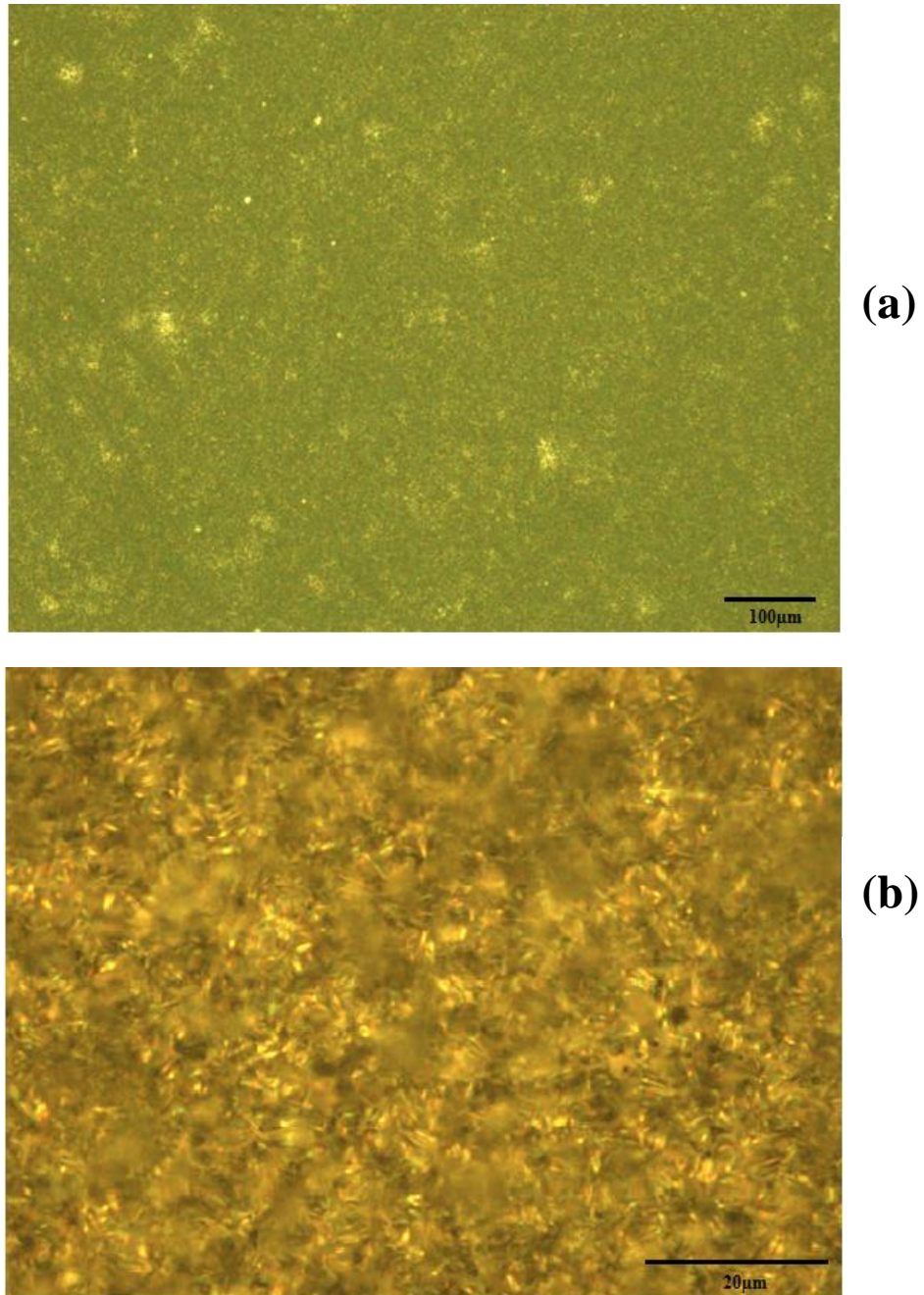


Figure 4-3: Optical Mic. Image of Additional ZnO NanoParticles Layer on NanoRods Layer 30 min, 50% Amplitude Taken from Sample(83) (a.10X b.100X Magnification Applied)

In Figure 4.3, ZnO nanoparticles on the nano rod is coated with spin coating. The surface of depletion layer expands. Therefore, we thought it would increase electrical efficiency. In Fig 4.3 image, brightness is lost. Even at some point blurry areas are available. We can estimate that the gap is filled with nanoparticles. Magnification images show the uniform distribution of ZnO nanoparticles on the FTO substrate.

4.1.2 Sectional Analysis

Disperse dye between the ZnO nano-rods is an important parameter. Length of the nanorods must exceed one micron. Otherwise, dye can not penetrate into sample and it will reduce the efficiency of the solar cell.

Nanorods, at room temperature, a maximum period is 0.8 cycle and the maximum power of 0.5 magnitude in a one hour 300 nanometers grow was observed. Therefore, this process was repeated 5 times and allowed to rise above 1.5 micron length of the nanorods.

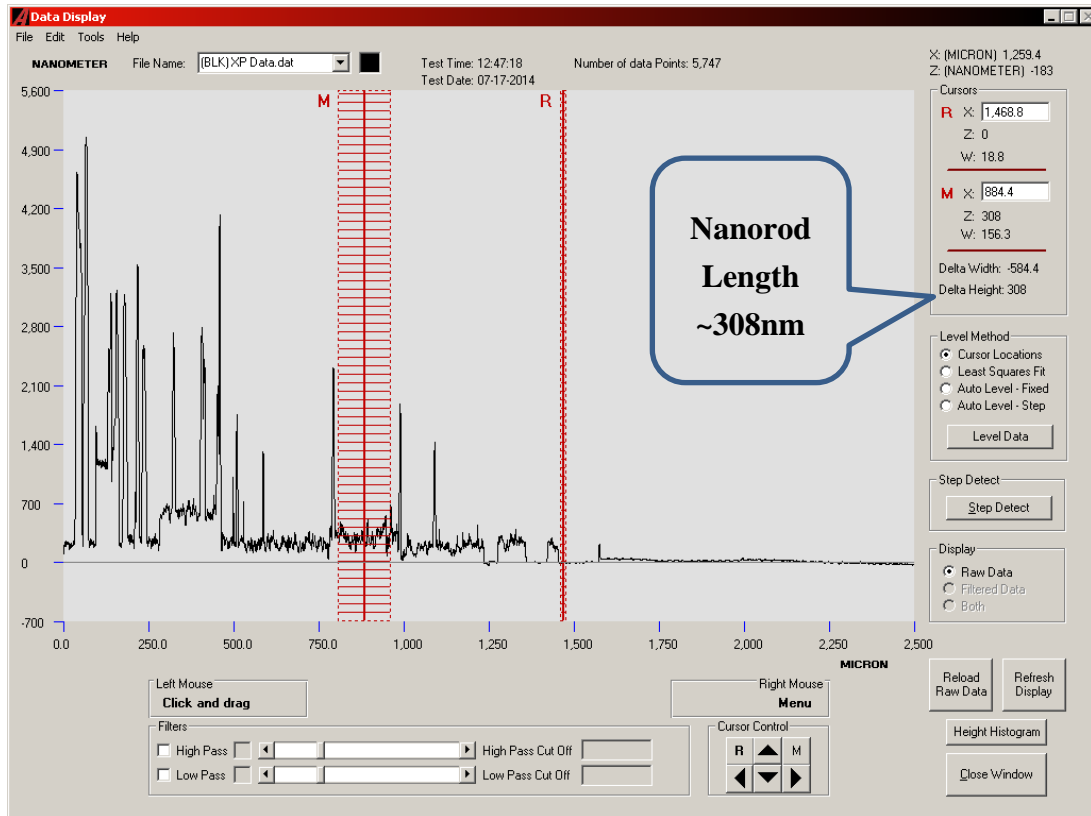


Figure 4-4: Profilometer Graph of ZnO Nanorod Length , 50% Amplitude Taken from Sample, Growth Time 60min

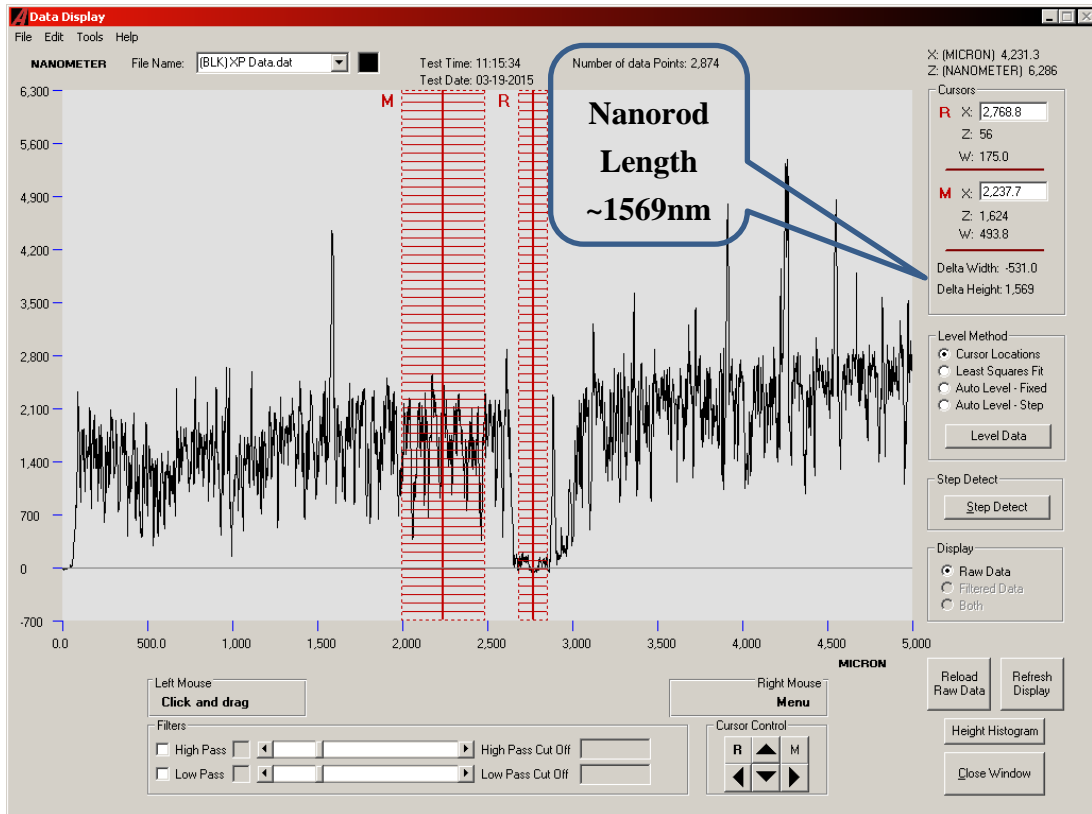


Figure 4-5: Profilometer Graph of ZnO Nanorod Length Taken from Sample, Growth Time 5x60min, 50% amplitude

The length of the nanorods grew to 1.5 microns so that the device could be structured.

4.1.3 AFM Analysis

The image shows seeds stuck to the FTO glass surface clearly. It also verifies the image of the optical microscope. The height of the nano-rods are outside the working area of the AFM, and thus AFM image could only be taken at seeding layer.

For atomic force microscopy images, Digital Instruments NanoScope III-A system is used. The average diameter of the length of the seeds was measured at 500nm.

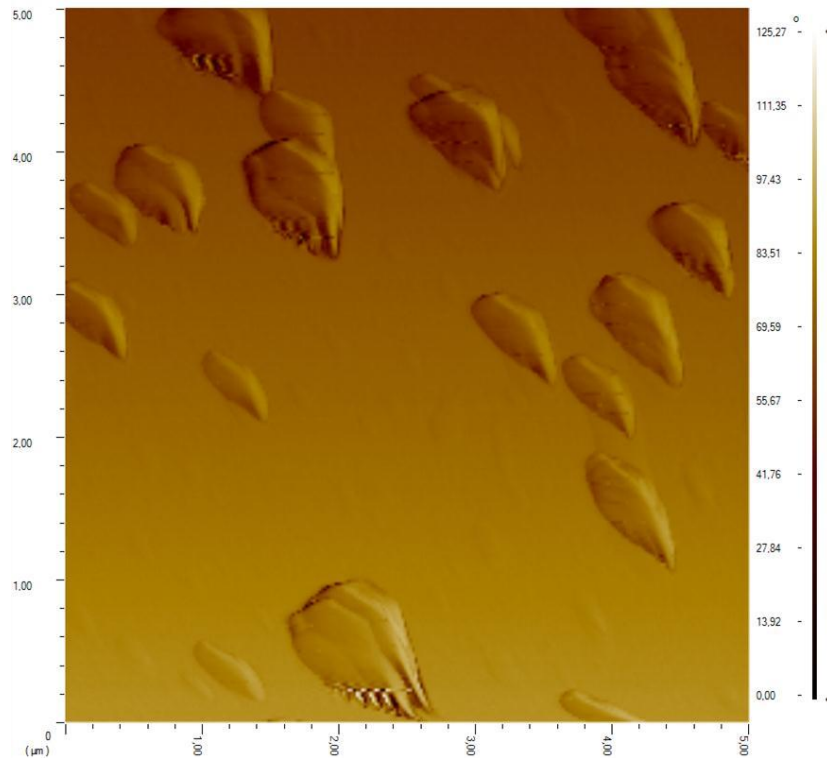


Figure 4-6: AFM Image of Seed ZnO Layer

4.1.4 Scanning Electron Microscopy Analysis (SEM)

One other morphological characterization device for ZnO nanorods is Scanning Electron Microscopy (SEM). Scanning Electron Microscope (SEM) images of the ZnO nanorods were taken at Düzce University. Device Brand: FEI, Device Model: Quanta 250 FEG and Waterloo Advanced Technology Laboratory, University of Waterloo, Zeiss of ULTRA Plus. Scanning Electron Microscope is a type of electron microscope producing an image by scanning the sample with a focused electron beam. Interaction of electrons with the electrons in the sample can be detected, through a variety of signals. These signals contain information about the surface and composition. SEM can take image in a better resolution than 1 nm and samples can be analyzed in high vacuum and low vacuum environment.

Images with different magnification were taken in 3 different areas. First, the SEM images of ZnO seed layer are placed in Fig 4.7. Then, the images of ZnO nanorods are placed in the Fig 4.8 Final image Fig 4.9. is taken from the coated ZnO nanoparticles on ZnO nano-rods.

We measured electrode morphology, size and diameter using SEM device. For seed layer, diameter of the covered surface area was 100nm on average while the height was about 50nm.

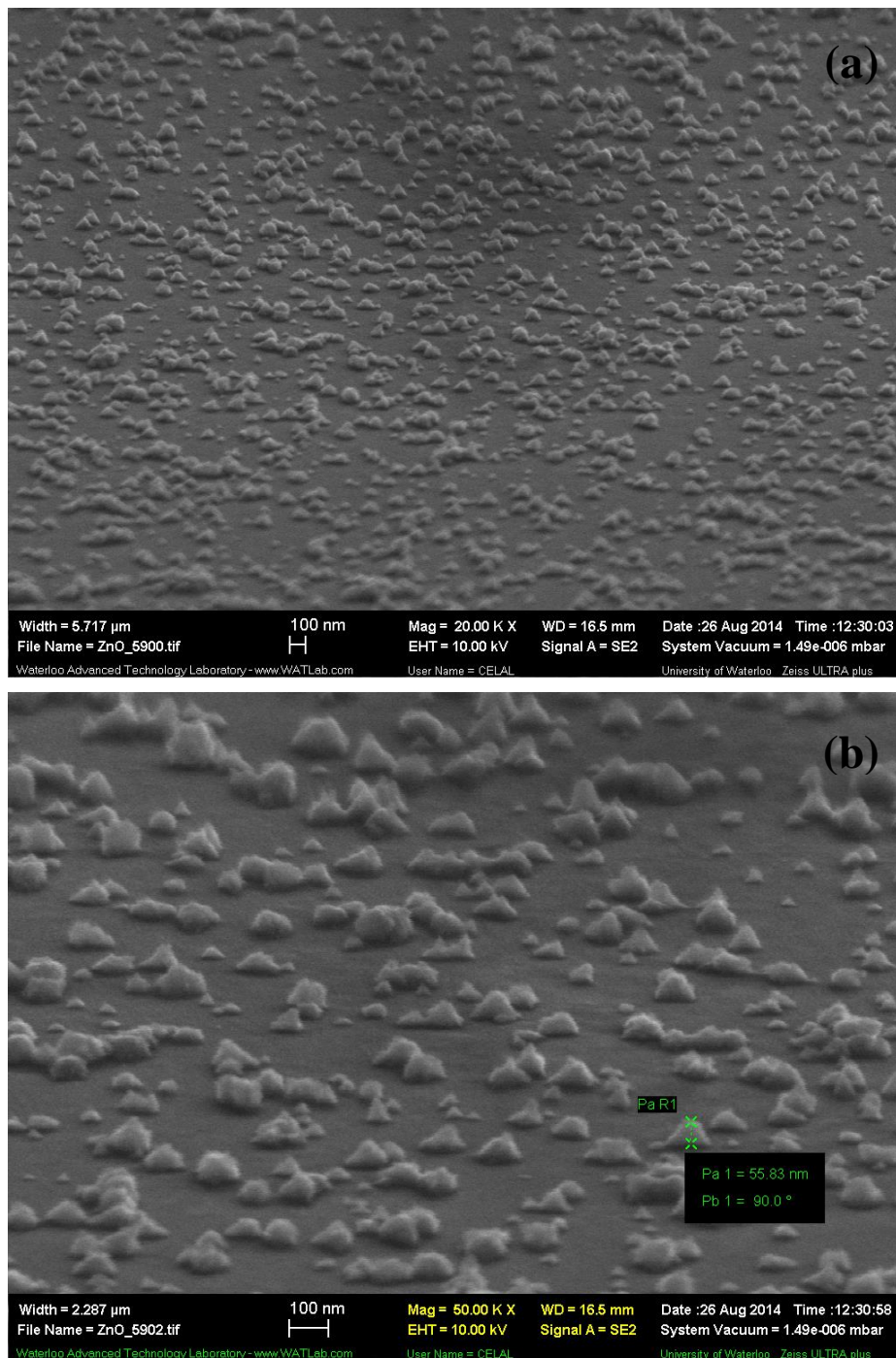


Figure 4-7: SEM Images of ZnO Seed Layer 30 min, 50% Amplitude Taken from Sample(59) (a) is Low Magnification(20000x Respectively) and (b) is High Magnification (50000x Respectively)

For nanorod layer, following the 5 fold growth process nanorod length grew to about 1.3 μ m and to 250nm.

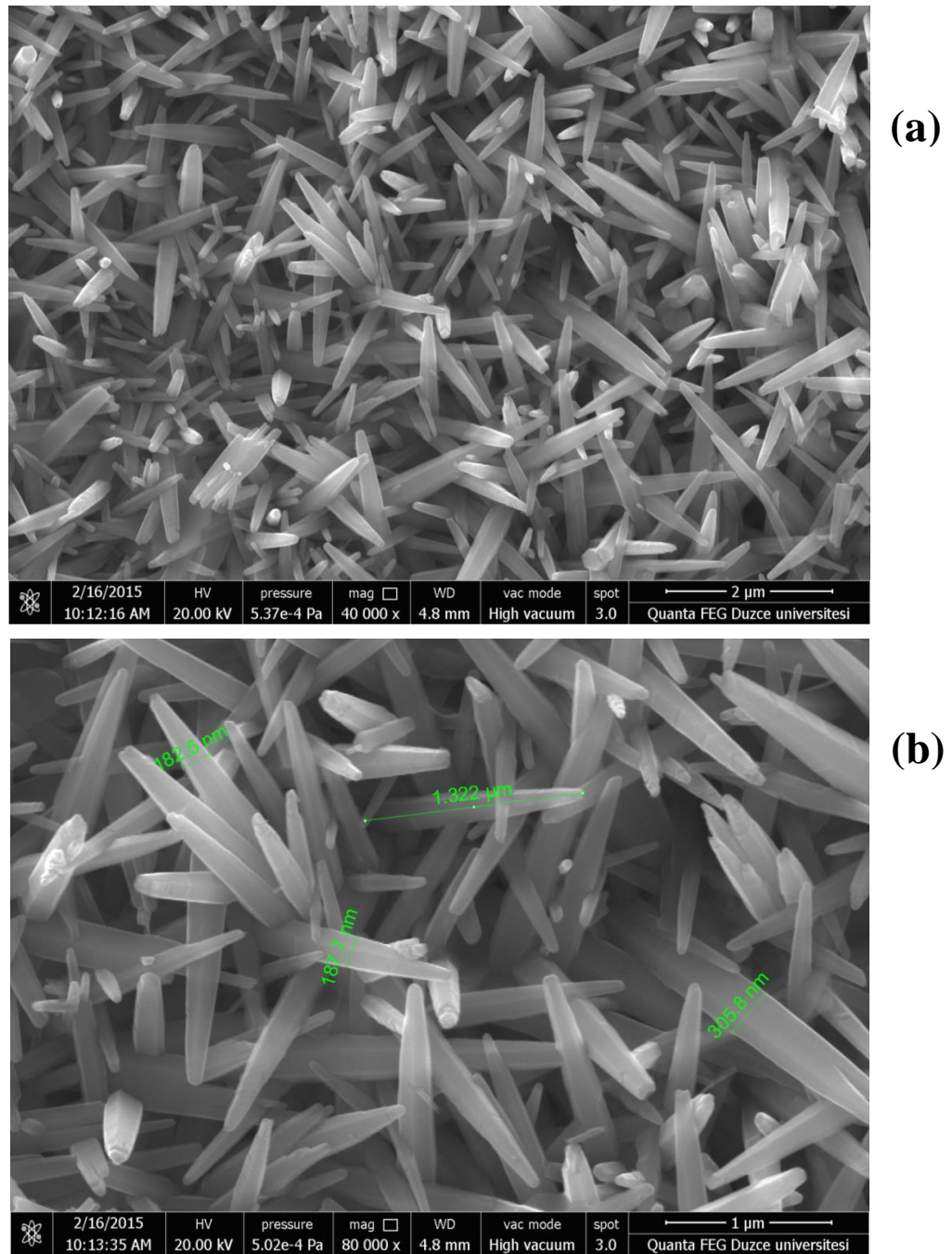
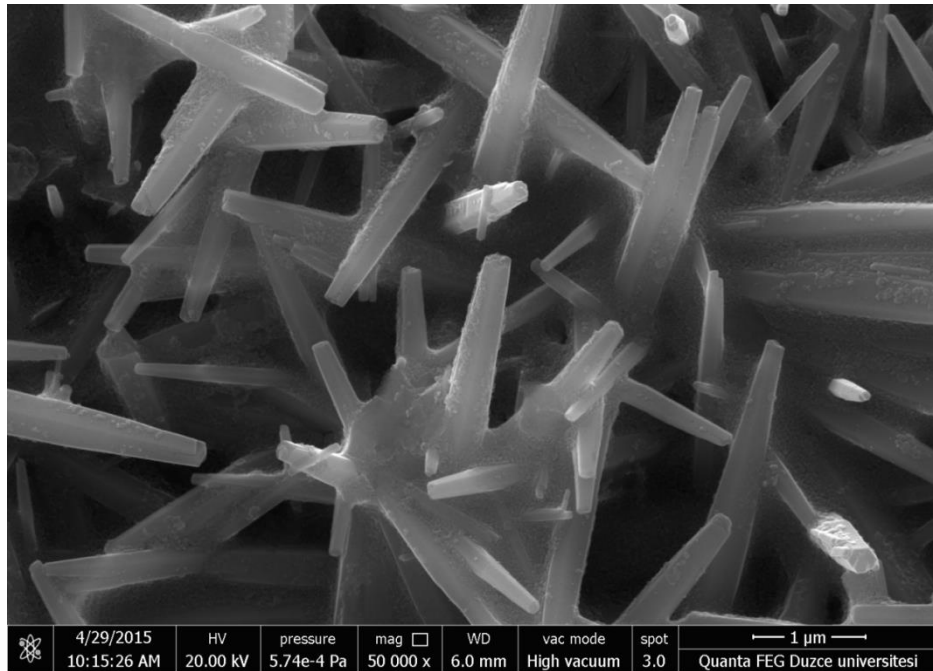
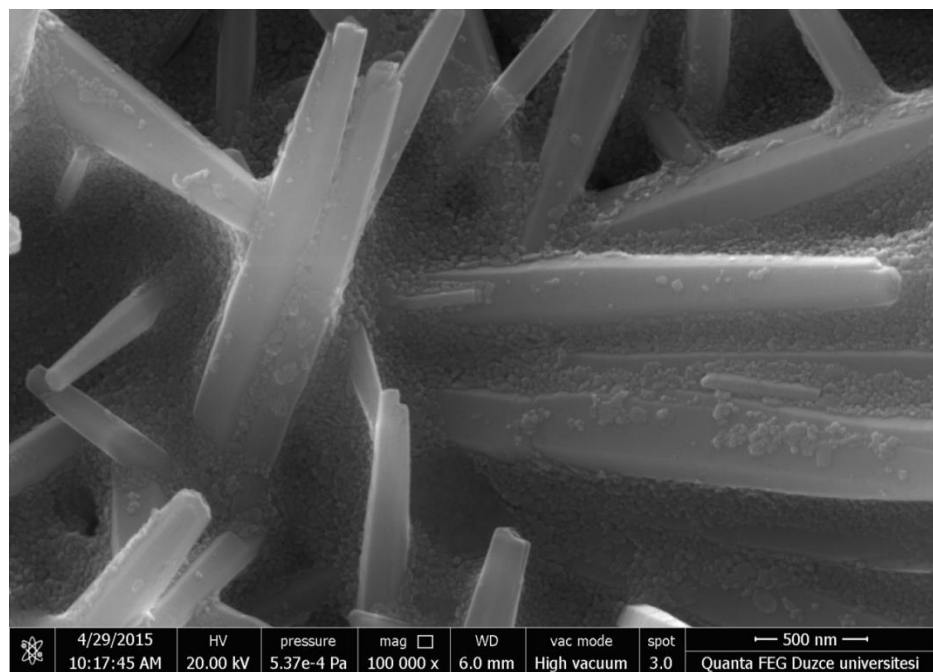


Figure 4-8: SEM Images of ZnO Nanorod Layer 5x60 min, 50% Amplitude Taken from Sample(68) (a)is Low Magnification(40000x Respectively) and (b) is High Magnification (80000x Respectively)



(a)



(b)

Figure 4-9: SEM Images of Additional ZnO 12.5% Concentration Nanoparticle Layer on ZnO Nanorod Layer 5x60 min, 50% Amplitude Taken from Sample. (a) is Low Magnification (50000x Respectively) and (b) is High Magnification (100000x Respectively)

We expect the surface area of nanorods to extend. Gaps between nanorods are closed, resulting in a drastically reduced PCE.

Figure 4.9 shows the SEM image was sonicated for 60 min at 50% amplitude of the ultrasonic probe. Dense, homogeneous growth was observed in this sample. Optical microscope images are consistent with the SEM images. SEM image clarity is better seen than the optical microscope. SEM images are proof of the huge density of ZnO nanorods grown on glass substrates. ZnO nanorods are combined at different directions on the substrate, where the seed layer of ZnO particles accumulates.

Duration of sonication applied to the component is an important parameter on the sonochemically grown ZnO nanorods. 30 minute sonication resulted ZnO nano rods with less density and lower aspect ratio. When sonication time was increased from 30 minutes to 60 minutes, more intense and longer ZnO nanorods were obtained. The average length of ZnO nanorods was ~ 300nm. As this length is not sufficient for dye absorption, the amplification process was repeated 5 times to obtain a nanorod length of ~1500nm.

The surface morphology of the ZnO structure has a rod-shaped structure. While some nanorods typically have a hexagonal shape, some have a tapered and sharp tip. Also some ZnO nanorods with a long sonication period form cluster, nano flowers or similar structures. Nanorods are in contact with each other and the Sn electrodes, creating a nanorod network.

4.2 Elemental Analysis

Elemental analysis of sonochemically grown ZnO nanorods was performed by Energy Dispersive X-ray Spectroscopy (EDS).

4.2.1 Energy Dispersive X-ray Spectroscopy Analysis (EDS)

EDS measurements were carried out after SEM images were taken in the same SEM. Composition of the ZnO nanorod was analyzed by energy dispersive spectroscopy (EDS). EDS spectrum of a ZnO nanorods is shown in Fig. 4.10. The major components of the ZnO nanorod based DSSC are zinc, oxygen and Sn. Zn has the highest amount in the EDS map, followed by oxygen and Sn. Sn originates from the FTO glass substrate; Ca and Si from the substrate of glass.

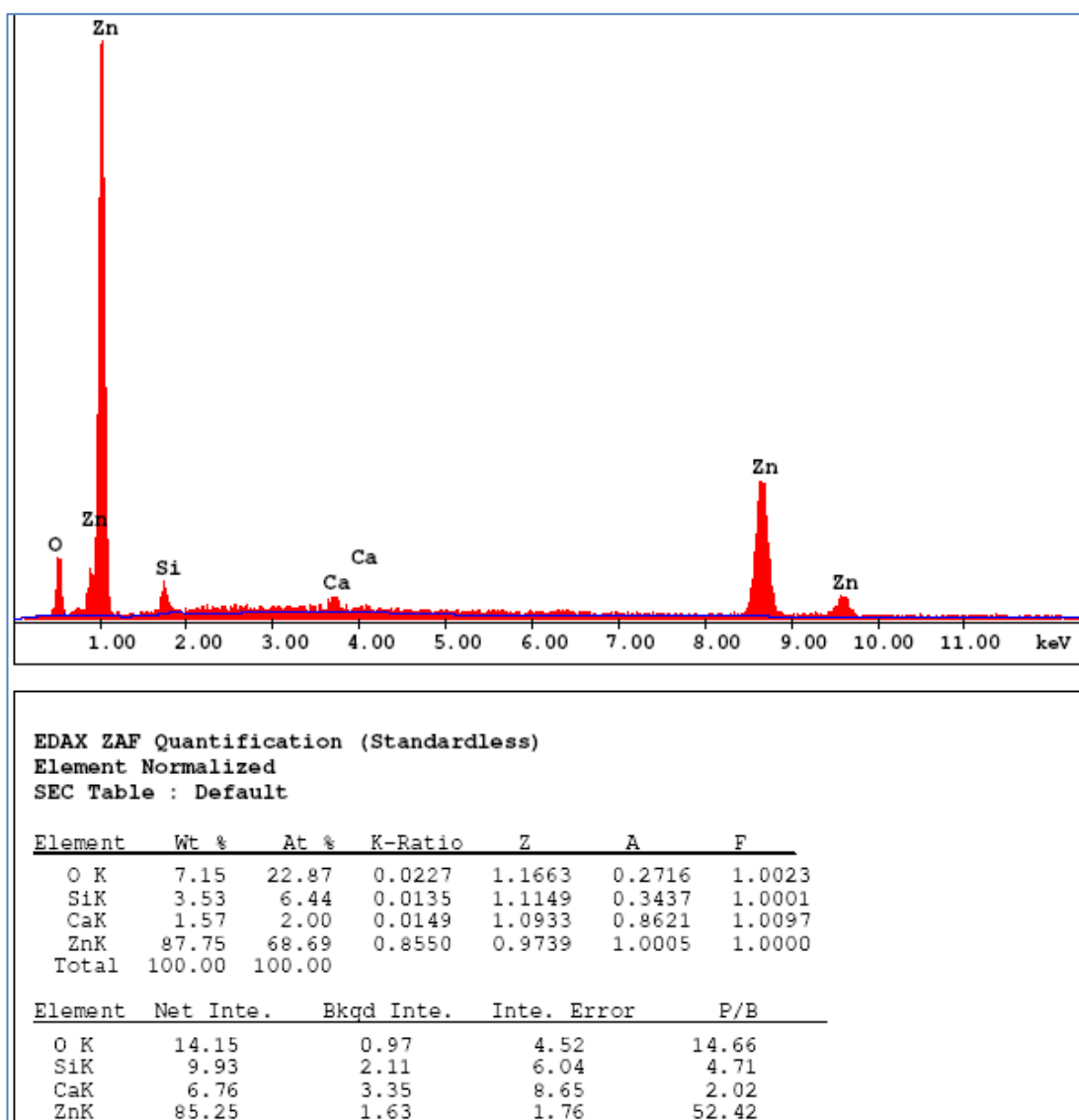


Figure 4-10: EDS Spectrum of ZnO Nanorod

4.3 Structural Analysis

4.3.1 XRD Analysis

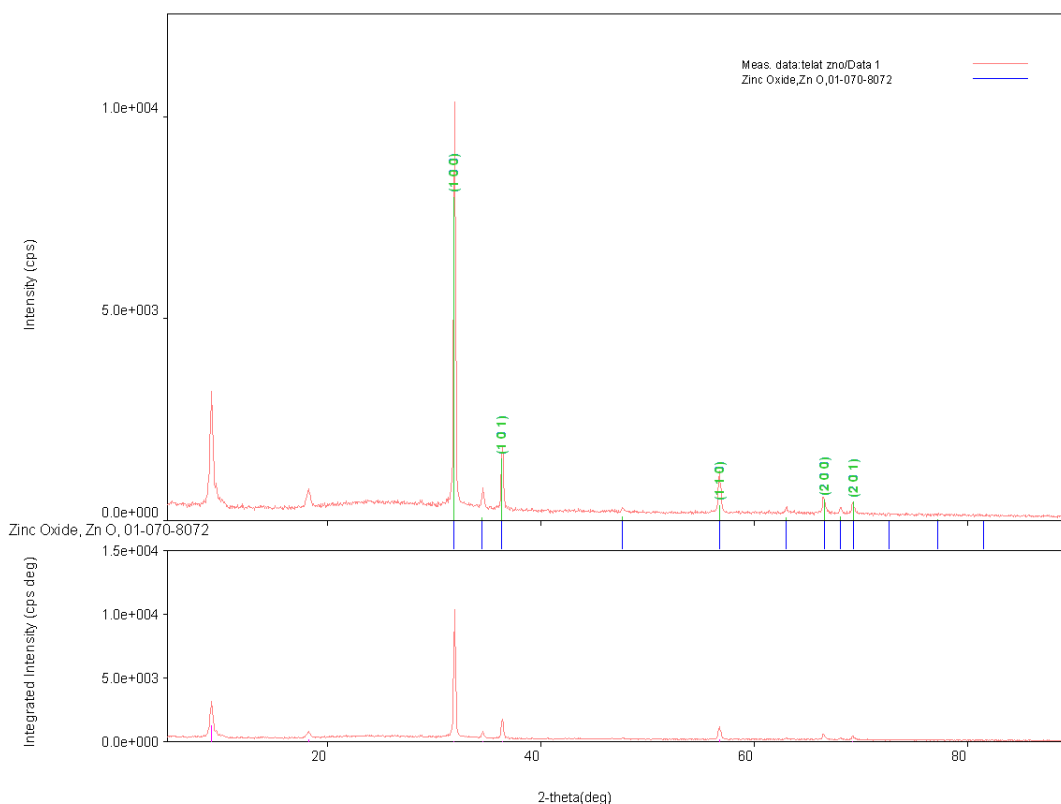


Figure 4-11: XRD Pattern of Sonochemical Growth ZnO Nanorods Taken from Second Device.

Figure 4-11, represents the XRD pattern of the sonochemically growth nanorods. The peaks at 31.84°, 34.52°, 36.33°, 56.71°, 68.13° degree represents the hexagonal wurtzite structure. Typical main peaks at 31.84° and 36.33° are related to 100 and 101 crystal orientations of hexagonal wurtzite structure. Compared to XRD pattern of nanoparticulated wurtzite ZnO (JPCDS card number: 36-1451) peaks at 47.63°, 68.13° and 69.18° couldn't be observed due to oriented structure of nanorods. The peaks below 20° do not correspond to the wurtzite hexagonal ZnO crystal structure. According to structural analysis from the database, these peaks correspond to the organometallic zinc compounds such as zincpropionate, which is attributed to incomplete oxidation reaction of organometallic zinc precursor (zinc (II) acetate or Zinc (II) nitrate) under sonochemical conditions.

4.3.2 Spectroscopic Analysis

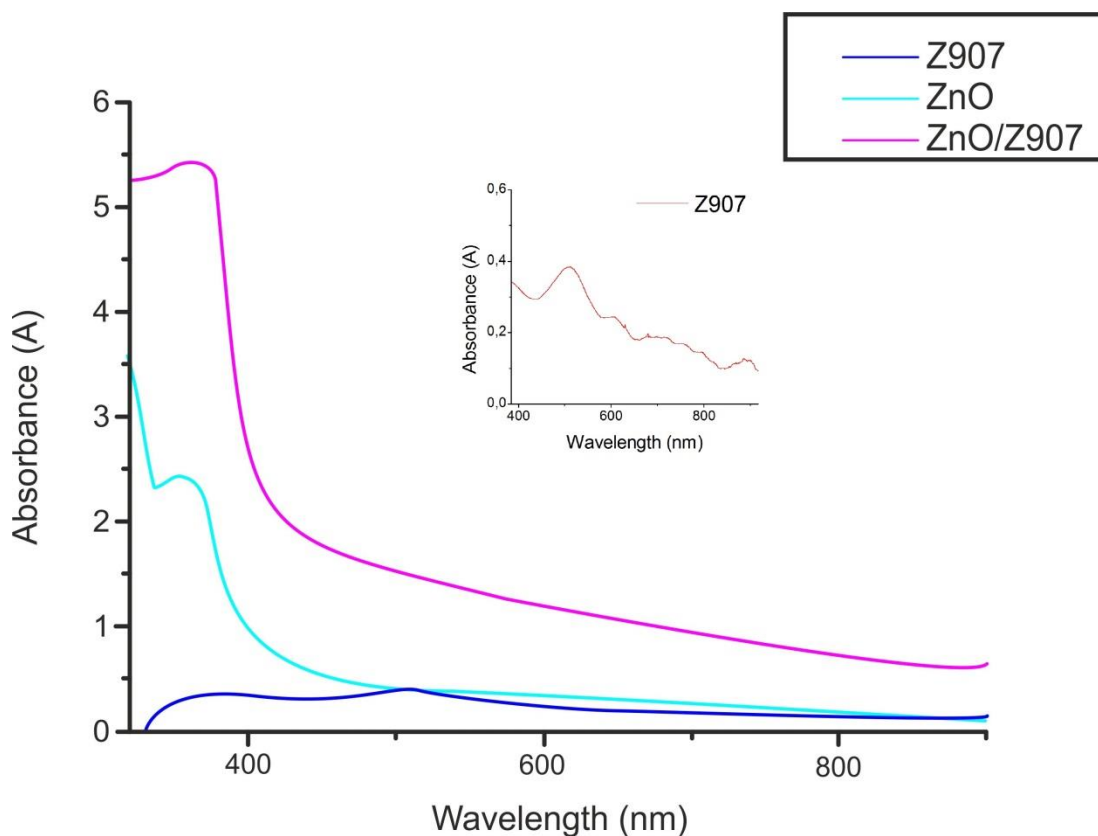


Figure 4-12: UV-Vis Spectroscopic Analysis Result

UV-V absorption spectra of ZnO nanorods and Z907 solution in ethanol (0.3 mM) adsorbed by ZnO nanorods are presented in Figure 4.12. Absorption onset for ZnO nanorods is at ~400 nm, corresponding to the optical band gap ($E_{G, opt}$) to ~3.2 eV in accordance with the literature.

Z907 in ethanol, exhibits three identical peaks at about 500 nm one main peak which correspond to π - π^* transition of the ligand and around 600 and 700 nm two broad peaks attributed to the metal to ligand charge transfer (MLCT) respectively. There is no significant change in the absorption bands on ZnO electrode.

4.4 Electrical Analysis

4.4.1 Current-Voltage (J-V) Characterization

Photovoltaic characterizations of the devices were performed by current density-voltage (J-V) measurement under standard conditions at $100\text{mW}/\text{cm}^2$ irradiation power with AM1.5 spectral distribution. The J-V curves were presented in Figure 4-14 and Figure 4-15. Four different devices fabricated with three different ZnO electrodes were compared. For the first device, sonication time was one hour. Thus, the lowest level of efficiency was obtained from device 1. Parameters presented in table 4-1 show device-1 exhibited lowest photovoltaic conversion efficiency (PCE) with lowest short circuit current of $0,32\text{ mA}/\text{cm}^2$. The reference device, device-2 is fabricated with ZnO electrode consisting of pure sonochemically grown nanorods. Device-3 and 4 consisted of sonochemically grown ZnO nanorods and additional layer of ZnO nanoparticles spin casted from 12.5% (w/v) and 25% (w/v) water based suspension respectively. Extracted photovoltaic parameters were summarized in Table 4-1. Device 2, sonicated for 5 hours to grow nanorods, exhibited highest photovoltaic conversion efficiency (PCE) %1.70 with highest short circuit current of $9.06\text{mA}/\text{cm}^2$.

Upon adding additional layer of ZnO nanoparticles from the 12.5% and 25% water suspension, PCE decreases drastically to 1.14% and 1.07%, respectively. It is interesting that PCE decreases drastically when the concentration of ZnO nanoparticles solution density increases. This result shows that, thicker layer of ZnO nanoparticles leads to lower charge collection at electrodes due to charge recombination and more getting trapped in the ZnO layer - short circuit current density (J_{sc}) is higher for device-3 compared to device-4, ($4,2\text{ mA}/\text{cm}^2$ and $3.55\text{ mA}/\text{cm}^2$ respectively).



Figure 4-13: The Production Phase of the Each Devices and Comparison of the Efficiency

Table 4-1: Electrical Chacterization Results of DSSC

Sample No	Properties of Sample	Active area cm ²	Voc mV	Jsc mA/cm ²	FF	Vmp mV	Jmp mA/cm ²	PCE %
Device 1	One Hour Growth	1	600	0.59	0.32	350	0.32	0.11
Device 1	One Hour Growth	1	590	0.60	0.34	330	0.36	0.12
Device 1	One Hour Growth	1	610	0.80	0.30	330	0.45	0.15
Device 1	One Hour Growth	1	590	0.83	0.32	330	0.49	0.16
Device 2	Five Hour Growth	1	620	9.06	0.30	320	5.30	1.70
Device 2	Five Hour Growth	1	600	8.12	0.34	320	5.17	1.66
Device 3	Five Hour Growth+Nanoparticles (%12.5)	1	540	4.20	0.50	360	3.16	1.14
Device 4	Five Hour Growth+Nanoparticles (%25)	1	560	3.55	0.54	380	2.82	1.07

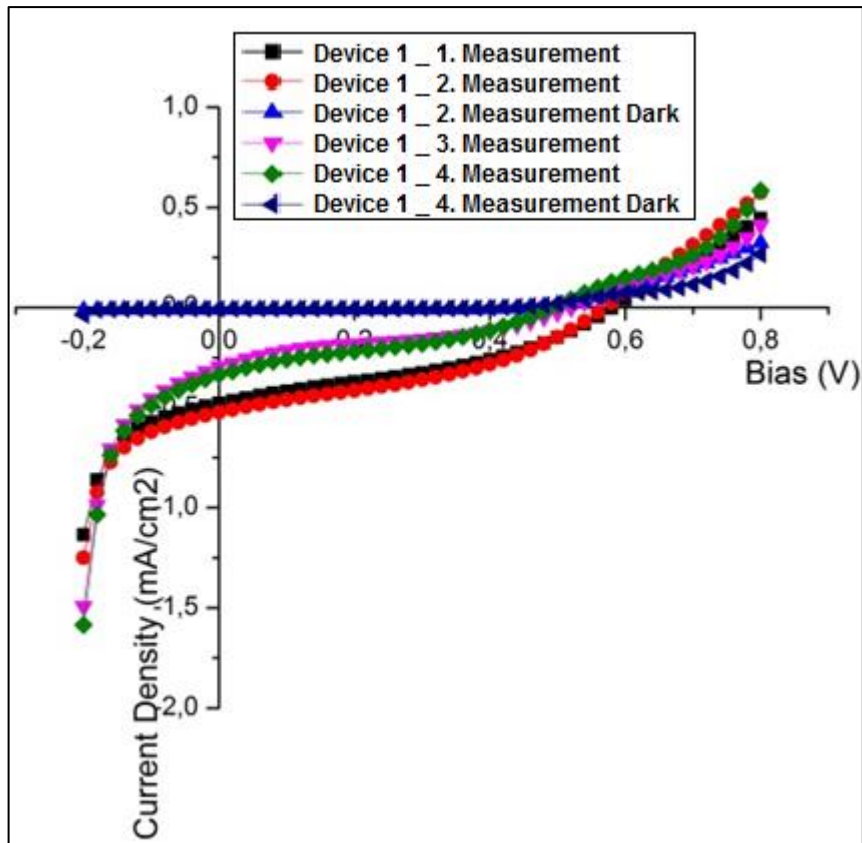


Figure 4-14: The Reference Device, Sonochemically Grown Nanorods in One Hour Without Nanoparticles. (Device1)

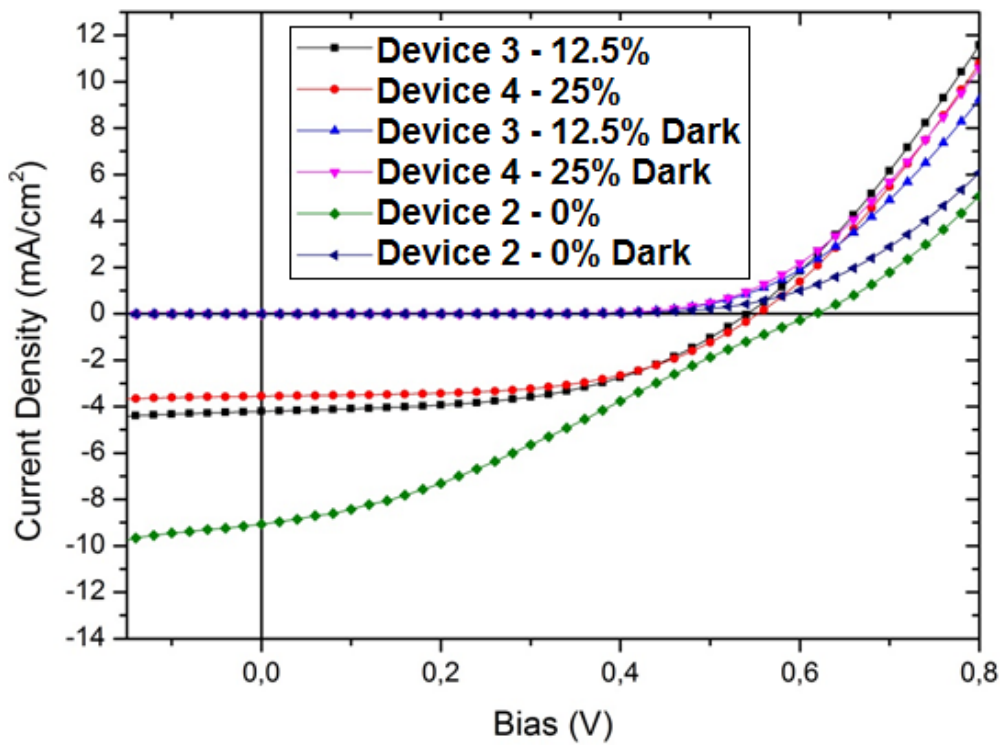


Figure 4-15: Sonochemically Grown Nanorods With Different Nanoparticle Ratios (Device 2-Device 3-Device 4)

4.4.2 Incident Photon to Current Conversion Efficiency (IPCE) Measurement

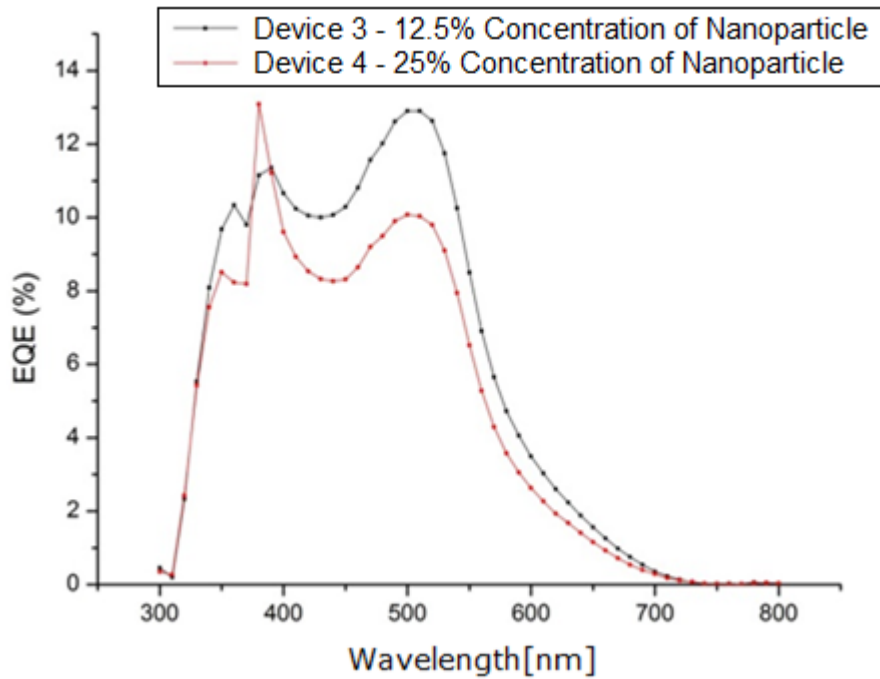


Figure 4-16: Incident Photon to Current Conversion Efficiency (IPCE) Result for Devices 3 and 4

Incident photon to current conversion efficiency (IPCE) measurements were performed under monochromatic light. IPCE spectra obtained for device-3 and device-4 were nearly identical. Device-3 yielded 13% EQE at 500 nm, while device-4 yielded 10% EQE, which is consistent with J_{sc} values obtained from J-V measurements.

CONCLUSION

In this thesis, there have been studies on the make of dye-sensitized solar cell with using sonochemical method of grown ZnO nanorods. Various electrical characterization and measurement techniques were applied to the obtained dye sensitized solar cells. Solar cells can be designed by the sonochemical method which does not harm the environment and with the low cost. There has not been any reports on sonochemically grown ZnO nanorods for fabricated dye sensitized solar cells. It is a new subject.

We observed that sonication period and amplitude adjustment play an essential role in the growth of ZnO nanorods on FTO substrate. Experimental results indicated that 0,8 cycle sonication period and 0,5 amplitude produced the best result, with ZnO nanorods densely grown on the FTO substrate. However, in the amplification process of sonication method, the negative effect of the sound waves scattered the elongation direction of the nanorod causing a non- uniform distribution. To minimize this adverse effect, we increased the distance between the sample and sonication probe.

In optimal conditions at ambient room temperature producing in a high concentration of oriented nanorods requires significantly less time than traditional growth techniques such as evaporation, chemical vapor deposition and sputtering.

Another reason for preferring the sonochemical method is due to low cost and fast fabrication process for ZnO nanorod production to meet the needs for low cost electronic, optoelectronic and energy conversion applications. Therefore, it can be inferred that sonochemical growth process reduces growth time drastically.

The nanorod length of 300nm exhibited 0.16% power conversion efficiency for the first device. This result indicated that the length of nanorods was not long enough for dye molecules to stick on the nanorods. Therefore, we fabricated another device with longer nanorods. We thought that, if the length of the nanorod is slightly longer that

would increase the power conversion efficiency. Therefore nanorod growth process was repeated by 5 consecutive periods. New solution was prepared for each cycle. Repeating the growth process for 5 times, an average nanorod length was obtained 1.5 micron and power conversion efficiency went up to 1.7% level.

In order to increase the surface area ZnO nanoparticles were coated on grown ZnO nanorods. As a result, we thought power conversion efficiency can be further increased when the dye was absorbed by on large surface area. So, we decided to fabricate the dye sensitized solar cell device.

For coating, Zinc Oxide Dispersion nanoparticles, which was bought from sigma Aldrich, were used.(As purchased Aldrich product code number of 721077). The average size of the nanoparticles are less than 35 nanometers and it is sold as dissolved (50%) in water.The solution was diluted to 12.5% NP/Water ratio. The nanorods, which length is 1.5 micron, were coated by this diluted solution by spin coating method. The third device was fabricated this way. After the characterization, it was observed that efficiency decreases compared with earlier devices.

Then, fresh nanoparticle solution with higher concentration (25%) was prepared. Fourth electrode was obtained by this solution and the fourth dye sensitize solar cell was fabricated. Although, the concentration of nanoparticles increased to 25%, power conversion efficiency further decreased.

Using SEM we closely observed the third and fourth devices, the nanorod surfaces are coated with nanoparticles, but the gaps between nanorods were filled by nanoparticles. As a result of this less dye molecules were able to penetrate into nanorod structure, and this resulted a decrease of Power Conversion Efficiency. Another explanation might be that since the mobility of the nanoparticles is much less than that of nanorods addition of nanoparticles causes decrease in the Power Conversion Efficiency.

Surface morphology, crystal structure and elemental analysis of the grown nanorod samples were characterized by Optical Microscope, AFM, SEM, EDS and XRD techniques, revealing an intensive expression of the ZnO nanorods.

We successfully fabricated DSSC devices basic on ZnO nanorods grown by sonochemical method. Fabricated devices' electrical characteristics suggest that

sonochemical growth method is very good candidate for low cost solar cell applications.

It was also observed that the seed layer is necessary for crystalline and densely grown nanorods network. Studies showed that ZnO nanorods are grown more uniformly on the surface of FTO substrate with seed layer than the one without seed layer.

The electrical measurements were carried out for different type DSSC device which are Seeding+Growth Nanorod and Seeding+Growth Nanorod+Nanoparticle. In order to neutralize the negative effects of atmospheric conditions, electrical measurements were taken in a glove box.

Future Works;

- ZnO nanorod will be grown by different growth parameters (temperatures, molarity, power, distance between sample and probe etc.
- ZnO nanorods can be replaced by TiO₂ nanorods and result might be compared.
- Different type of nanoparticles can be tried.
- Different pH values can be tried to get different nanostructure.

REFERENCES

1. Hatfield C.B.,1997,Nature,387,121p
2. Service, R. F. Science 2005, 309, 548.
3. Van Zolingen, R. J. C.; Van de Sanden, M. C. M.; Janssen, R. A. J. Solar Cells, Technische Universiteit Eindhoven, 2010.
4. Chapin D., 1954, Construction of Power Photocells,1-26-54&2-23-54, Book 20349, Loc. 124-11-02,AT&T Archives,Warren,NJ
5. Alsema E.A.,2000,Prog.Photovoltaics,8,17p
6. Gratzel M., 2006,Prog.Photovoltaic:Res Appl., 14, 429p
7. Robertson N., 2006 Angew. Chem.,118,2398p;2006, Angew Chem.Int. Ed., 45, 2338p
8. Regan B.O. and Gratzel M.,1991, Nature, 35, 737p
9. Avinash P. Nayak, Aaron Katzenmeyer, Yasu Gosho, Sonochemical Synthesis of Zinc Oxide Nanowire Arrays on Silicon and Glass Substrates
10. Ballıpınar F., Çinko Oksit (ZnO) Nanoyapıların Organik Güneş Pillerinde Uygulanması
11. Zhang, H., Feng, J., Wang, J., Zhang, M., (2007). Preparation of ZnO nanorods through wet chemical method. Material Letters, 61, 5202-5205.
12. Minemato, T., Mizuta. T., Takakura, H., Hamakawa, Y., (2007) Antireflective coating fabricated by chemical bath deposition of ZnO for spherical Si Solar Cells, Solar Energy Materials and Solar Cells, 91, 191-194.
13. Zhang, H., Feng, J., Wang, J., Zhang, M., (2007). Preparation of ZnO nanorods through wet chemical method. Material Letters, 61, 5202-5205.
14. Kalita, G., Masahira, M., Koichi, W., ve Umeno, M., (2010).Nanostuctured morphology of P3HT:PCBM bulk heterojunction solar celss, Solid-State Electronics 54:447-451
15. Spanggaard, H., Krebs, F., (2004). A brief history of th development of organic and polymeric photovoltaics, Solar Energy Materials & Solar Energy 83: 125-146
16. <http://lasp.colorado.edu/~bagenal/3720/CLASS4/4Sunlight.html>
17. Moser, J. 1987, vol. 177, pp. 133-166
18. O' Regan,“ A low-cost high-efficiency solar cell based on dyesensitised colloidal TiO₂ films” A low-ature 1991,353,737-740
19. Nazeeruddin, “Engineering of efficient panchromatic sensitisers for nanocrystalline TiO₂ –Based Solar Cells”J. Am. Chem. Soc. 2001. 123, 1613 - 1624
20. Van Zolingen, R. J. C.; Van de Sanden, M. C. M.; Janssen, R. A. J. SolarCells, Technische Universiteit Eindhoven, 2010.
21. Hwang, S.; Lee, J. H.; Park, C.; Lee, H.; Kim, C.; Park, C.; Lee, M. H.;Lee, W.; Park, J.; Kim, K.; N. G.;Park, Kim, C. Chem. Commun. 2007, 4887.
22. Boschloo, G.; Hagelman, L.; Hagfeldt, A. J. Phys. Chem. B 2006, 110, 13144.

23. Hara, K.; Kurashige, M.; Ito, S.; Shinpo, A.; Suga, S.; Sayama, K.; Arakawa, H. *Chem. Commun.* 2003, 252.
24. Wang, Z. S.; Cui, Y.; Hara, K.; Dan-oh, Y.; Kasada, C.; Shinpo, A. *Adv. Mater.* 2007, 19, 1138.
25. Kim, S.; Choi, H.; Baik, C.; Song, K.; Kang, S. O.; Ko, J. *Tetrahedron* 2007, 63, 11436.
26. Edvinsson, T.; Li, C.; Pschirer, N.; Sch_neboom, J.; Eickemeyer, F.; Sens, R.; Boschloo, G.; Herrmann, A.; M_llen, K.; Hagfeldt, A. *J. Phys. Chem. C* 2007, 111, 15137.
27. Kim, C.; Choi, H.; Kim, S.; Baik, C.; Song, K.; Kang, M. S.; Kang, S. O.; Ko, J. *J. Org. Chem.* 2008, 73, 7072.
28. Mishra A.; Fischer, M. K. R.; Bauerle P. *Angew. Chem. Int. Ed.* 2009, 48, 2474.
29. Bach, U.; Lupo, D.; Comte, P.; Moser, J. E.; Weissörtel, F.; Salbeck, J.; Spreitzer, H.; Gratzel, M. *Nature*, 1998, 395, 583.
30. O'Regan, B.; Schwartz, D. J. *Appl. Phys.* 1996, 80, 4749.
31. Sanadeera, R.; Fukuri, N.; Saito, Y.; Kitamura, T.; Wada, Y.; Yanagida, S. *Chem. Commun.* 2005, 2259.
32. Murakoshi, K.; Kogure, R.; Yanagida, S. *Chem Lett*, 1997, 5, 471.
33. O'Regan, B.; Schwarz, D. T. *Chem. Mater.* 1998, 10, 1501.
34. Barbe, C. J.; Arendse, F.; Comte, P.; Jirousek, M.; Lenzenmann, F.; Shklover, V.; Gratzel, M. *J. Am. Ceram. Soc.* 1997, 80, 3157.
35. Günes, S.; Neugebauer, H.; Sariciftci, N. S. *Chem. Rev.* 2007, 107, 1324.
36. Wöhrle, D.; Meissner, D. *Adv. Mater.* 1991, 3, 129.
37. Qin H.; Wenger, S.; Xu, M.; Gao, F.; Jing, X.; Wang, P.; Zakeeruddin, S.M.; Gratzel M. *J. Am. Chem. Soc.* 2008, 130, 9202.
38. Halls, J. J. M.; Pichler, K.; Friend, R. H.; Moratti, S. C.; Holmes, A. B. *Appl. Phys. Lett.* 1996, 68, 3120.
39. Theander, M.; Yartsev, A.; Zigmantas, D.; Sundström, V.; Mammò, W.; Andersson, M. R.; Inganäs, O. *Phys. Rev. B* 2000, 61, 12957.
40. Haugeneder, A.; Neges, M.; Kallinger, C.; Spirkl, W.; Lemmer, U.; Feldmann, J.; Scherf, U.; Harth, E.; Gügel, A.; Müllen, K. *Phys. Rev. B* 1999, 59, 15346.
41. Stübinger, T.; Brütting, W. *J. Appl. Phys.* 2001, 90, 3632.
42. Markov, D. E.; Amsterdam, E.; Blom, P. W. M.; Sieval, A. B.; Hummelen, J. C. *J. Phys. Chem. A* 2005, 109, 5266.
43. P. Poizot, S. Laruelle, S. Grugeon, L. Dupont and J.M. Tarascon, *Nature*, 407, 496 (2000).
44. A.C. Dillon, A.H. Mahan, R. Deshpande, P.A. Parilla, K.M. Jones, S-H. Lee, *Thin Solid Films*, 516, 794 (2008)
45. H. Huang, E.M. Kelder and J. Schoonman, *J. Power Sources*, 97-98, 114 (2001)
46. G.H. Lee, J. G. Park, Y.M. Sung, K.Y. Chung, W.Cho and D.W. Kim, *Nanotech.* 20 295205 (2009).
47. P. Limthongkul, H Wang and Y.M. Chiang, *Chem.Mater.*, 13, 2397 (2001).
48. A. Koichi, K. Masashi and M. Yoshihiro, *Denryoku Chuo Kenkyujo Enerugi Gijutsu Kenkyjo Kenkyu Hokoku*, M04014, 19 (2005)
49. M. Asamoto, S. Miyake, K. Sugihara and H. Yahiyo, *Electrochem. Comm.*, 11, 1508 (2009)

50. T. Takeguchi, Y. Kani, T. Yano, R. Kikuchi, K. Eguchi, K. Tsujimoto, Y. Uchida, A. Ueno, K. Omoshiki, M. Aizawa, *J. Power Sources* 112 588 (2002).
51. M. Mamak, N. Coombs and G. Ozin, *J. Am. Chem. Soc.* 122, 8932 (2000).
52. P.H. Larsen, Metal oxide solid state fuel cells; Patent Application, <http://www.faqs.org/patents/app/20090061279>
53. S. Colodrero, A. Mihi, L. Haggman, M. Ocana, G. Boschloo, A. Hagfeldt and H. Miguez, *Adv. Mater.*, 21, 766 (2009)
54. L. Chen, Z. Hong, G. Li and Y. Yang, *Adv. Mater.*, 21, 1434 (2009)
55. E.L. Beltran, P. Prené, C. Boscher, P. Belleville, P. Buvat and C. Sanchez, *Adv. Mater.*, 18, 2579 (2006)
56. H.J. Snaith and L.S. Mende, *Adv. Mater.*, 19, 3187 (2007)
57. M. Gratzel, *Nature*, 414, 338 (2001).
58. V. Wood, M.J. Panzer, J.E. Halpert, J.M. Caruge, M.G. Bawendi and V. Bulovic, *Nanolett.* 3, 3581 (2009).
59. J.M. Caruge, J.E. Halpert, V. Wood, V. Bulovic and M.G. Bawendi, *Nature Photonics*, 2, 247 (2008).
60. S.A. Haque, S. Koops, N. Tokmoldin, J.R. Durrant, J. Huang, D.D.C. Bradley and E. Palomares, *Adv. Mater.* 19, 683 (2007).
61. P.D. Ye, B. Yang, K.K. Ng, J. Bude, G.D. Wilk, S. Halder and J.C.M. Hwang, *Appl. Phys. Lett.*, 86, 063501 (2005).
62. P.D. Ye, G.D. Wilk, B. Yang, J. Kwo, H.J.L. Gossman, M. Frei, J.P. Mannaerts, M. Sergent, M. Hong, K.K. Ng, *J. Electron. Mater.* 33, 912 (2004).
63. M. Lee, S.I. Kim, C. B. Lee, H. Yin, S. Ahn, B. S. Kang, K. H. Kim, J.C. Park, C. J. Kim, I. Song, S. W. Kim, G. Stefanovich, J. H. Lee, S. J. Chung, Y. H. Kim, Y. Park, *Adv. Func. Mater.* 19, 1587 (2008).
64. M. Wu, X.Z. Bo, J.C. Stum, S. Wagner, *IEEE TRANS. ELECTRON. DEVICES*, 49, 1093 (2002).
65. M. Hepel, S. Hazelton, *Electrochim. Acta*, 50, 5278 (2005).
66. P. Mahata, T. Aarthi, G. Madras, and S. Natarajan, *J. Phys. Chem. C*, 111, 1665 (2007).
67. D. Zhao, C. Chen, Y. Wang, W. Ma, J. Zhao, T. Rajh, L. Zang, *Environ. Sci. Technol.*, 42, 308 (2008).
68. C. Chen, W. Zhao, P. Lei, J. Zhao, N. Serpone, *Chem. Eur. J.*, 10, 1956 (2004).
69. A. Khaleel, P.N. Kapoor and K.J. Klabunde, *Nanostructured Mater.*, 11, 459 (1999).
70. J. Mizsei and V. Lantto, *Sensors and Actuators B: Chemical* 6, 223 (1992).
71. A. Kolmakov, M. Moskovits, *Annu. Rev. Mater. Res.*, 34, 151 (2004).
72. E. Comini, G. Faglia, G. Sberveglieri, Z. Pan and Z.L. Wang, *Appl. Phys. Lett.*, 81, 1869 (2002).
73. C. Yu, Q. Hao, S. Saha, L. Shi, X. Kong, Z.L. Wang, *Appl. Phys. Lett.*, 86, 063101 (2005).
74. C.S. Rout, M. Hegde, A. Govindaraj, C.N.R. Rao, *Nanotech.* 18 205504 (2007).
75. G. Sarala Devi, S. Manorama, V.J. Rao, *Sensor Actu. B*, 28, 31 (1995).
76. W. Yuanda, T. Maosong, H. Xiuli, Z. Yushu, D. Guorui, *Sensor Actu. B*, 79, 187 (2001).
77. V. I. Stroganov, M. I. Kostenko, *J. Appl. Spect.*, 33, 1016 (2004).
78. B.D. Clymer, D. Gillfillan, *Appl. Opt.*, 30, 4390 (1990).

79. T. P. Osedach, N. Zhao, L.Y. Chang, S. M. Geyer, A. C. Arango, J. C. Ho, M. Bawendi, V. Bulovic, *Microsyst. Tech. Lab. Ann. Res. Rep.* (2009). 78
80. N. Suzuki, H. Tanaka, T. Kawai, *Adv. Mater.*, 20, 909 (2008).
81. L.-D. Sun, Z.-G. Yan, Y.-C. Pang, L.-P. You, C.-H. Yan, *J. Phys. Chem. C* 111, 13022 (2007).
82. I.-B. Shim, C.S. Kim, *J. Magne. Magnetic Mater.*, 272, 1571(2004).
83. M. Diaconu, H. Schmidt, M. F.-Morariu ,G. Güntherodt, H. Hochmuth, M. Lorenz, M. Grundmann, *Phys. Lett. A*, 351, 323 (2006).
84. P.V. Radovanovic, N.S. Norberg, K.E. McNally, D.R. Gamelin, *J. Am. Chem. Soc.*124,15192 (2002).
85. R. Bazzi, M.A. F.- Gonzalez, C. Louis, K. Lebbou, C. Dujardin, A. Brenier, W. Zhang, O. Tillement, E. Bernstein, P. Perriat, *J. Luminescence*, 102, 445 (2003). 80
86. Y. Pan, Q. Su, H. Xu, T. Chen, W. Ge, C. Yang, M. Wu, *J. Solid State Chem.* 174, 69 (2003).
87. Q.X. Zheng, B. Li , M. Xue , H.D. Zhang ,Y.J .Zhan, W.S. Pang, X.T. Tao, M.H. Jiang, *J. Super Crit. Fluids*, 46, 123 (2008).
88. M. Vasile, P.Vlazan, P.S.froloaga, I. Grozescu, N.M. Avram, E. Rusu, *Phys. Scr. T*, 135, 014046 (2009).
89. K. Mukae, K. Tsuda, I. Nagasawa, *Jap. J. Appl. Phys.*, 16, 1361 (1977).
90. X. Wang, Y. Ding, C. J. Summers, Z. L. Wang, *J. Phys. Chem. B* 108, 8773 (2004).
91. D. S. Ginley, C. Bright, *Mater. Res. Soc. Bull.* 25,15 (2000).
92. T. Fukano, T. Motohiro, T. Ida, H. Hashizume, *J. Appl. Phys.* Doi: 10.1063/1.1866488.
93. P.K. Manoj, B. Josef, V.K. Vaidyan, D.S.D. Amma, *Ceram. Int.* 33, 273 (2007).
94. H.Y. Kim, J.H. Kim, M.O. Park, S. Im, *Thin Solid Films*, 93, 398 (2001)
95. Q. Yang, X. Jiang, X. Guo, Y. Chen, L. Tong, *Appl. Phys. Lett.*, 94,101108 (2009).
96. http://en.wikipedia.org/wiki/Sputter_deposition
97. http://www.icmm.csic.es/fis/english/evaporacion_electrones.html
98. A. Umar, S. Lee, Y.H.Im , Y.B. Hahn, *Nanotech.* 16, 2462 (2005).
99. A. Umar, S. Lee, Y.S. Lee, K.S. Nahm, Y.B. Hahn, *J. Cryst. Growth*, 277, 479 (2005).
100. S.-W. Kim ,S. Fujita , H.-K. Park, B. Yang, H.-K. Kim, D.H. Yoon, *J. Cryst. Growth*, 292, 306 (2006).
101. A.-J. Cheng, Y. Tzeng, Y. Zhou, M. Park, T.-H. Wu, C. Shannon, D. Wang, W. Lee, *Appl. Phys. Lett.* 92, 092113 (2008).
102. B.H. Juárez, P.D. García, A. Blanco, C. López, *Adv. Mater.* 17, 2761 (2005).
103. D.C. Kim, B.H. Kong, H.K. Cho, *J. Mater. Sci: Mater. Electron.* 19, 760 (2008).
104. J.Y. Park, I.O. Jung, J.H. Moon, B.-T. Lee, S.S. Kim, *J. Cryst. Growth*, 282, 353 (2005)
105. Zhuo Chen, T. Salagaj, C. Jensen, K. Strobl, Mim Nakarmi and Kai Shum1, First Nano, a division of CVD Equipment Cooperation, 1860 Smithtown Avenue, Ronkonkoma, NY 11779, USA
106. http://www.aliexpress.com/reactor-vessel_reviews.html

107. Bohac P., and Gauckler L.J. 2000, Oxygen Ion and Mixed Conductors and their Technological Applications, Kluwer Academic Publishers, Dordrecht, 271
108. D.C. Kim, B.H. Kong, H.K. Cho, J. Mater. Sci: Mater. Electron. 19, 760 (2008).
109. J.Y. Park, I.O. Jung, J.H. Moon, B.-T. Lee, S.S. Kim, J. Cryst. Growth, 282, 353 (2005)
110. Zhuo Chen, T. Salagaj, C. Jensen, K. Strobl, Mim Nakarmi and Kai Shum¹, First Nano, a division of CVD Equipment Cooperation, 1860 Smithtown Avenue, Ronkonkoma, NY 11779, USA
111. http://www.aliexpress.com/reactor-vessel_reviews.html
112. Bohac P., and Gauckler L.J. 2000, Oxygen Ion and Mixed Conductors and their Technological Applications, Kluwer Academic Publishers, Dordrecht, 271
113. Zhitao, H., Sisi, L., Jinkui, C. and Yong, C., Controlled growth of well-aligned ZnO nanowire arrays using the improved hydrothermal method. Journal of Semiconductors, 2013. 34(6): p. 063002-1-6.
114. Gedanken, A., "Using sonochemistry for the fabrication of nanomaterials", Ultrasonics -Sonochemistry, 200404
115. www.europeansocietysonochemistry.eu
116. Jaisai, M., Baruah, S., and Dutta, J. , Paper modified with ZnO nanorods – antimicrobial studies. Journal of Nanotechnol., 2012. 3: p. 684–691.
117. Liu, T.-Y., Liao, H-C., Ling, C-C., Hu, S-S. and Chen, S-Y., Immobilization of protein on arrayed ZnO nanorods grown on thermoplastic polyurethane(TPU) substrate for biomedical application. Langmuir, 2006. 22: p. 5804-5809.
118. Liua, Z.W., Ong, C. K., Yu, T. and Shen, Z. X. , Catalyst-free pulsed-laser-deposited ZnO nanorods and their room temperature photoluminescence properties. Applied Physics letters, 2006. 88: p. 053110.
119. Chang, P., Fan, Z., Tseng, W., Wang, D., Chiou, W., Hong, J. and Lu, J. G. . , ZnO Nanowires Synthesized by Vapor Trapping CVD Method. Chemistry of Materials, 2004. 16: p. 5133.
120. Azadeh, A., Amin, A. M. and Ali, M. , Sonochemically assisted synthesis of ZnO nanoparticles; A novel direct method. Iran J. Chem. Chem. Eng. , 2011. 30: p. 3.
121. Rusli, N., et al., Growth of High-Density Zinc Oxide Nanorods on Porous Silicon by Thermal Evaporation. Materials, 2012. 5(12): p. 2817-2832.
122. Suslick, K.S., Sonochemistry. Kirk-Othmer Encyclopaedia of Chemical Technology, 1998. 26: p. 517-541.
123. Roshan, A.H., Kazemzadeh, S. M., Vaezi M. R. and Shokuhfar, A., The effect of sonication power on the sonochemical synthesis of titania nanoparticles. Journal of Ceramic Processing Research., 2011. 12(3): p. 299-303.
124. Pholnak, C., Sirisathitkul, C., Suwanboon, S. and Harding, D. J., Effects of Precursor Concentration and Reaction Time on Sonochemically Synthesized ZnO Nanoparticles. Material Research, 2013.
125. Azadeh, A., Amin, A. M. and Ali, M. , Sonochemically assisted synthesis of ZnO nanoparticles; A novel direct method. Iran J. Chem. Chem. Eng. , 2011. 30: p. 3.

126. Nayak, A.P., Katzenmeyer, A., and Gosho, Y., Sonochemical Synthesis of Zinc Oxide Nanowire Arrays on Silicon and Glass Substrates. . Proceedings of The National Conference On Undergraduate Research (NCUR) 2010.
127. Jung, S.-H., Oh, E., Lee, K.-H., Jeong, S.-H., Yang, Y. and Park, C. G. , Fabrication of Diameter-tunable Well-aligned ZnO Nanorod Arrays via a Sonochemical Route. Bulletin of the Korean Chemical Society, 2007. 28(9): p. 1457.
128. Oh, E.a.J., S-H. , Sonochemical Method for Fabricating a High-performance ZnO Nanorod Sensor for CO Gas Detection. Journal of the Korean physical society., 2011. 59(1): p. 8-11.
129. Vabbina, P.K., Nayyar, P., Nayak, A. P., Katzenmeyer, A.M., Logeeswaran V.J., Pala, N., Saif Islam, M. and Talin A.A. , Synthesis of Crystalline ZnO Nanostructures on Arbitrary Substrates at Ambient Conditions. Proc. of SPIE 2010. 8106 81060H-1.
130. Goswami, S.K., Lee, B. W., and Eunsoon, O., Effect of Precursors on Optical and Structural Properties of ZnO Nanorods Synthesized by Sonochemical Method. . Journal of the Korean Physical Society 2011. 59(3): p. 2313-2317.
131. Rusli, N., et al., Growth of High-Density Zinc Oxide Nanorods on Porous Silicon by Thermal Evaporation. Materials, 2012. 5(12): p. 2817-2832.
132. Das, S.N., Kar, J. P., Xiong, J. and Myoung, J-M., Synthesis of ZnO Nanowire by MOCVD Technique: Effect of Substrate and Growth Parameter. Nanotechnology and Nanomaterial, 2012.
133. Liu, X., Wu, X., Cao, H. and Chang R. P. H., Growth mechanism and properties of ZnO nanorods synthesized by plasma-enhanced chemical vapor depositio. Journal of applied physics, 2004. 95(6): p. 1341-1347.
134. Bae, C.H., Park, S. M., Ahn, S. E., Oh, D-J., Kim, G. T. and Ha, J. S., Sol-gel synthesis of sub-50 nm ZnO nanowires on pulse laser deposited ZnO thin films. Applied Surface Science 2006. 253: p. 1758-1761.
135. Nayak, A.P., Katzenmeyer, A., and Gosho, Y., Sonochemical Synthesis of Zinc Oxide Nanowire Arrays on Silicon and Glass Substrates. . Proceedings of The National Conference On Undergraduate Research (NCUR) 2010.
136. Palumbo, M., Henley, S. J., Lutz, T., Stolojan, V. and Silva, S. R. P, A fast sonochemical approach for the synthesis of solution processable ZnO rods. JOURNAL OF APPLIED PHYSICS 2008. 104: p. 074906.
137. Robert A. Wilson, Heather A. Bullen, Department of Chemistry, Northern Kentucky University, Highland Heights, KY 41099., Introduction to Scanning Probe microscopy (SPM) Basic Theory Atomic Force Microscopy (AFM)
138. http://en.wikipedia.org/wiki/Atomic_force_microscopy
139. <http://www.purdue.edu/remlrs/sem.html2014>
140. http://www.chemistry.co.nz/henry_moseley.htm
141. Robert Edward Lee, Scanning electron microscopy and X-ray microanalysis, Prentice-Hall (1993)
142. http://pruffle.mit.edu/atomiccontrol/education/xray/xray_diff.php

CURRICULUM VITAE

Name Surname: Telat GÜLER

Place and Date of Birth: 13 April 1977/ Izmir, TURKEY

E-Mail: telat_guler@hotmail.com

B.Sc.: Industrial Automation Technology Teacher

Professional Experience and Rewards:

2013 to - date: Nanotechnology Master Program, Institute of Science / Gediz University, İzmir / TURKEY.

2006 – 2015: International Teacher Training Center in İZMİR

2003 – 2006: Mazhar Zorlu Vocational and Technical High School, Industrial Automation Technology Teacher, Izmir/Turkey

1999 – 2003: Buca Vocational and Technical High School, Electronic Teacher, Izmir/Turkey

Qualifications

- 1. Foreign languages:** English
- 2. Computer skills:** Windows; Microsoft Office (Word, Excel, Power Point); Scientific Graphing and Data Analysis Softwares (Origin); AutoCad, Solidworks.
- 3. Training Seminars Given by Myself**

PLC Programming (Siemens,Omron,Telemecaniques,Mitsubishi,Festo,Delta)

Control Systems

Sensor Technologies

Factory Automation Technologies

Flexible Manufacture System on Factory Automation

Industrial Network-Communication

SCADA (Supervisory Control And Data Acquisition)

Electric-Electronic

Microcontroller Systems

4. International Certifications(JAPAN,SPAIN,GERMANY)

➤ JAPAN International Cooperation Agency Program of the Government of Japan (04.08.2004-24.03.2005)

Education for Industrial Automation Technology and Computerized Machine Control for Mechanical Automation- Essential for Cleaner Production (Kitakyushu International Techno-cooperative Association and the related institutions.)

Oita University

Kyushu Institute of Technology

Kinki University

School of Humanity-Oriented Science and Engineering

Kumamoto University

Krosaki Harima Corporation

Mitsubishi Heavy Industries,Ltd.

Toshiba Mitsubishi-Electric System Corporation

Yaskawa Elektric Corporation

Japan Steel Works Ltd.

➤ SMC Competence Center (Vitoria / SPAIN) (Flexible Manufacturing Systems) (19.01.2009 - 23.01.2009)

System Installation

Planning of Workflow

Programming

Troubleshooting

Using industrial communications protocols such DeviceNet and Profibus in Automation Systems

Reading technical document and learning how to prepare it.

➤ Manufacturing Execution System (Vitoria / SPAIN) (26.01.2009 – 30.01.2009)

Automate Management of Recipes

Production Reporting

Product or materials tracking.

Measure and manage operational equipment efficiency (OEE)

Ease management of resources, including inventory and personel.

Manufacturing

Supplay Chain Management

Process Management

Data Warehouse.

➤ **Teacher Training System of Spain (Vitoria / SPAIN) (02.02.2009 – 06.02.2009)**

Selecting trainees and inviting them to the courses conducted.

Planning process of courses

Preparing and updating course curriculum

Evaluation and monitoring in courses and seminars.

Education management in Teacher Training Center.

➤ **Industrial Automation Training Techniques and Instruments (GERMANY) (16.01.2012 - 27.01.2012)**

Automation Technology/PLC Training Packages

Electrical Engineering/Electronic Training Packages

Mechatronics and factor automation

Mobile mechatronic learning system Robotino

Pneumatics and hydraulics Training Packages

Process automation and close-loop control technology

Simulating system and virtual learning environment